

Tumor-associated CD19⁺ macrophages induce immunosuppressive microenvironment in hepatocellular carcinoma

Junli Wang^{1,2,#}, Wanyue Cao^{1,2,#}, Jinyan Huang^{2,7}, Yu Zhou², Rujia Zheng^{2,7}, Yu Lou^{1,2}, Jiaqi Yang^{1,2}, Jianghui Tang^{1,2}, Mao Ye^{1,2}, Zhengtao Hong^{1,2}, Jiangchao Wu^{1,2}, Haonan Ding^{1,2}, Yuquan Zhang^{1,2}, Jianpeng Sheng^{2,5,6}, Xinjiang Lu^{2,8}, Pinglong Xu^{2,5,9}, Xiongbin Lu^{1,2}, Xueli Bai^{1,2,3,4,5,6}, Tingbo Liang^{1,2,3,4,5,6}, Qi Zhang^{1,2,3,4,5,6,*}

¹ Department of Hepatobiliary and Pancreatic Surgery, the First Affiliated Hospital, Zhejiang University School of Medicine, Hangzhou 310003, China.

² Zhejiang Provincial Key Laboratory of Pancreatic Disease, the First Affiliated Hospital, Zhejiang University School of Medicine, Hangzhou 310003, China.

³ Clinical Research Center of Hepatobiliary and Pancreatic Diseases, Zhejiang Province, Hangzhou 31003, China.

⁴ The Innovation Center for the Study of Pancreatic Diseases of Zhejiang Province, Hangzhou 310003, China.

⁵ Zhejiang University Cancer Center, Hangzhou 310063, China.

⁶ MOE Joint International Research Laboratory of Pancreatic Diseases, Hangzhou 310003, China.

⁷ Biomedical Big Data Center, the First Affiliated Hospital, Zhejiang University School of Medicine, Hangzhou 31003, China.

⁸ Department of Physiology, Zhejiang University School of Medicine, Hangzhou 310063, China.

⁹ Life Sciences Institute, Zhejiang University, Hangzhou 310063, China

These authors contributed equally.

*Correspondence: qi.zhang@zju.edu.cn (Q.Z.).

Abstract

Tumor-associated macrophages are a key component that contributes to the immunosuppressive microenvironment in human cancers. However, therapeutic targeting of macrophages has been a challenge in clinic due to the limited understanding of their heterogeneous subpopulations and distinct functions. Here, we identify a unique and clinically relevant CD19⁺ subpopulation of macrophages that is enriched in many types of cancer, particularly in hepatocellular carcinoma (HCC). The CD19⁺ macrophages exhibit increased levels of PD-L1 and CD73, enhanced mitochondrial oxidation, and compromised phagocytosis, indicating their immunosuppressive functions. Targeting CD19⁺ macrophages with anti-CD19 chimeric antigen receptor T (CAR-T) cells inhibited HCC tumor growth. We identify PAX5 as a primary driver of up-regulated mitochondrial biogenesis in CD19⁺ macrophages, which depletes cytoplasmic Ca²⁺, leading to lysosomal deficiency and consequent accumulation of CD73 and PD-L1. Inhibiting CD73 or mitochondrial oxidation enhanced the efficacy of immune checkpoint blockade therapy in treating HCC, suggesting great promise for CD19⁺ macrophage-targeting therapeutics.

Keywords

Hepatocellular carcinoma, tumor-associated CD19⁺ macrophage, tumor immunosuppressive microenvironment, PAX5, immune checkpoint blockade

Significance

Hepatocellular carcinoma (HCC) remains a lethal malignancy with limited therapeutic options. Our study reveals the critical role of CD19⁺ tumor-associated macrophages in driving HCC progression through enhanced mitochondrial oxidation, and lysosomal dysfunction mediated by the Pax5-[Ca²⁺]-TFEB axis with PD-L1 and CD73 overexpression, . Importantly, targeting CD19⁺ macrophages via CD19 CAR-T cells or CD73 blockade significantly enhances antitumor immunity, offering a promising combinatorial immunotherapy strategy. Our findings provide novel insights into the immunosuppressive tumor microenvironment and present a transformative approach to improve outcomes for HCC patients.

Introduction

Liver cancer has emerged as the third leading cause of cancer-related death worldwide, with hepatocellular carcinoma (HCC) being the predominant pathological subtype¹. Current therapies for treating hepatocellular carcinoma (HCC) comprise surgical resection, liver transplantation, locoregional therapies, and systemic treatments including targeted therapies and immunotherapy². Surgical resection and liver transplantation offer the best chance for a cure, but are only options for a small subset of patients diagnosed at an early stage. Locoregional therapies, including radiofrequency ablation and transarterial chemoembolization, are used for intermediate stages of HCC or when surgery is not feasible. Systemic treatments, like tyrosine kinase inhibitors (e.g., sorafenib and lenvatinib) and immune checkpoint inhibitors (e.g., atezolizumab, nivolumab and pembrolizumab), have expanded treatment options for the majority of patients with advanced HCC that misses the window for surgical intervention³. Despite these advancements, the 5-year overall survival rates for HCC remain below 20%⁴. These therapies face significant challenges in the clinic, including tumor heterogeneity, which leads to variable treatment responses, and the immunosuppressive tumor microenvironment (TME), which hampers the efficacy of immunotherapies^{5, 6}.

The immunosuppressive microenvironment of HCC is characterized by a complex interplay of various cell types that collectively inhibit effective anti-tumor immune responses. Key players include myeloid-derived suppressor cells (MDSCs), which accumulate and inhibit T cell activation⁷. Regulatory T cells (Tregs) suppress cytotoxic T cell function, while cancer-associated fibroblasts (CAFs) produce extracellular matrix components and cytokines that further support an immunosuppressive milieu⁸. Particularly, tumor-associated macrophages (TAMs) are the most abundant in HCC that promotes tumor growth and suppresses inflammation⁹. These various types of stroma

cells interact through direct contact and the release of soluble factors, creating a TME that hinders immune-mediated tumor eradication¹⁰.

Macrophages exhibit different features in the presence of different inducers, such as lipopolysaccharide and interleukin-4, which lead to the two classic polarizations of macrophages, defining as M1 and M2 macrophages¹¹. TAMs are believed to promote tumor progression by reprogramming local immunosuppression, inducing angiogenesis and drug resistance, and promoting tumor cell invasion. Phenotypically, despite being considered to have an M2-like polarization¹², TAMs are noncanonical and dynamically altered in response to stimuli within the TME. Consequently, the binary classification of macrophages is inadequate for describing them within the highly heterogeneous TME, both spatially and temporally¹³. Studies have identified specific TAM subgroups, such as PD-1⁺ TAMs in colon cancer, TREM1⁺ TAMs in hepatocellular carcinoma, and CD169⁺ TAMs in glioblastoma^{14, 15, 16}. These subgroups have diverse or even contradictory effects on tumor progression, suggesting that precise interventions targeting certain TAM subgroups, rather than the wholesale removal of M1, M2 or all TAMs in the TME, are likely to achieve better anti-tumor efficacy. Therefore, understanding the full spectrum of TAMs is crucial for developing therapeutic approaches that target macrophages in HCC.

In the present study, we identified a unique subgroup of CD19⁺ TAMs that are enriched in a number of solid tumor types, particularly in HCC. As a transmembrane glycoprotein, CD19 is considered as a biomarker and functionally crucial for the regulation of B cell receptor signaling in both the early and late stages of B cell development. Interestingly, a recent analysis of single-cell RNA sequencing (scRNA-seq) data defined a transdifferentiated cell types in the ischemic brain that was characterized by co-expression of B-cell markers and several macrophage markers¹⁷, suggesting a potential role of CD19 in macrophages. Here, we elucidated the clinical relevance,

cellular functions, and molecular features of CD19⁺ TAMs and determined the underlying regulatory mechanisms of their immunosuppressive characteristics. Based on these findings, we propose that targeting CD19⁺ TAMs or mitigating their pro-tumoral effects could be a promising strategy for treating HCC.

Methods

A detailed description of the methods used in the study can be found in the Supplementary information.

Clinical specimens

The collection and application of clinical samples were approved by the ethics committee of the First Affiliated Hospital, Zhejiang University School of Medicine. All patients' informed consent was obtained.

Cell culture

THP-1 cells, Hepa1-6 and Plat-E cells were obtained from the American Type Culture Collection (ATCC, Manassas, VA), immortalized murine bone marrow-derived macrophages (iBMDMs) were provided by Jingying Zhang at Zhejiang University. THP-1 cells were cultured in Roswell Park Memorial Institute medium (RPMI 1640, Gibco, Carlsbad, CA). Hepa1-6 and Plat-E cells were cultured in high-glucose Dulbecco's modified Eagle's medium (DMEM, Gibco). Media were supplemented with 10% fetal bovine serum (FBS, Gibco) and 1% penicillin/streptomycin (Sigma-Aldrich, Saint Louis, MO), and maintained at 37.0 ± 0.2 °C in a humidified incubator with 5.0% CO₂.

BMDMs were isolated from femurs and tibia of adult C57BL/6 mice (The Model Animal Research Center of Nanjing University, Nanjing, China) and cultured in RPMI 1640 medium containing 50 ng/ml recombinant murine macrophage colony-stimulating factor (M-CSF, Peprotech, Rocky Hill, NJ) for 5-day differentiation.

Mouse models

All mice were bred under pathogen-free conditions. Animal experiments were approved by the ethics committee of The First Affiliated Hospital, Zhejiang University School of Medicine. Lyz-Cre mice were obtained from The Jackson Laboratory (Bar Harbor, ME). Homozygous muMT mice were provided by Prof. Chao Wang at Zhejiang University. Pax5flox/flox and CD19flox/flox mice were purchased from Cyagen Biosciences (Suzhou,

China). C57BL/6 (CD45.2) mice were purchased from The Model Animal Research Center of Nanjing University (Nanjing, China). Mice at 6-12 weeks of age were used for animal experiments.

For in situ mice model, a 20 μ l suspension consisting of 50% Matrigel Basement Membrane Matrix (Corning, Teterboro, NJ) and 50% phosphate buffered saline (PBS; Cienry, Hangzhou, China) with Hepa1-6 cells in combination with macrophages were injected into the liver of mice. For syngeneic model, Hepa1-6 cells with 100 μ l PBS were inoculated subcutaneously into the left or right flanks of mice. Sacrificed tumors were processed for further experiments.

Transfection of lentiviral vectors and siRNA

THP-1 cells and iBMDMs were seeded in 6-well plates at a density of 2×10^5 cells/ml and infected with lenti-*PAX5* or lenti-*TFEB*, lenti-*NC* (Jikai, Shanghai, China). Stably transduced cells were purified using fluorescence activated cell sorting for further experiments. For siRNA transfection, 1.5×10^5 per well THP-1 cells were seeded in 24-well plates and transfected with human *TFEB* siRNA (Santa Cruz Biotechnology, Santa Cruz, CA) using lipofectamine RNAimax (ThermoFisher Scientific, Waltham, MA) for 48 hours according to manufacturer's protocols.

Targeted anti-CD19 CAR-T cell therapy

CD19⁺/CD19⁻ macrophages were isolated from the spleens of mice (CD45⁺CD11b⁺F4/80⁺CD19⁺), and were mixed with Hepa1-6 cells to establish subcutaneous xenograft model at the left (CD19⁺ macrophages) or right (CD19⁻ macrophages) flank of C57BL/6 or *muMT* mice. Anti-CD19 CAR-T cells were prepared and expanded. Mice were randomly assigned into groups for T cell infusion (1×10^7 cells in 100 μ L PBS), and were sacrificed after 14 days. Harvested tumors were processed for subsequent experiments.

ImageStream analysis

Single-cell suspensions were stained and observed using an ImageStream II system (Amnis Corp, Seattle, WA) to identify CD19⁺ macrophages, CD19⁻ macrophages, and B cells. Totally 1×10^5 single and focus cells were collected and analyzed by IDEASTM 6.2 software (Amnis Corp).

Multiplex immunohistochemistry (mIHC)

HCC and para-tumor were prepared into slides with 4- μ m thickness. mIHC was performed using Opal™ 6-Plex Detection Kits (Akoya Biosciences, Marlborough, MA) according to the manufacturer's instructions.

Single-cell RNA sequencing (scRNA-seq) and RNA-seq

ScRNA-seq libraries were constructed using a Chromium Single Cell 3' Library and Gel Bead Kit v3.1 (10 x Genomics) according to the manufacturer's protocol. RNA-seq was performed using the Illumina HiSeq XTEN platform (Illumina, San Diego, CA, USA) at Novogene Co. Ltd (Beijing, China).

Statistical analysis

Statistical analysis was conducted using GraphPad Prism 8 (GraphPad Inc., La Jolla, CA).

Results

CD19⁺ macrophages are enriched in HCC

A group of tumor tissue samples (n=30) from patients with HCC were analyzed with mass cytometry (CyTOF) for profiling their tumor immune microenvironment ⁶. Unexpectedly, we identified a subgroup of TAMs expressing CD19 at a level comparable to that in B cells in the tumors (**Figure 1A**). To validate the presence of CD19⁺ TAMs, we further conducted immune profiling analysis of HCC samples in a 41-patient cohort. Approximately a half (29 out of 41) of the HCC samples had a considerable proportion (>20% of total TAMs) of CD19⁺ TAMs. The existence of a CD19⁺ subpopulation in the TAMs was further confirmed using immunofluorescence (**Figure 1B**), ImageStream (**Figures 1C and S1A**) and flow cytometry (**Figures 1D and S1B**). Additionally, we applied multiplex immunohistochemical (mIHC) staining on tumors and their adjacent normal tissues using CD14, CD68, CD19, and CD20 markers to demonstrate CD19⁺ TAMs at the single-cell level (**Figure 1E**). Conventional macrophage markers, CD11b and CD68/CD14, were used to confirm their macrophage identity. Notably, the proportion of CD19⁺ TAMs was much higher in HCC than in adjacent normal tissue or peripheral blood (**Figures 1B and 1D**). In terms of cell size, the CD19⁺ TAMs had greater FSC/SSC (forward scatter/side scatter) values in flow cytometry than those of B cells, suggesting their macrophage cell lineage rather than a B cell lineage (**Figure S1C**).

Next, we wanted to determine whether CD19⁺ TAMs exist in other types of solid tumors. In a total of six types of human solid tumors, including HCC, CD19⁺ TAMs are enriched (**Figure 1F**) compared with those in peripheral blood and normal tissues. In particular, HCC, renal carcinoma, colorectal cancer, pancreatic cancer, and gastric cancer had a median proportion of CD19⁺ TAMs over 20% of total TAMs. Similarly, we detected CD19⁺ macrophages in various normal tissues and peripheral blood in mice

(**Figure S1D**). Moreover, the proportion of CD19⁺ macrophages did not correlate with that of B cells in these tissues (**Figures S1E and S1F**), further suggesting that they are not derived from B cells. The results collectively suggest that CD19⁺ macrophages naturally exist in the body but are enriched in solid tumors.

CD19⁺ TAMs are associated with poor clinical outcomes in HCC

As no previous study reported this subgroup of TAMs, we wanted to examine the clinical relevance of CD19⁺ macrophages in HCC. A human HCC tissue microarray was co-immunostained with anti-CD19 and anti-CD68 antibodies (**Figure S2A**). In a total of 191 tissue samples with valid co-immunostaining, we found that the abundance (shown as density) of CD19⁺ TAMs was positively correlated with tumor size (**Figure S2B**) and tumor cell differentiation (**Figure S2C**), but not with disease stages (**Figure S2D**), suggesting CD19⁺ TAMs may be recruited at early stage of tumor initiation for creating immunosuppressive TME. Importantly, HCC patients with greater density of CD19⁺ TAMs had worse overall survival (hazard ratio 3.12, 95% confidential interval 1.23–7.89) and disease-free survival (**Figures 2A and S2E**). By contrast, the density of total TAMs had no correlation with overall survival of these patients (**Figure 2B**). Consistent with its clinical relevance, the density of CD19⁺ TAMs was positively correlated with tumor cell proliferation, as indicated by Ki-67 staining in human HCC samples (**Figure 2C**). TME analysis of the HCC tissue microarray indicated that a high density of CD19⁺ TAMs was associated with increased infiltration of Tregs but reduced infiltration of CD8⁺ T cells (**Figure S2F**). Furthermore, in a prospective cohort of HCC patients treated with anti-PD-1 antibodies (NCT03732547), we observed a notable correlation between a favorable tumor response (partial response or stable disease) and elevated CD19⁺ TAMs levels, rather than total TAMs levels (**Figures 2D, and 2E**), suggesting that CD19⁺ TAM-associated immunosuppression can be overcome, at least partially, by immune

checkpoint blockade therapy.

CD19⁺ TAMs possess immunosuppressive abilities and promote HCC growth

To study the role of CD19⁺ TAMs in shaping the TME, we further analyzed the CyTOF data from the 41 patients with HCC (the same cohort analyzed in **Figure 1A**). CD19⁺ TAMs represent a major subgroup of TAMs, accounting for approximately 30% of TAMs and 5% of CD45⁺ cells in the tumors (**Figure S2G**). The CD19⁺ and CD19⁻ subsets of TAMs showed a sharp difference at the level of the M2 macrophage marker CD163 (**Figure S2H**). The proportion of CD19⁺ TAMs was also negatively correlated with the abundance of total T, CD4⁺ and CD8⁺ T cells (**Figure S2I**). In-depth analysis showed that the proportion of CD19⁺ TAMs was positively correlated with that of PD-1⁺ effector memory T cells (TEMs), but negatively correlated with that of CD127⁺ TEMs (**Figure S2I**), consistent with the clinical data in (**Figures 2D and 2E**). These data strongly suggest that CD19⁺ TAMs possess immunosuppressive abilities.

To determine the role of CD19⁺ macrophages in tumor growth in vivo, we isolated CD19⁺ and CD19⁻ macrophages from mouse spleen and mixed them with mouse HCC cells (Hepa 1-6) to generate orthotopic syngeneic mouse models (**Figure S3A**). The presence of CD19⁺ macrophages significantly promoted tumor growth in comparison to CD19⁻ macrophages (**Figure 2F**). Meanwhile, the number of infiltrating CD8⁺ T cells was much lower, but Gr-1⁺ cells were more abundant in tumors with CD19⁺ macrophages (**Figures S3B and S3C**). To test the clinical potential of targeting CD19⁺ macrophages in HCC, we developed mouse chimeric antigen receptor T (CAR-T) cells specifically targeting mouse CD19 (see details in **Supplementary Methods**) for adoptive T cell therapy (**Figure S3D**). The growth of the tumors with CD19⁺ macrophages, but not with CD19⁻ macrophages, was significantly inhibited when the tumor-bearing mice received

anti-CD19 CAR-T cells. This inhibition was not observed in the mice treated with control CAR-T cells for tumors containing either CD19⁺ or CD19⁻ macrophages (**Figures 2G and S2E**). To exclude the possibility that the inhibition is associated with B cells that are also positive for CD19, we tested the anti-tumor effect of the anti-CD19 CAR-T in *muMT* mice that lack mature B cells¹⁸. Low levels of B cells in *muMT* mice were verified by flow cytometry (**Figure S3F**). GFP⁺ anti-CD19 CAR-T cells were infiltrated into tumors in *muMT* mice (**Figure S3G**) and CD19⁺ macrophages were effectively depleted by the anti-CD19 CAR-T treatment (**Figure S3H**). The similar anti-tumor effect of anti-CD19 CAR-T cells was observed in the tumors with CD19⁺ macrophages (**Figure 2H**), independent of the B cell levels in the mice. These results highlight the role of CD19⁺ macrophages in HCC progression and suggested CD19⁺ macrophages are a potential clinical target for HCC treatment.

CD19⁺ TAMs exhibit a distinct gene expression profile

To understand the molecular features of CD19⁺ macrophages, we isolated CD19⁺ TAMs, CD19⁻ TAMs and B cells from three HCC patients, and conducted scRNA-seq analysis for a total of 52,749 cells (**Figures 3A and S4A**). TAMs were annotated by a high expression level of *CD11b*, *CD14* and *CD68*, while B cells were identified by *CD45*, *CD19* and *CD79A*. CD19⁺ TAMs, CD19⁻ TAMs and B cells were clustered (**Figure 3B**). We next characterized the transcriptional profiles of the three types of cells (**Figure 3C**). CD19⁺ TAMs exhibited a distinctive gene signature, among which ribonuclease 1 (*RNASE1*), selenoprotein P (*SELENOP*) and apolipoprotein E (*APOE*) are closely associated with cell metabolism. CD19⁻ TAMs expressed high levels of genes encoding small calcium-binding proteins in the S100 family including *S100A9*, *S100A8* and *S100A4*. Interestingly, CD19⁺ TAMs and B cells both express high levels of genes (*IGHG1*, *IGLC1* and *IGKC*) encoding immunoglobulin proteins. Furthermore, CD19⁺ TAMs

appeared to be in proximity to M2-like macrophages, while CD19⁻ TAMs were close to M1 macrophages to some extent, although no definite associations were found (**Figures 3D and S4B**). Genes in metabolic pathways and lysosome were significantly enriched in CD19⁺ TAMs (**Figure 3E**). Specifically, CD19⁺ TAMs had higher expression levels of genes associated with mitochondrial functions and higher mitochondria scores (**Figures 3F and 3G**). The gene expression profiling analysis demonstrated that CD19⁺ macrophages are a subgroup of cells distinct from CD19⁻ macrophages and B cells.

Based on the scRNA-seq data analysis, we identified a 10-gene signature capable of distinguishing between CD19⁺ and CD19⁻ macrophages. This signature includes five genes specific to CD19⁺ TAMs (*RNASE1*, *APOE*, *APOA2*, *APOC1*, *SELENOP*) and five genes specific to CD19⁻ TAMs (*S100A9*, *S100A8*, *S100A4*, *FCN1*, *VCAN*) (**Figure S4C**). The mRNA expression profiles of these 10 genes effectively differentiate CD19⁺ TAMs from CD19⁻ TAMs, aligning well with their protein levels determined by flow cytometry (**Figures S4D and S4E**). This 10-gene signature was also applied to analyze two public scRNA-seq datasets (Bioproject: PRJCA010606 and PRJCA007744) (**Figures S5A, S5B, S5C and S6A, S6B, S6C**). The defined CD19⁺ TAMs are highly enriched in HCC compared to normal adjacent tissues and show a higher level of mitochondrial activity than CD19⁻ TAMs (**Figures S5D, S5E and S6D, S6E**).

CD19⁺ TAMs are highly proliferative and immunosuppressive

Given the high mitochondria score of CD19⁺ TAMs in HCC, we next analyzed the metabolic activity of mitochondria based on the expression levels of oxidative phosphorylation (OXPHOS)-related genes, including NADH dehydrogenase members, cytochrome c oxidase subunit members, and ATP synthase membrane subunit members

in CD19⁺ TAMs and CD19⁻ TAMs. Overall, a majority of these genes was significantly up-regulated in CD19⁺ TAMs (**Figure 4A**). Seahorse analysis of cell metabolism showed remarkably enhanced mitochondrial respiration of CD19⁺ macrophages, including both basal and maximal respiratory capacities (**Figure 4B**). The energetic feature of CD19⁺ macrophages may lead to the alterations of their functions and cell activities. First, CD19⁺ TAMs showed much compromised phagocytotic activity (**Figure 4C**). Second, we found that the proportion of CD19⁺ TAMs was significantly higher in large tumors than in small ones in an HCC syngeneic mouse model (**Figure S7A**), consistent with their clinical relevance in human HCC. CD19⁺ TAMs showed higher levels of Ki-67 expression than CD19⁻ TAMs from the same tumor, both in mice and patients (**Figures S7B and S7C**). The enhanced proliferation of CD19⁺ TAMs was confirmed using an orthotopic mouse model and 5-ethynyl-2'-deoxyuridine (EdU) assays (**Figure S7D**). Therefore, we reasoned that abundance of CD19⁺ TAMs in tumors, especially large ones, is likely due to their high proliferation rate.

As CD19⁺ TAMs are a biomarker for poor clinical outcomes of anti-PD-1 immunotherapy in patients with HCC (**Figures 2D and 2E**), it was not of much surprise to see increased PD-L1 levels in CD19⁺ TAMs compared to CD19⁻ TAMs (**Figure 4D**). During the HCC metabolite analysis⁶, we were particularly interested in adenosine, a primary immunosuppressive metabolite present in high levels in the TME of most solid tumors¹⁹. In the metabolite data from the analysis using liquid chromatography with tandem mass spectrometry (LC-MS/MS), we observed significant associations between the concentrations of adenosine diphosphate (ADP), adenosine monophosphate (AMP), and adenosine and the abundance of CD19⁺ TAMs in human HCC tumors (**Figure S7E**). Factors that contribute to adenosine production include hypoxia, high cell turnover, and particularly, the expression of CD73, a 5'-nucleotidase (NT5E) that converts autocrine

and paracrine danger signals of ATP to anti-inflammatory adenosine²⁰. Given its pivotal role in regulating the ADP/AMP/adenosine conversion²¹, CD73 has been an emerging therapeutic target for immune checkpoint blockade^{22, 23}, and numerous CD73-targeted antibodies and small-molecule inhibitors are currently undergoing clinical testing for cancer therapy²⁴. As expected, we observed significantly elevated levels of CD73 in CD19⁺ TAMs (**Figure 4D**). Biochemical assay verified a high 5'-nucleotidase activity of CD73 in the CD19⁺ TAMs (**Figure 4E**). As an indicator of their immunosuppressive functions, CD19⁺ macrophages significantly inhibited the proliferation of total T cells, CD4⁺ T cells, and CD8⁺ T cells when these cells were isolated from the clinical tumor samples and co-cultured in vitro in mixed lymphocyte reaction (MLR) assays (**Figure 4F**).

PAX5 is a master regulator for CD19⁺ macrophages

CD19 is important for B cell development and differentiation²⁵. Therefore, it is intriguing to determine whether CD19 expression is essential for the immunosuppressive activity of CD19⁺ TAMs. To this end, *CD19^{ΔMφ} (CD19^{flox/flox};Lyz-Cre)* mice were generated to establish orthotopic mouse HCC tumor models with macrophage-specific knockout of CD19. Unexpectedly, no differences in orthotopic tumor growth were observed between *CD19^{ΔMφ}* mice and their littermate controls (**Figure 5A**), although CD19 expression was depleted in literally all the macrophages in the *CD19^{ΔMφ}* mice (**Figure 5B**). These results suggest that CD19 can only be used as a biomarker for the CD19⁺ macrophages, but functionally dispensable for this subgroup of macrophages in the tumor. Among upstream regulators of CD19, PAX5 is the key transcription factor that governs the expression of CD19^{26, 27}. We found that CD19⁺ TAMs indeed had up-regulated expression of PAX5 at both mRNA and protein levels (**Figures 5C, 5D, and 5E**). Thus, we reasoned that PAX5 may play a role in the CD19⁺ macrophages. Exogenous overexpression of *PAX5* in human THP-1 cells (a model for macrophage-related cell activities) induced the

expression of CD19, CD73 and PD-L1 (**Figures 5F and 5G**). Similar results were observed in mouse immortalized bone marrow-derived macrophages (iBMDMs) (**Figure 5H**). Functionally, overexpression of *PAX5* impaired phagocytosis in the mouse iBMDMs (**Figure S8A**). Collectively, *PAX5* appears to be a master regulator for the essential features of CD19⁺ macrophages in the tumor.

In the human THP-1 cells, overexpression of *PAX5* also profoundly enhanced mitochondrial respiration in terms of basal respiration, maximal respiration and ATP production (**Figure 5I**). Electron microscopy analysis demonstrated that the number of mitochondria was much higher in the THP-1 cells with *PAX5* overexpression (**Figure 5J**). The increased number of mitochondria and decreased mitochondrial superoxide levels were detected by flow cytometry in these cells (**Figure 5K**). Importantly, *PAX5* significantly enhanced the expression of PGC-1 α , a potent inducer of mitochondrial biogenesis (**Figure S8B**)²⁸. Additionally, *PAX5*-overexpressing THP-1 cells presented a higher level of adenosine in the culture medium than control cells, consistent with increased CD73 activity (**Figures S8C and S8D**). Since cellular metabolism is tightly related to macrophage functions¹⁵, we asked whether regulation of mitochondrial metabolism affected CD73 activity in CD19⁺ macrophages. Antimycin, an OXPHOS inhibitor, dramatically impaired CD73 activity (**Figure S8D**). Induction of reactive oxide species by diamide, rather than their removal by N-acetyl-cysteine (NAC), also inhibited CD73 activity. By contrast, blocking CD19 with neutralizing antibodies or inhibiting glycolysis with 2-deoxy-d-glucose (2-DG) had no effect on the CD73 activity (**Figure S8D**). Therefore, mitochondrial metabolism, but not CD19-associated cell signaling regulate the functions of CD19⁺ macrophages in the tumor. Consistent with the cell studies, conditional knocked out of *Pax5* in mouse macrophages (*Pax5*^{fllox/fllox}; *Lyz-Cre*, named as *Pax5* ^{Δ M ϕ}) drastically inhibited the growth of orthotopically injected

Hepa1-6-derived tumors (**Figures 5L, S8E, S8F, and S8G**). As expected, depletion of PAX5 efficiently decreased the protein levels of CD19, CD73, and PD-L1 in the macrophages of these mice (**Figure S8H**). Collectively, these results suggested that PAX5, instead of CD19, plays a central role in the regulation of CD19⁺ macrophages in the tumor.

PAX5 induces PD-L1 and CD73 in a post-transcriptional manner

Interestingly, *PAX5* overexpression in human THP1 cells did not significantly induce the mRNA levels of *PD-L1* and *CD73* (**Figure 6A**), indicating post-transcriptional regulation of PAX5 in CD19⁺ macrophages. We performed CUT&Tag (**C**leavage **U**nder **T**argets and **T**agmentation) and RNA-seq assays on human THP-1 cells with or without *PAX5* overexpression and identified global expression changes of genes that are transcriptionally regulated by PAX5 (**Figure 6B**). Among these changes, genes associated with lysosome pathways were the second most significantly enriched, behind the genes involved in phagocytosis (**Figure 6C**), suggesting that PAX5 may control target protein degradation via lysosome. Heat shock cognate 71-kDa protein (HSC70) is a chaperon protein that brings target proteins to lysosomes for degradation in cells²⁹. We identified three KFERQ-like motifs, which are potential binding sites to HSC70, in both PD-L1 and CD73 (**Figure 6D**). Coimmunoprecipitation assays validated protein interactions between HSC70 and PD-L1 or CD73 (**Figure 6E**). In lysosome function assays, we observed that lysosomes were significantly inhibited upon *PAX5* overexpression (**Figures 6F and S6G**). Meanwhile, both CD73 and PD-L1 were induced when *PAX5*-overexpressing THP-1 cells were treated with inhibitors of lysosomal proteolysis (NH₄Cl and leupeptin) (**Figure 6H**).

Because decreased number of lysosomes were seen in the *PAX5*-overexpressing

THP-1 cells, we speculated that PAX5 may also regulate the activity of TFEB (Transcription Factor EB), a master regulator of lysosomal biogenesis (**Figure S9A**)³⁰, in the nucleus. We found that nuclear TFEB levels were dramatically diminished in *PAX5*-overexpressing cells (**Figures 6I and S9B**). Knockdown of TFEB inhibited lysosomal functions and increased PD-L1 and CD73 protein levels, similar to the effects of *PAX5* overexpression (**Figures S9C, S9D, and S9E**). Overexpression of TFEB offset the effects of *PAX5* overexpression, leading to reduced levels of PD-L1 and CD73 in the *PAX5*-overexpressing cells (**Figures S9F and S9G**). We sought to delineate the mechanism by which PAX5 regulates the nuclear translocation of TFEB. TFEB subcellular translocation is regulated primarily by Ca²⁺ signaling or mTOR-mediated phosphorylation^{31, 32}. While no change in mTOR expression was observed in the *PAX5*-overexpressing cells (data not shown), we reasoned that increasing calcium uptake by mitochondria, due to their up-regulated biogenesis in CD19⁺ TAMs, may impact Ca²⁺ signaling in the cytosol³². Using a fluorescent probe, we found an increased level of mitochondrial Ca²⁺ and, accordingly, a decreased level of cytosolic Ca²⁺ in *PAX5*-overexpressing THP-1 cells (**Figure 6J**). Treatment with IACS-010759 (an OXPHOS inhibitor) or ionomycin (a Ca²⁺ ionophore) significantly increased the cytosolic level of Ca²⁺ and thus promoted the nuclear level of TFEB (**Figures S9H and S9I**). These results suggested that PAX5 modulates the Ca²⁺ shuttling between mitochondria and the cytosol, consequently inhibiting the nuclear translocation of TFEB and lysosomal activity, which eventually increases the levels of CD73 and PD-L1 by inhibiting their lysosomal degradation.

Blocking CD19⁺ TAMs enhances the efficacy of immune checkpoint blockade therapy

Given the role of CD19⁺ TAMs in HCC progression, we wanted to determine

whether they could be a therapeutic target in treating HCC. In a syngeneic HCC tumor model, we first depleted macrophages in mice using clodronate liposomes every other day for four doses (**Figures S10A, S10B, and S10C**) prior to mouse Hepa1-6-derived tumor models establishment (**Figure S10D**)^{33, 34}. Control or *Pax5*-overexpressing iBMDMs were then infused into these mice to test their effects on tumor growth (**Figure S10D**). As expected, *Pax5*-overexpressing iBMDMs promoted greater tumor growth than wild-type iBMDMs (**Figure S10E**). In another orthotopic mouse model without systemic depletion of macrophages, *Pax5*-overexpressing iBMDMs also imposed a profound pro-tumor effect (**Figure 7A**). Immunohistochemical analysis revealed that *Pax5*-overexpressing iBMDMs limited the tumor infiltration of CD8⁺ T cells (**Figure 7B**), indicating an immunosuppressive TME.

CD19⁺ TAMs create an immunosuppressive tumor microenvironment with increased levels of PD-L1 and CD73. We next tested whether the combination of PD-L1 and CD73 blockade had a synergistic effect on tumor control (**Figure 7C**). Anti-CD73 neutralizing antibodies or a small-molecule inhibitor of CD73 significantly enhanced the anti-tumor effect of anti-PD-L1 antibodies in an orthotopic HCC mouse model (**Figure 7D**). These effects are solely dependent on PAX5 in the CD19⁺ macrophages, as PD-L1 and CD73 blockade did not affect tumor progression in the *Pax5*^{ΔMφ} mice (**Figure S10F**). In the presence of anti-PD-L1 antibodies, CD73 blockade significantly increased the tumor infiltration of CD8⁺ T cells, as well as CD4⁺ T cells and natural killer cells. Tumor cell proliferation was greatly suppressed, as indicated by reduced Ki-67 staining (**Figures S11**).

Because induced mitochondrial respiration is critical for the functions of CD19⁺ TAMs, we tested whether inhibiting mitochondrial respiration of CD19⁺ TAMs had a similar

anti-tumor effect. The OXPHOS inhibitor IACS-010759 exhibited an improved anti-tumor effect when combined with anti-PD-L1 antibodies in the orthotopic mouse HCC tumor model (**Figure 7E**). The combination of PD-L1 blockade and OXPHOS inhibition also significantly promoted tumor infiltration of immune cells, including CD4⁺ T cells and CD8⁺ T cells (**Figures S12**). Collectively, therapeutic approaches targeting CD73 or OXPHOS in CD19⁺ TAMs show great promise for improving the anti-tumor efficacy of immunotherapy for HCC.

Discussion

TAMs play a crucial role in shaping the immunosuppressive tumor microenvironment. However, the heterogeneity of TAMs and the mechanisms by which they contribute to tumor progression remain elusive. In this study, we identified CD19⁺ macrophages enriched in a number of human tumor tissues. A high density of CD19⁺ macrophages within tumors is associated with poor clinical outcomes and reduced response to immunotherapy in patients with HCC. It was previously known that B cell progenitors, and even mature B cells, can be induced to adopt the gene expression patterns, morphology, and functions of macrophages³⁵. Overexpression of transcription factor C/EBP in differentiated B cells leads to their rapid reprogramming into macrophages by inhibiting the B cell commitment transcription factor PAX5 and downregulation of its target CD19³⁵. Interestingly, CD19⁺ macrophages retain high expression levels of PAX5 and CD19. Despite its essential role in B cell differentiation and signaling, CD19 itself appears to be dispensable for the pro-tumor functions of CD19⁺ TAMs, at least in HCC. Depletion of CD19 in our preclinical mouse models had no notable effect on tumor growth (**Figure 5A**). The abundance of CD19⁺ macrophages was also not correlated with the numbers of B cells in the tissues (**Figure S1F**). In addition, cell morphology and size analysis suggest that CD19⁺ TAMs is not likely to originate from a B cell lineage (**Figures 1C and S1C**). Further studies are warranted to determine whether CD19⁺ TAMs are recruited from circulating non-resident macrophages or functionally switched from tissue-resident macrophages.

PAX5 is a deciding regulator for B-lineage commitment³⁶, and is usually undetectable in macrophages. However, PAX5 remains as a key player that drives immunosuppressive functions in the CD19⁺ TAMs. *PAX5*-overexpressing macrophages phenocopied CD19⁺ macrophages with all known characteristics, including enhanced

oxidative phosphorylation, increased proliferative capacity, compromised phagocytic activity, and up-regulated levels of PD-L1 and CD73. However, CD19 does not seem to be transactivated in CD19⁺ macrophages as it does in B cells. Instead, PAX5 induces the CD19 protein level in the macrophages by inhibiting its lysosomal degradation. This differential regulation may distinguish signaling networks between B cells and macrophages. It is now unclear how PAX5 is highly expressed in CD19⁺ macrophages. This study is the first report showing a potential lineage crossing between B cells and macrophages in the tumor microenvironment. We observed varying levels of CD19⁺ macrophages in the circulation and organs of both humans and mice, indicating the possible existence of these cells since embryonic development. This suggests that lineage restriction during hematopoietic stem cell differentiation may not be as stringent as previously thought, allowing for the generation of a small population of "hybrid cells."

CD19⁺ TAMs are immunosuppressive due to their high levels of PD-L1 and CD73. CD73 expression in solid tumors has been identified as an independent biomarker of poor prognosis in clinic^{37, 38}. Recent evidence has indicated that CD73 is selectively expressed in a diverse range of immune cell types, including T cells, natural killer cells, and macrophages³⁹. The expression of CD73 on macrophages is closely associated with M2 polarization and resistance to anti-PD-1 antibodies^{21, 40}. Our study demonstrated that PAX5 increases the levels of CD73 and PD-L1 by compromising lysosomal activity due to decreased nuclear translocation of TFEB in CD19⁺ macrophages. The elevated activity of CD73 in these macrophages leads to increased adenosine production, which supports cancer cell proliferation in the tumor microenvironment. Given the hyperactivity of OXPHOS in CD19⁺ TAMs, the combined inhibition of CD73 and OXPHOS, along with immune checkpoint blockade, presents a promising therapeutic approach for treating HCC and potentially other tumors enriched with CD19⁺ TAMs.

In this study, we explored potential therapeutic strategies to deplete or inhibit CD19⁺ TAMs, including CD19-targeted CAR-T cells, CD73 blockade, and OXPHOS inhibitors. CD19-targeted CAR-T therapies have consistently demonstrated high antitumor efficacy in both pediatric and adult patients with relapsed B-cell acute lymphoblastic leukemia, chronic lymphocytic leukemia, and B-cell non-Hodgkin lymphoma⁴¹. However, their clinical application in non-hematologic solid tumors remains to be established^{42, 43}. Our results from a preclinical HCC model indicate significant translational potential for CD19-targeted CAR-T therapy in treating solid tumors with high levels of CD19⁺ TAMs. CD73 blockade has demonstrated antitumor effects in preclinical experiments by eliciting an effective immune response, including enhanced NK cell activity, improved CD4⁺ and CD8⁺ T cell function, and elevated levels of proinflammatory cytokines²². Beyond macrophages, CD73 expression on tumor cells and Tregs also suppresses antitumor immunity²¹. Thus, targeting CD73 may exert multifaceted effects in cancer treatment. Finally, OXPHOS inhibitors have become a focus in cancer therapeutics, enhancing treatment responses in various cancers, including melanomas, lymphomas, colorectal cancers, leukemias, and pancreatic ductal adenocarcinoma^{44, 45}. However, the clinical efficacy of OXPHOS inhibitors is influenced by the complex TME. Our study suggests that OXPHOS inhibition may enhance clinical efficacy by targeting and suppressing CD19⁺ TAMs in cancer immunotherapy.

In summary, we identified a new subgroup of CD19⁺ TAMs, which show immunosuppressive capacity and promoted HCC progression. Mechanistically, CD19⁺ TAMs are primarily driven by PAX5 and have up-regulated PD-L1 and CD73 levels. Elimination of these macrophages by CD19-specific CAR-T cells or functional inhibition of them by inhibiting CD73 or OXPHOS sensitized HCC to immunotherapy.

Acknowledgements

This work was supported by National Key Research & Development Program (No. 2020YFA0804300), National Natural Science Foundation of China (Nos. 82071865, 82403723, 81871320, 32321002, 82188102, 92359304), Zhejiang Provincial Natural Science Funds (Nos. LR20H160002, HDMD22H319373), Zhejiang Provincial Key Research & Development Program (No. 2021C03063), Zhejiang Provincial Medical and Health Technology Project (No. WKJ-ZJ-2403), and Zhejiang Provincial Traditional Chinese Medicine Science and Technology Project (GZY-ZJ-KJ-23025). We thank Jianfeng Wang from the Zhejiang Provincial Key Laboratory of Pancreatic Disease for sample collection. Dr. Qi Zhang also gratefully acknowledges the support of K.C.Wong Education Foundation.

Author contributions

T.L. and Q.Z. conceived the project. Q.Z., J.W. and J.S. designed the experiments. Q.Z., J.W., Y.Z., J.Y., M.Y., J.Z., J.W., J.W., and Z.H. performed most of the experiments under the supervision of T.L., X.B, X.L and P.X. R.Z., Y.L, X.L., and J.H. performed the bioinformatic analysis. Q.Z. and J.W. wrote the manuscript and the other authors made critical revisions.

Competing Interests statement

The authors declare no competing interests.

Lead contact

Further information and requests for resources and reagents should be addressed to Qi

Zhang (qi.zhang@zju.edu.cn).

Materials availability

Plasmids, cell lines and mice generated in this study will be made available with a

completed Materials Transfer Agreement by the lead contact upon request.

Data and code availability

All data generated or analyzed during this study are included in this manuscript (and its supplementary information files). Human sequencing data were deposited in Genome Sequence Archive (GSA) (GSA: HRA008143). All processed sequencing data are available via <https://www.scidb.cn/en/s/b63uAr>. Any additional information required to reanalyze the data reported in this paper is available from the lead contact upon request.

Reference

1. Sung H, Ferlay J, Siegel RL, Laversanne M, Soerjomataram I, Jemal A, Bray F: (2021).Global Cancer Statistics 2020: GLOBOCAN Estimates of Incidence and Mortality Worldwide for 36 Cancers in 185 Countries. *CA: a cancer journal for clinicians* 71(3):209-249.
2. Forner A, Llovet JM, Bruix J: (2012).Hepatocellular carcinoma. *Lancet (London, England)* 379(9822):1245-1255.
3. Gordan JD, Kennedy EB, Abou-Alfa GK, Beg MS, Brower ST, Gade TP, Goff L, Gupta S, Guy J, Harris WP *et al*: (2020).Systemic Therapy for Advanced Hepatocellular Carcinoma: ASCO Guideline. *Journal of Clinical Oncology* 38(36):4317-4345.
4. Vogel A, Meyer T, Sapisochin G, Salem R, Saborowski A: (2022).Hepatocellular carcinoma. *Lancet (London, England)* 400(10360):1345-1362.
5. Marra F, Tacke F: (2014).Roles for chemokines in liver disease. *Gastroenterology* 147(3):577-594.e571.
6. Zhang Q, Lou Y, Yang J, Wang J, Feng J, Zhao Y, Wang L, Huang X, Fu Q, Ye M *et al*: (2019).Integrated multiomic analysis reveals comprehensive tumour heterogeneity and novel immunophenotypic classification in hepatocellular carcinomas. *Gut* 68(11):2019-2031.
7. Kalathil S, Lugade AA, Miller A, Iyer R, Thanavala Y: (2013).Higher frequencies of GARP(+)/CTLA-4(+)/Foxp3(+) T regulatory cells and myeloid-derived suppressor cells in hepatocellular carcinoma patients are associated with impaired T-cell functionality. *Cancer research* 73(8):2435-2444.
8. Shen KY, Zhu Y, Xie SZ, Qin LX: (2024).Immunosuppressive tumor microenvironment and immunotherapy of hepatocellular carcinoma: current status and prospectives. *Journal of hematology & oncology* 17(1):25.
9. Noy R, Pollard JW: (2014).Tumor-associated macrophages: from mechanisms to therapy. *Immunity* 41(1):49-61.

10. Binnewies M, Roberts EW, Kersten K, Chan V, Fearon DF, Merad M, Coussens LM, Gabrilovich DI, Ostrand-Rosenberg S, Hedrick CC *et al*: (2018).Understanding the tumor immune microenvironment (TIME) for effective therapy. *Nature medicine* 24(5):541-550.
11. Murray PJ: (2017).Macrophage Polarization. *Annu Rev Physiol* 79:541-566.
12. Mantovani A, Sozzani S, Locati M, Allavena P, Sica A: (2002).Macrophage polarization: tumor-associated macrophages as a paradigm for polarized M2 mononuclear phagocytes. *Trends in immunology* 23(11):549-555.
13. DeNardo DG, Ruffell B: (2019).Macrophages as regulators of tumour immunity and immunotherapy. *Nat Rev Immunol* 19(6):369-382.
14. Wu Q, Zhou W, Yin S, Zhou Y, Chen T, Qian J, Su R, Hong L, Lu H, Zhang F *et al*: (2019).Blocking Triggering Receptor Expressed on Myeloid Cells-1-Positive Tumor-Associated Macrophages Induced by Hypoxia Reverses Immunosuppression and Anti-Programmed Cell Death Ligand 1 Resistance in Liver Cancer. *Hepatology (Baltimore, Md)* 70(1):198-214.
15. Gordon SR, Maute RL, Dulken BW, Hutter G, George BM, McCracken MN, Gupta R, Tsai JM, Sinha R, Corey D *et al*: (2017).PD-1 expression by tumour-associated macrophages inhibits phagocytosis and tumour immunity. *Nature* 545(7655):495-499.
16. Kim HJ, Park JH, Kim HC, Kim CW, Kang I, Lee HK: (2022).Blood monocyte-derived CD169(+) macrophages contribute to antitumor immunity against glioblastoma. *Nature communications* 13(1):6211.
17. Wang R, Li H, Ling C, Zhang X, Lu J, Luan W, Zhang J, Shi L: (2023).A novel phenotype of B cells associated with enhanced phagocytic capability and chemotactic function after ischemic stroke. *Neural regeneration research* 18(11):2413-2423.

18. Kitamura D, Roes J, Kühn R, Rajewsky K: (1991).A B cell-deficient mouse by targeted disruption of the membrane exon of the immunoglobulin mu chain gene. *Nature* 350(6317):423-426.
19. Allard B, Allard D, Buisseret L, Stagg J: (2020).The adenosine pathway in immuno-oncology. *Nature reviews Clinical oncology* 17(10):611-629.
20. Junger WG: (2011).Immune cell regulation by autocrine purinergic signalling. *Nat Rev Immunol* 11(3):201-212.
21. Antonioli L, Pacher P, Vizi ES, Haskó G: (2013).CD39 and CD73 in immunity and inflammation. *Trends in molecular medicine* 19(6):355-367.
22. Zhang B: (2010).CD73: a novel target for cancer immunotherapy. *Cancer research* 70(16):6407-6411.
23. Vijayan D, Young A, Teng MWL, Smyth MJ: (2017).Targeting immunosuppressive adenosine in cancer. *Nature reviews Cancer* 17(12):765.
24. Alcedo KP, Bowser JL, Snider NT: (2021).The elegant complexity of mammalian ecto-5'-nucleotidase (CD73). *Trends in cell biology* 31(10):829-842.
25. Depoil D, Fleire S, Treanor BL, Weber M, Harwood NE, Marchbank KL, Tybulewicz VL, Batista FD: (2008).CD19 is essential for B cell activation by promoting B cell receptor-antigen microcluster formation in response to membrane-bound ligand. *Nature immunology* 9(1):63-72.
26. Tedder TF: (2009).CD19: a promising B cell target for rheumatoid arthritis. *Nature reviews Rheumatology* 5(10):572-577.
27. Chung EY, Psathas JN, Yu D, Li Y, Weiss MJ, Thomas-Tikhonenko A: (2012).CD19 is a major B cell receptor-independent activator of MYC-driven B-lymphomagenesis. *The Journal of clinical investigation* 122(6):2257-2266.
28. Finck BN, Kelly DP: (2006).PGC-1 coactivators: inducible regulators of energy metabolism in health and disease. *The Journal of clinical investigation*

116(3):615-622.

29. Cuervo AM, Mann L, Bonten EJ, d'Azzo A, Dice JF: (2003).Cathepsin A regulates chaperone-mediated autophagy through cleavage of the lysosomal receptor. *The EMBO journal* 22(1):47-59.
30. Settembre C, Di Malta C, Polito VA, Garcia Arencibia M, Vetrini F, Erdin S, Erdin SU, Huynh T, Medina D, Colella P *et al*: (2011).TFEB links autophagy to lysosomal biogenesis. *Science (New York, NY)* 332(6036):1429-1433.
31. Roczniak-Ferguson A, Petit CS, Froehlich F, Qian S, Ky J, Angarola B, Walther TC, Ferguson SM: (2012).The transcription factor TFEB links mTORC1 signaling to transcriptional control of lysosome homeostasis. *Science signaling* 5(228):ra42.
32. Medina DL, Di Paola S, Peluso I, Armani A, De Stefani D, Venditti R, Montefusco S, Scotto-Rosato A, Prezioso C, Forrester A *et al*: (2015).Lysosomal calcium signalling regulates autophagy through calcineurin and TFEB. *Nature cell biology* 17(3):288-299.
33. Van Rooijen N, Sanders A: (1994).Liposome mediated depletion of macrophages: mechanism of action, preparation of liposomes and applications. *Journal of immunological methods* 174(1-2):83-93.
34. Moreno SG: (2018).Depleting Macrophages In Vivo with Clodronate-Liposomes. *Methods in molecular biology (Clifton, NJ)* 1784:259-262.
35. Xie H, Ye M, Feng R, Graf T: (2004).Stepwise reprogramming of B cells into macrophages. *Cell* 117(5):663-676.
36. Hodawadekar S, Yu D, Cozma D, Freedman B, Sunyer O, Atchison ML, Thomas-Tikhonenko A: (2007).B-Lymphoma cells with epigenetic silencing of Pax5 trans-differentiate into macrophages, but not other hematopoietic lineages. *Experimental cell research* 313(2):331-340.
37. Ma XL, Shen MN, Hu B, Wang BL, Yang WJ, Lv LH, Wang H, Zhou Y, Jin AL, Sun YF

- et al*: (2019).CD73 promotes hepatocellular carcinoma progression and metastasis via activating PI3K/AKT signaling by inducing Rap1-mediated membrane localization of P110 β and predicts poor prognosis. *Journal of hematology & oncology* 12(1):37.
38. Supernat A, Markiewicz A, Welnicka-Jaskiewicz M, Seroczynska B, Skokowski J, Sejda A, Szade J, Czapiewski P, Biernat W, Zaczek A: (2012).CD73 expression as a potential marker of good prognosis in breast carcinoma. *Applied immunohistochemistry & molecular morphology : AIMM* 20(2):103-107.
39. Beavis PA, Stagg J, Darcy PK, Smyth MJ: (2012).CD73: a potent suppressor of antitumor immune responses. *Trends in immunology* 33(5):231-237.
40. Eichin D, Laurila JP, Jalkanen S, Salmi M: (2015).CD73 Activity is Dispensable for the Polarization of M2 Macrophages. *PloS one* 10(8):e0134721.
41. Cappell KM, Kochenderfer JN: (2023).Long-term outcomes following CAR T cell therapy: what we know so far. *Nature reviews Clinical oncology* 20(6):359-371.
42. The Lancet O: (2021).CAR T-cell therapy for solid tumours. *The Lancet Oncology* 22(7):893.
43. Albelda SM: (2024).CAR T cell therapy for patients with solid tumours: key lessons to learn and unlearn. *Nature reviews Clinical oncology* 21(1):47-66.
44. Ashton TM, McKenna WG, Kunz-Schughart LA, Higgins GS: (2018).Oxidative Phosphorylation as an Emerging Target in Cancer Therapy. *Clinical cancer research : an official journal of the American Association for Cancer Research* 24(11):2482-2490.
45. Yap TA, Daver N, Mahendra M, Zhang J, Kamiya-Matsuoka C, Meric-Bernstam F, Kantarjian HM, Ravandi F, Collins ME, Francesco MED *et al*: (2023).Complex I inhibitor of oxidative phosphorylation in advanced solid tumors and acute myeloid leukemia: phase I trials. *Nature medicine* 29(1):115-126.

Figure legends

Figure 1. CD19⁺ macrophages are enriched in HCC (See also Figure S1).

(A) Visualized tSNE representation of the immune cell subtypes in human HCC tissues, including CD19⁺ TAMs, CD19⁻ TAMs, and B cells (left) and CD19 protein expression levels in these three clusters (right). Clusters are differently color-coded and annotated in the figure. Data were generated from CyTOF. (B) Representative immunofluorescence images of CD19⁺ TAMs in HCC tissue and adjacent normal tissue. Scale bar, 50 μ m. White arrows indicate CD19⁺ TAMs. (C) ImageStream showing CD19⁺ TAMs, CD19⁻ TAMs and B cells in HCC tissue at a single-cell level. $\times 40$ magnification. (D) Representative flow cytometry plots showing CD19 expression on TAMs in HCC tissue, adjacent normal tissue, and peripheral blood. (E) Multiplex IHC assay was used to identify CD19⁺ macrophages and B cells in formalin-fixed and paraffin-embedded HCC and adjacent normal tissues. Different colors indicate CD14 (yellow), CD68 (green), CD20 (orange), CD19 (red), and DAPI (blue). CD19⁺ macrophages are identified as CD14⁺CD68⁺CD20⁻CD19⁺, whereas B cells are identified as CD14⁻CD68⁻CD20⁺CD19⁺. Scale bars, 50 μ m. (F) Flow cytometry quantification of CD19⁺ TAMs proportion in different types of cancer. n (hepatocellular carcinoma) = 28, n (renal cancer) = 11, n (colorectal cancer) = 11, n (pancreatic ductal adenocarcinoma) = 13, n (breast cancer) = 12, n (gastric cancer) = 6. Data are presented as the mean \pm SEM. A paired two-tailed *t*-test was used in F. **P* < 0.05; ****P* < 0.001. *****P* < 0.0001.

Figure 2. CD19⁺ TAMs are associated with poor clinical outcome and immunotherapy response (See also Figure S2 and S3).

(A) Kaplan-Meier curves showing overall survival of HCC patients with a high (> median) or low (< median) ratio of CD19⁺ TAMs. Data are derived from immunofluorescence co-staining of human HCC tissue microarray. n = 149. (B) Kaplan-Meier curves show overall survival of HCC patients with a high or low TAMs ratio. Data are derived from immunofluorescence co-staining of human HCC tissue microarray. n = 149. (C) Correlation analysis between Ki-67⁺ cells and CD19⁺ TAMs density in HCC tissues. Data are derived from immunofluorescence co-staining of human HCC tissue microarray. n = 156. Scale bar, 50 μ m; 100 μ m. (D) Representative images of immunofluorescence co-staining of CD19 and CD68 in human HCC tissues from the responders and non-responders in a cohort of patients treated with anti-PD-1 antibody. Scale bar, 25 μ m. (E) Representative magnetic resonance images showing a responder and a non-responder before and after anti-PD-1 antibody treatment from (D) (top panel). Quantification of total TAMs and CD19⁺ TAMs density in all the responders and non-responders from (D) (bottom panel). Tumors are indicated by red circles or arrows. n = 17. PR, partial response; SD, stable disease; PD, progressive disease. (F) Splenic CD19⁺ and CD19⁻ macrophages were sorted and separately mixed with 5×10^5 Hepa1-6 cells at the ratio of 1:5, and then injected into the liver of mice. Images and weight of the tumors were showed at 14 days post-inoculation. n = 5 per group. Tumors are indicated by red circles. (G) Splenic CD19⁺ macrophages and CD19⁻ macrophages were separately mixed with 5×10^5 Hepa1-6 cells at the ratio of 1:5, and then inoculated subcutaneously (s.c.) into mice. When tumors reached 35 to 45 mm², mice were received intravenous injection (i.v.) with GFP⁺ control CAR-T cells or GFP⁺ anti-CD19 CAR-T cells (1×10^7 cells in 100 μ L of PBS). The harvested tumors were analyzed. n = 5 per group. (H) Splenic CD19⁺ macrophages and CD19⁻ macrophages were mixed with 5×10^5 Hepa1-6 cells at

the ratio of 1:5, and then inoculated subcutaneously in the left and right flanks of *muMT* (lacking mature B cells) or wild-type (WT) mice. When tumors reached 35 to 45 mm², mice were received intravenous injection with GFP⁺ control CAR-T cells or GFP⁺ anti-CD19 CAR-T cells (1×10^7 cells in 100 μ L of PBS). The harvested tumors were analyzed. n = 5 per group. Data are presented as the mean \pm SEM. Log-rank test (**A**, **B**), Pearson correlation test (**C**), unpaired two-tailed *t*-test (**E**, **F**, **H**), or paired two-tailed *t* test (**G**) were used for statistical analysis. **P* < 0.05; ***P* < 0.01; ****P* < 0.001, NS, not significant.

Figure 3. CD19⁺ TAMs display a distinct gene expression profile (See also Figure S4, S5 and S6).

(A) Schematic diagram of scRNA-seq experimental strategy for human HCC tissues. n = 3. (B) UMAP plot analysis showing HCC samples (top panel) and cell types in the samples (bottom) as indicated. (C) Heatmap showing the top 10 upregulated genes in CD19⁺ TAMs, CD19⁻ TAMs and B cells, respectively. (D) mRNA expression levels of classical M1 and M2 macrophage marker genes in CD19⁺ TAMs, compared with CD19⁻ TAMs. Bubble size and color represent the percentages and relative levels, respectively, of upregulated or downregulated genes as indicated at the x axis. (E) Bar chart showing the top-ranked biological pathways in CD19⁺ TAMs from KEGG enrichment analysis of the scRNA-seq data in (A). (F) t-SNE plots showing the expression levels of mitochondrion-related genes in CD19⁺ and CD19⁻ TAMs. (G) Violin plot analysis of mitochondrion-related gene expression levels in CD19⁺ and CD19⁻ TAMs. Data are mean ± SEM; An unpaired two-tailed *t*-test was used in (G). *****P* < 0.0001.

Figure 4. CD19⁺ TAMs are highly proliferative and immunosuppressive (See also Figure S7).

(A) Relative expression levels of mitochondrial metabolism-related genes in CD19⁺ TAMs and CD19⁻ TAMs in human HCC tissue. (B) Mitochondrial OCR measurement in CD19⁺ TAMs and CD19⁻ TAMs (5×10^5 cells per well). $n = 3$ independent experiments. (C) Flow cytometry histograms and quantification showing the phagocytic ability in CD19⁺ TAMs and CD19⁻ TAMs. $n = 3$ independent experiments. (D) Flow cytometry histograms and quantification showing the levels of PD-L1 and CD73 in CD19⁺ TAMs and CD19⁻ TAMs. $n = 5$ independent experiments. (E) Normalized 5'-nucleotidase (CD73) specific activity of CD19⁺ TAMs and CD19⁻ TAMs lysate. $n = 3$ independent experiments. (F) Co-culture of CD19⁺ TAMs or CD19⁻ TAMs with CD3⁺ T, CD4⁺ T, CD8⁺ T cells at different ratios for 72 h. $n = 3$ independent experiments. Data are mean \pm SEM.; Unpaired two-tailed *t*-test (B, E), paired two-tailed *t* test (C, D), or two-way ANOVA test (F) were used. * $P < 0.05$; ** $P < 0.01$; *** $P < 0.001$.

Figure 5. PAX5 is a master regulator for CD19⁺ macrophages (See also Figure S8).

(A) Tumor images and weights of orthotopic HCC model in *CD19^{ΔMφ}* (*CD19^{flox/flox};Lyz-Cre*) and littermate wildtype mice. n = 4 per group. (B) Representative flow cytometrical images and quantification showing the proportion of CD19⁺ TAMs in the tumors from (A). (C) *PAX5* mRNA expression level in CD19⁺ TAMs and CD19⁻ TAMs. (D) Flow cytometry histograms and quantification showing protein expression levels of PAX5 in CD19⁺ TAMs and CD19⁻ TAMs. n = 5 independent experiments. (E) Western blotting analysis of PAX5 expression level in CD19⁺ TAMs and CD19⁻ TAMs. Relative PAX5 blot intensities were shown. (F) Representative flow cytometry histograms showing the levels CD19, PD-L1, and CD73 in THP-1 cells with or without *PAX5* overexpression. (G) Western blotting analysis of CD19, PD-L1, and CD73 levels in THP-1 cells with or without *PAX5* overexpression. (H) Representative flow cytometry histograms showing the levels of CD19, PD-L1, and CD73 in iBMDM with or without *Pax5* overexpression. (I) Mitochondrial OCR measurement in THP-1 cells with or without *PAX5* overexpression (5×10^5 cells per well). n = 3 independent experiments. (J) Electron microscopy images and quantification showing mitochondrias in THP-1 cells with or without *PAX5* overexpression. scale bar: 0.5 μm or 0.2 μm. n = 5 independent experiments. (K) Representative flow cytometry histograms showing mitochondrial number (mitotracker), and mitochondrial ROS level (MitoSOX) in THP-1 cells with or without *PAX5* overexpression. (L) Tumor images and sizes of orthotopic HCC model in *Pax5^{ΔMφ}* (*Pax59^{flox/flox};Lyz-Cre*) and littermate control mice. n= 5 per group. Data are mean ± SEM; One-way ANOVA with Welch's correction (A), unpaired two-tailed *t*-test (B,I, J, L), or paired two-tailed *t* test (C, D) were used. **P* < 0.05; ***P* < 0.01; ****P* < 0.001; *****P* < 0.0001; NS, not significant.

Figure 6. PAX5 induces PD-L1 and CD73 in a post-transcriptional manner (See also Figure S9).

(A) mRNA expression levels of *CD73*, and *PD-L1* in THP-1 cells with or without *PAX5* overexpression. $n = 3$ independent experiments. (B) Venn diagram showing the number and percentage of share genes in Cut&Tag and RNA-seq analyses of THP-1 cells with *PAX5* overexpression. (C) WebGestalt analysis of enriched biological pathways in the shared genes in (B). (D) KFERQ finder V0.8 identified KFERQ-like motifs in PD-L1 and CD73. (E) Immunoprecipitation (IP) of HSC70 followed by immunoblotting (IB) analyses for HSC70, PD-L1, and CD73 in THP-1 cells with or without *PAX5* overexpression. (F) Representative immunofluorescence images and quantification of LysoTracker (red) in THP-1 cells with or without *PAX5* overexpression or not. Blue color indicates DAPI staining; scale bar, 25 μm . $n = 3$ independent experiments. (G) Representative flow cytometry histograms and quantification showing the lysosome quantity assessed by LysoSensor fluorescence expression in THP-1 cells with or without *PAX5* overexpression. $n = 3$ independent experiments. (H) Western blotting detection of PD-L1 and CD73 in THP-1 cells with *PAX5* overexpression, or treated with inhibitors of lysosomal proteolysis (NH_4Cl , 20mM and leupeptin, 100 μM), or inhibitor of proteasome (MG132, 5 μM). LC3B is used as a marker of lysosomal proteolysis inhibition. (I) Western blotting detection of cytosol and nuclear TFEB in THP-1 cells with or without *PAX5* overexpression. (J) Fluorescent probe indicates relative Ca^{2+} levels in mitochondria (Rhod2) and cytoplasm (Calbryte™ 630^{AM}) in THP-1 cells with or without *PAX5* overexpression. Fluorescence was measured every 30s for 30 minutes. $n = 3$ repeats. Data are mean \pm SEM; An unpaired two-tailed *t*-test (A, F, G), or two-way ANOVA test (J) were used. * $P < 0.05$; ** $P < 0.01$; *** $P < 0.001$; **** $P < 0.0001$; NS, not significant.

Figure 7. Blocking CD19⁺ TAMs enhances the efficacy of immune checkpoint blockade therapy (See also Figures S10, S11, and S12).

(A) Hepa1-6 cells (5×10^5) were mixed with iBMDMs (with or without *Pax5* overexpression) at a ratio of 1:1, and orthotopically injected into the livers of C57BL/6 mice. Tumor images and sizes were showed at 15 days post-inoculation. Tumor sites were indicated by red dotted line in liver. $n = 5$ per group. (B) Representative immunohistochemical images and quantification showing the infiltrated CD8⁺ T cells in the tumors of (A). Scale bar, 50 μm . (C) Schematic diagram illustrating targeted therapy of CD73 and PD-L1 for CD19⁺ TAMs in HCC. Tumors were established by inoculating 5×10^5 Hepa1-6 cells and iBMDMs with *Pax5* overexpression at the ratio of 1:1. Seven days post-inoculation, mice were treated as indicated. i.p, intraperitoneal injections; i.g, oral gavage. (D) Tumor images and sizes of (C). $n = 5$ per group. Tumor sites were indicated by red dotted line in the liver. (E) Tumor images and sizes in the in vivo experiment targeting OXPHOS and PD-L1 in CD19⁺ TAM. Tumors were established by inoculating 5×10^5 Hepa1-6 cells and iBMDMs with *Pax5* overexpression at the ratio of 1:1. Seven days post-inoculation, mice were treated as indicated. $n = 5$ per group. Tumor sites were indicated by red line in the liver. Data are mean \pm SEM; Unpaired two-tailed *t*-test (A, B), or unpaired one-way ANOVA with Welch's correction (D, E) were used. * $P < 0.05$; ** $P < 0.01$.

Inventory of Supplemental Information

- **Supplementary Methods**
- **Figures S1-S12 and Figure S legends.**
- **Supplementary Table S1-8.**

Supplementary Table S1. Patients' clinical information, related to **Figure 1**, **Figure 2**, and **Figure S2**.

Supplementary Table S2. Sequences of primer for transgenic mice genotyping, related to **Figure 5**. and **Figure S8**.

Supplementary Table S3. CyTOF antibody panel, related to **Figure 1** and **Figure S2**.

Supplementary Table S4. CD19 CAR sequences, related to **Figure 2** and **Figure S3**.

Supplementary Table S5. qRT-PCR Primer sequences, related to **Figure 4** and **Figure 6**.

Supplementary Table S6. Differentially expressed genes (DEGs) in CD19⁺ TAMs, CD19⁻TAMs, and B cells (data from sc-RNA seq), related to **Figure 3**.

Supplementary Table S7. Classical M1 and M2 macrophage marker genes expression in CD19⁺ TAMs and CD19⁻ TAMs, related to **Figure 3**.

Supplementary table 8. Key resources table.

Fig. 1

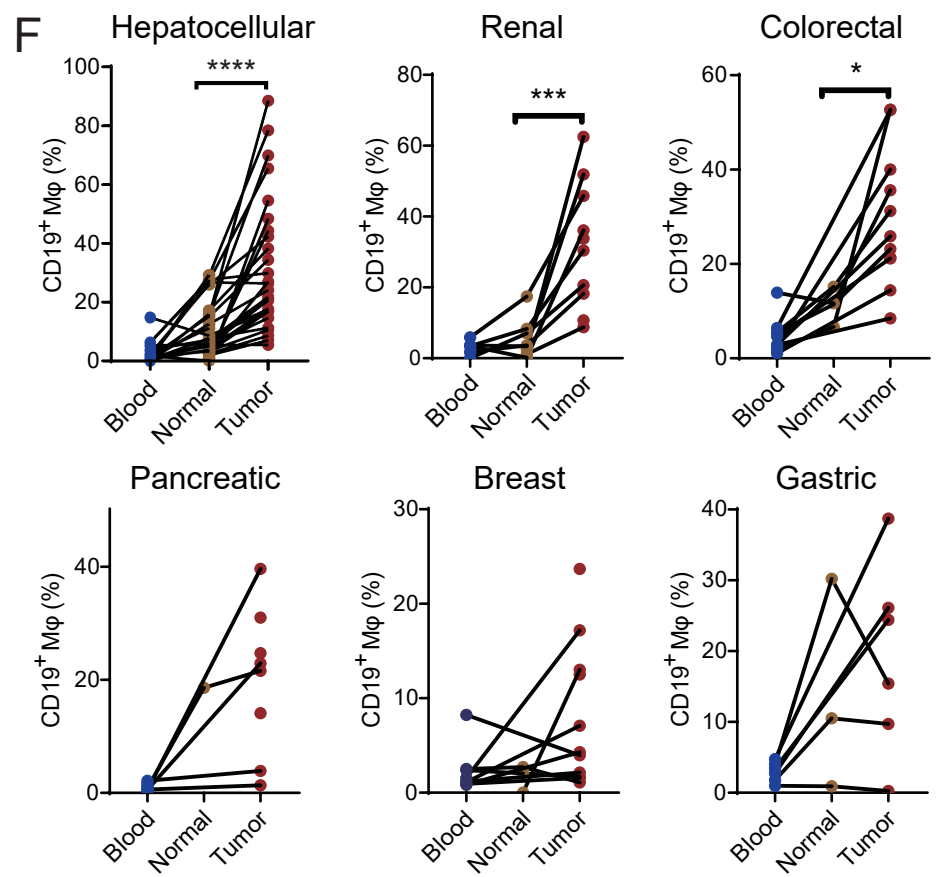
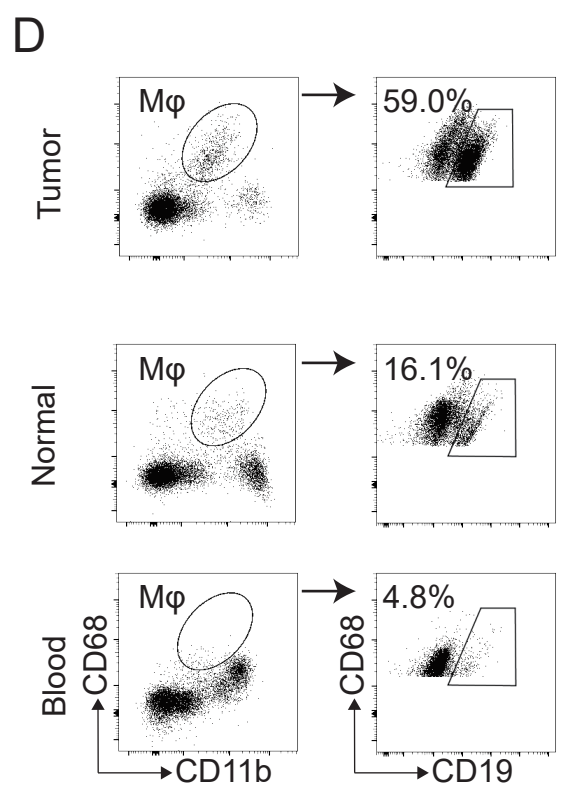
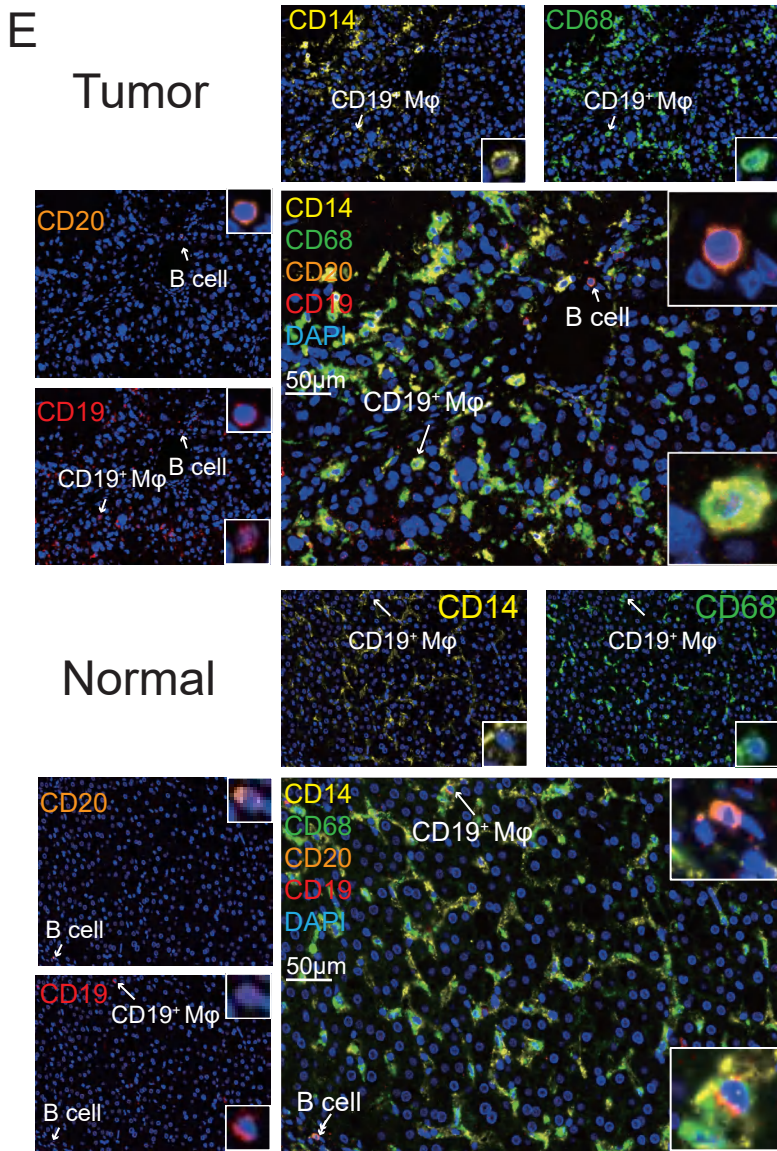
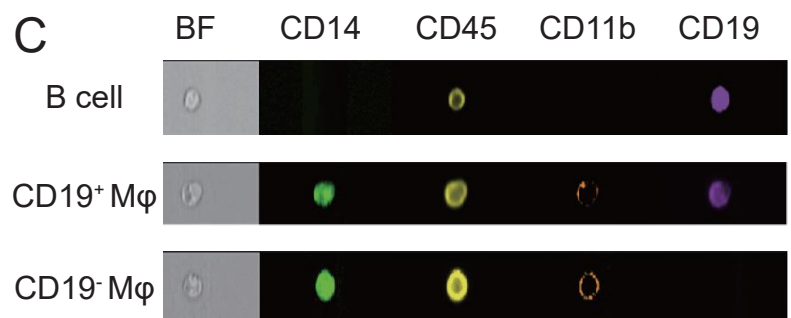
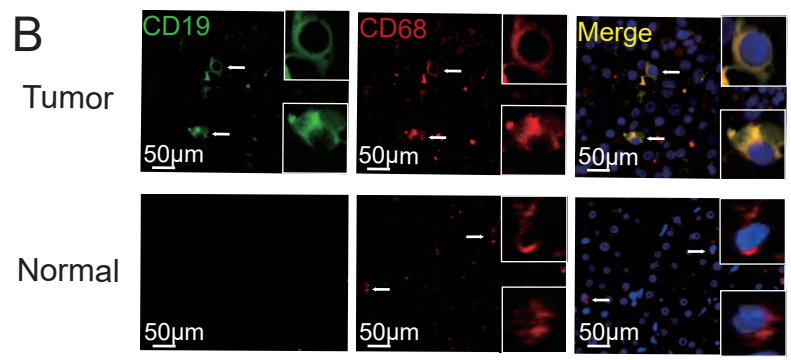
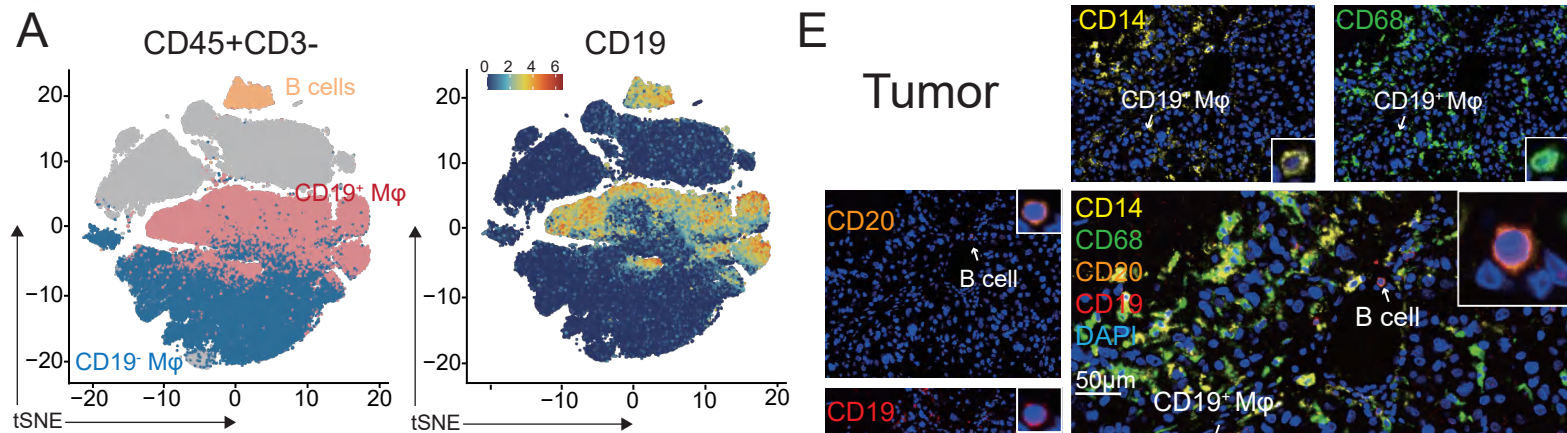


Fig. 2

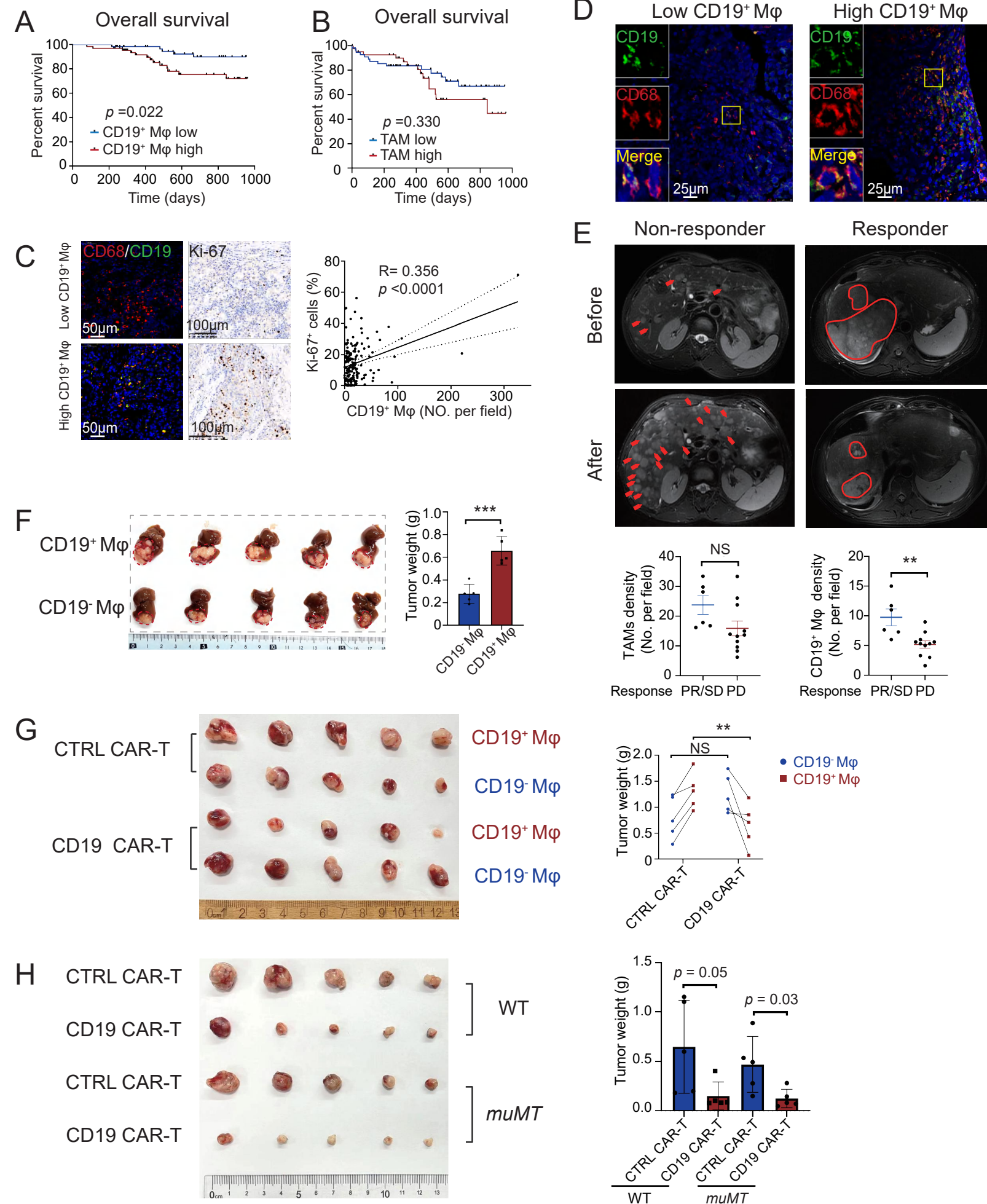


Fig.3

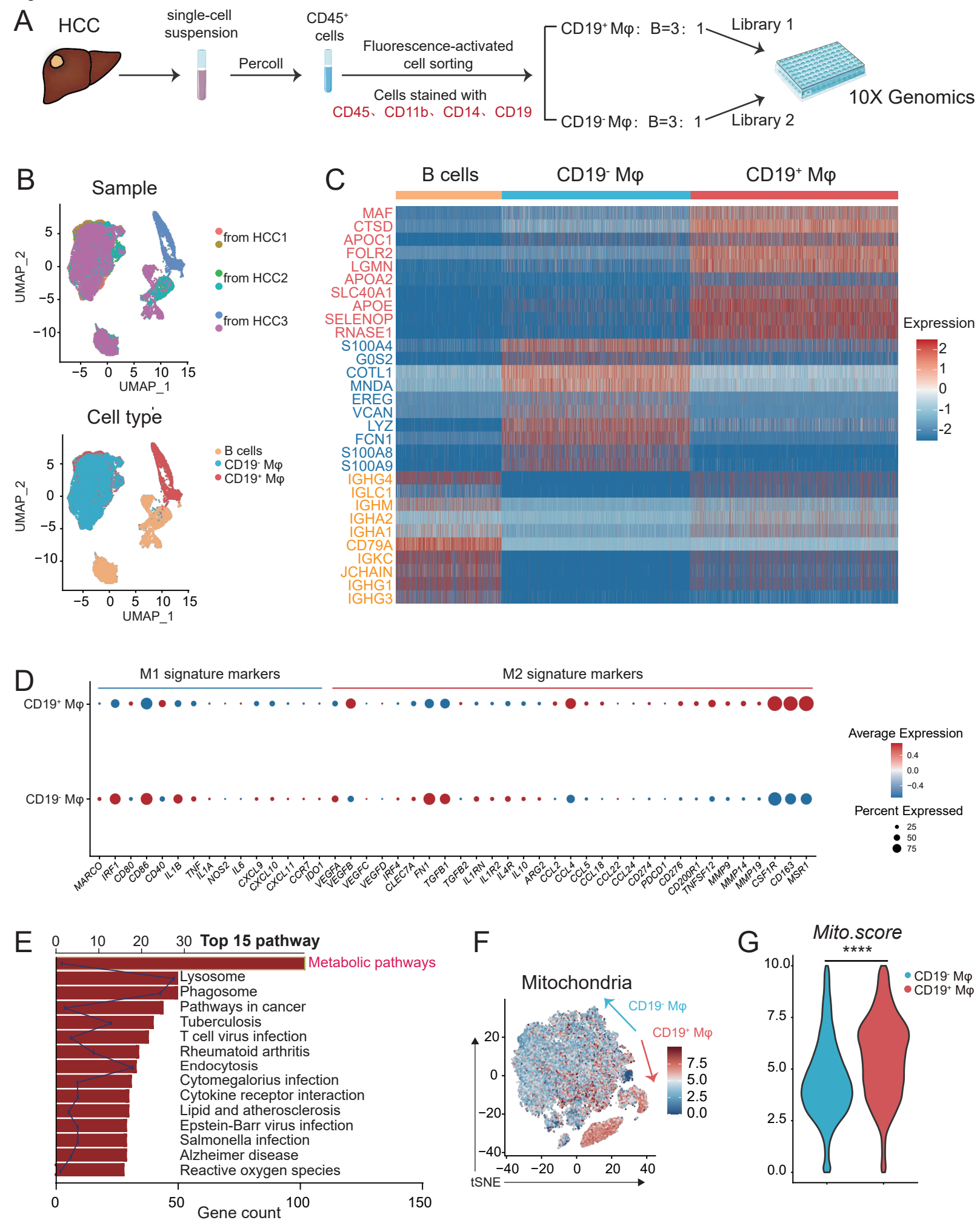


Fig. 4

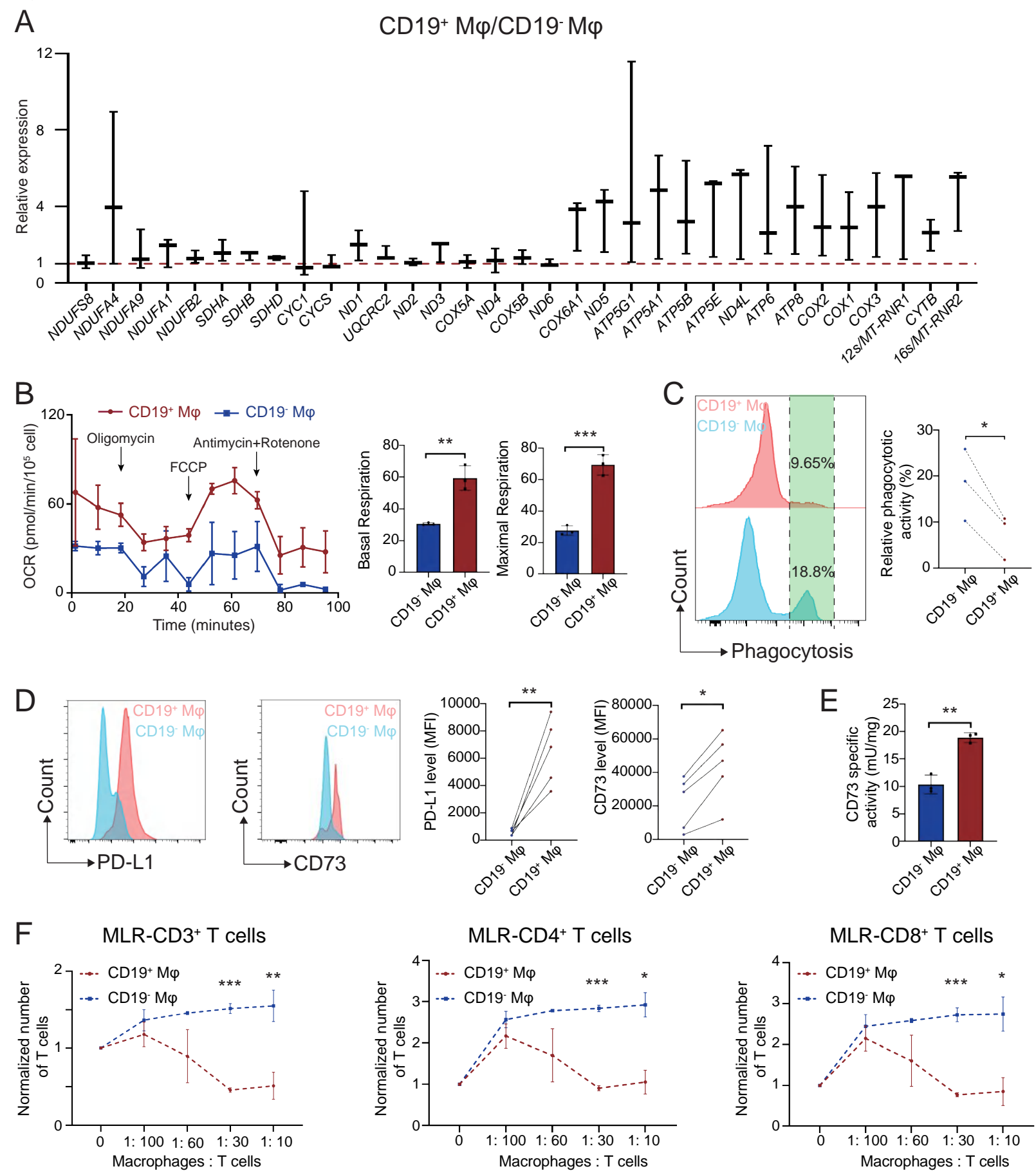


Fig. 5

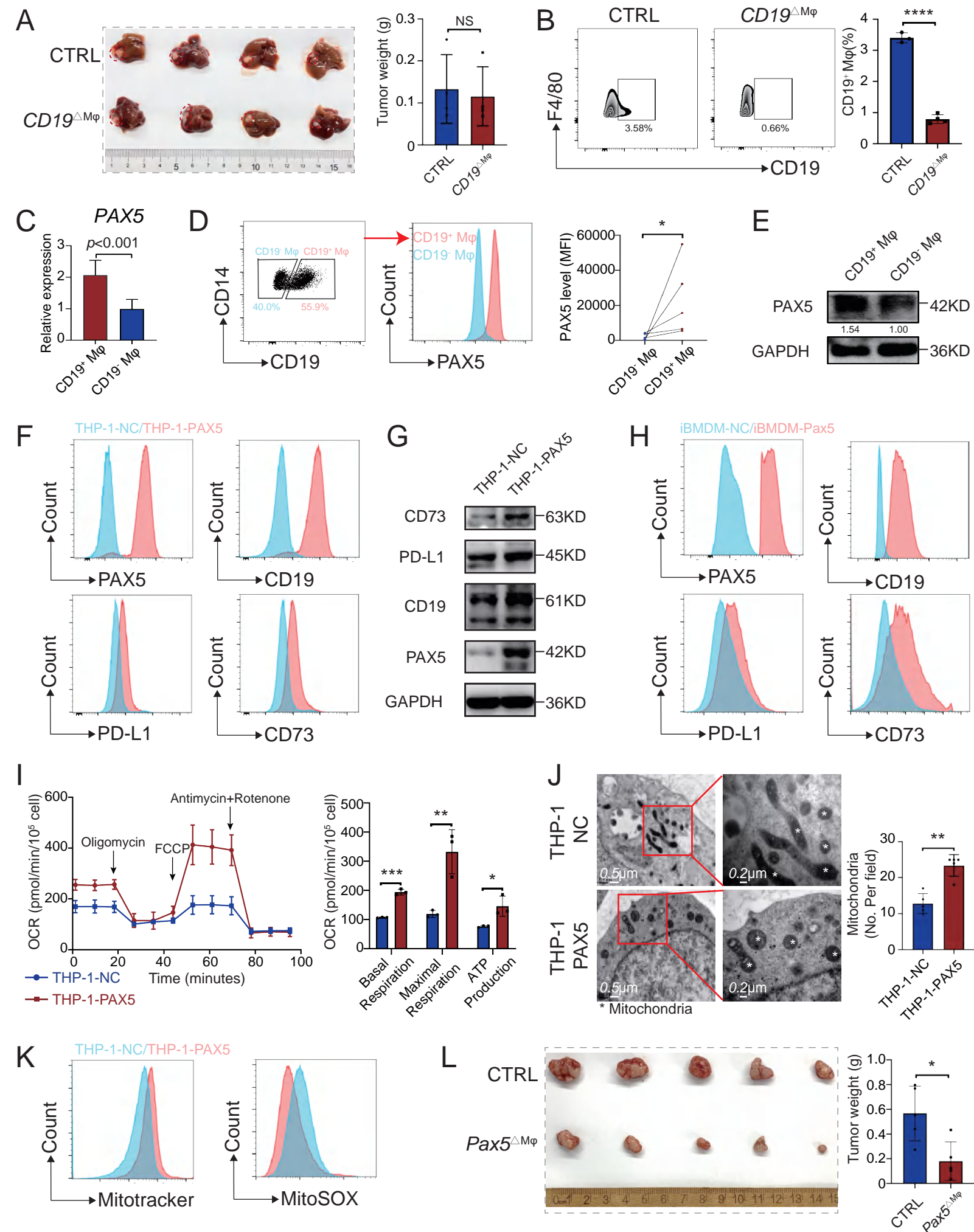
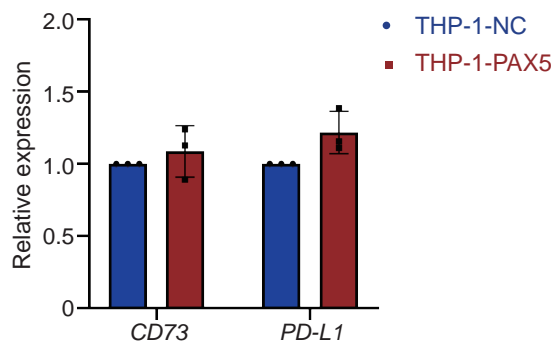
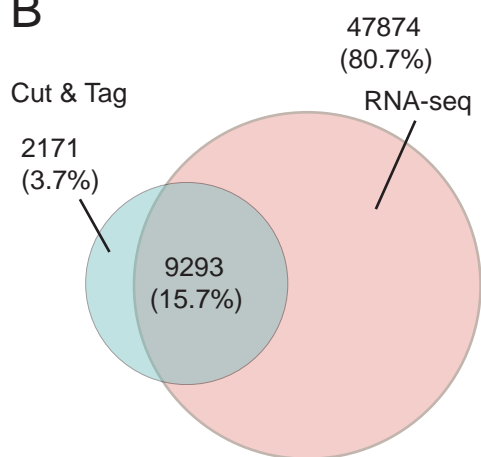


Fig. 6

A



B

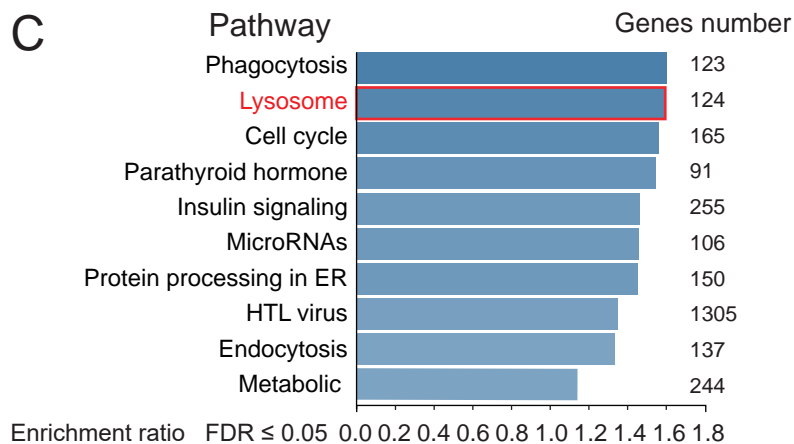


D

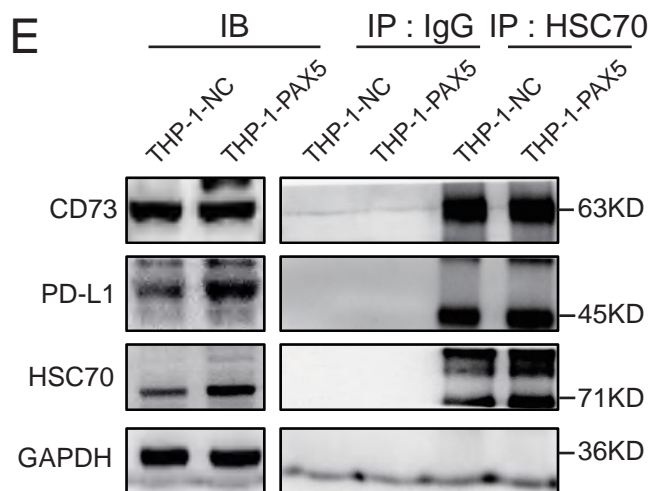
KFERQ Finder

protein name	PD-L1	CD73
UniProt ID	Q9NZQ7	P21589
motif	DLKVQ LLKDQ DVKLQ	FTKVQ VDKLN DRVVK
motif_type	canonical canonical canonical	phos.act. acetyl.act. acetyl.act.

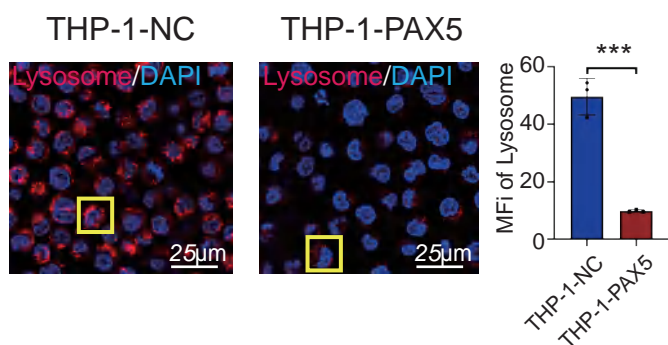
C



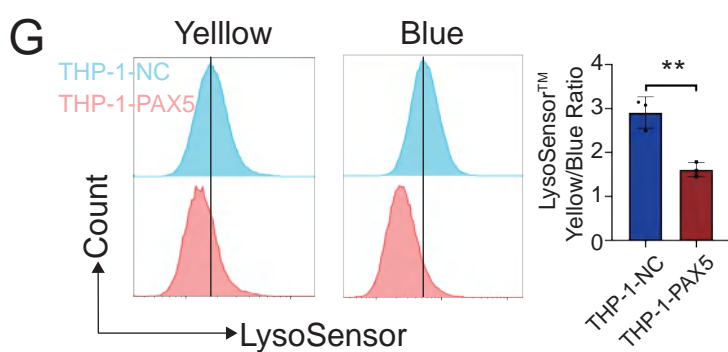
E



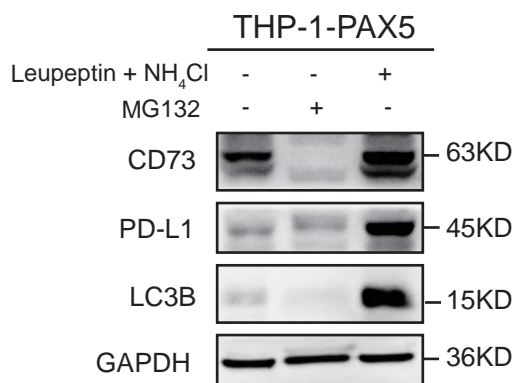
F



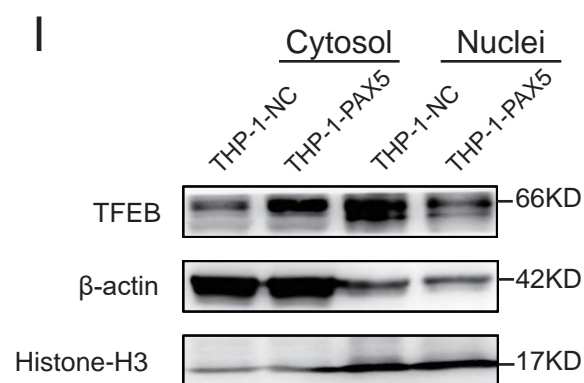
G



H



I



J

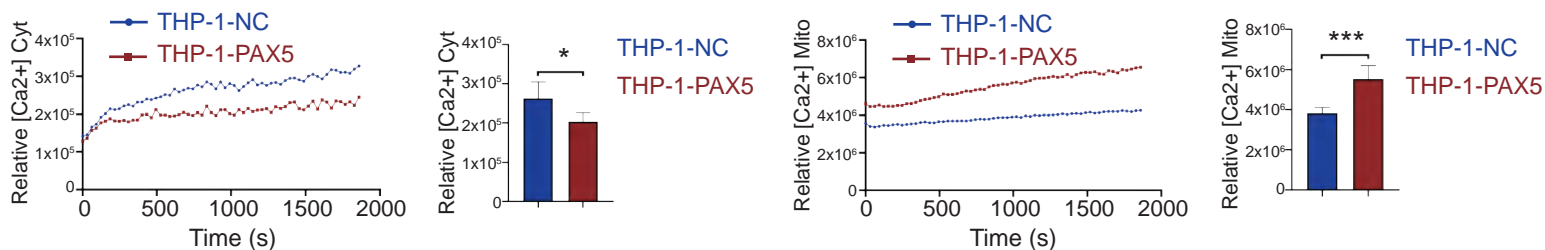
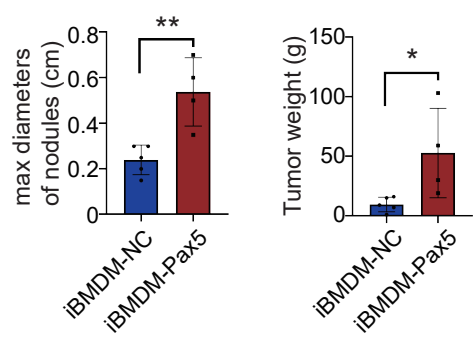
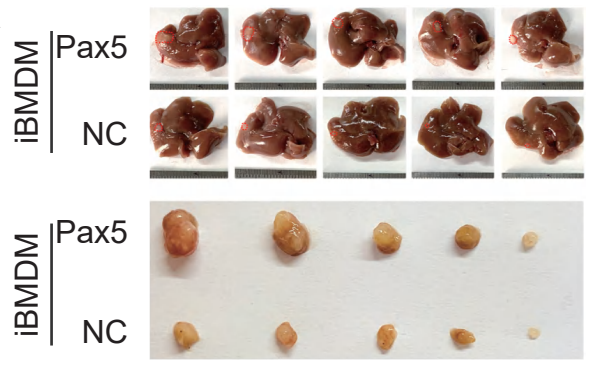
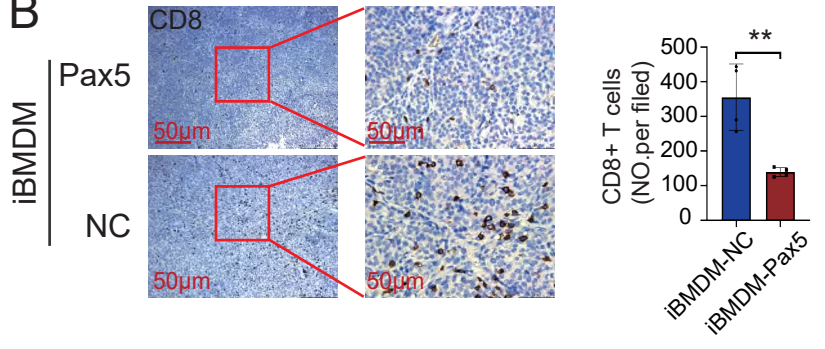


Fig. 7

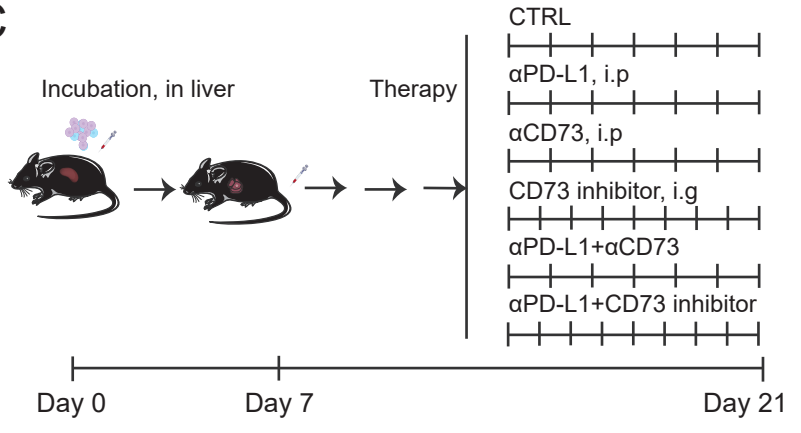
A



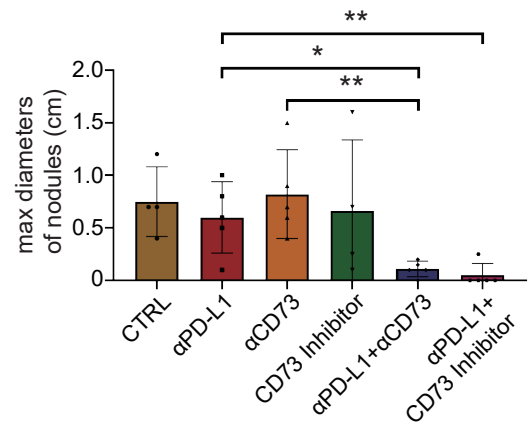
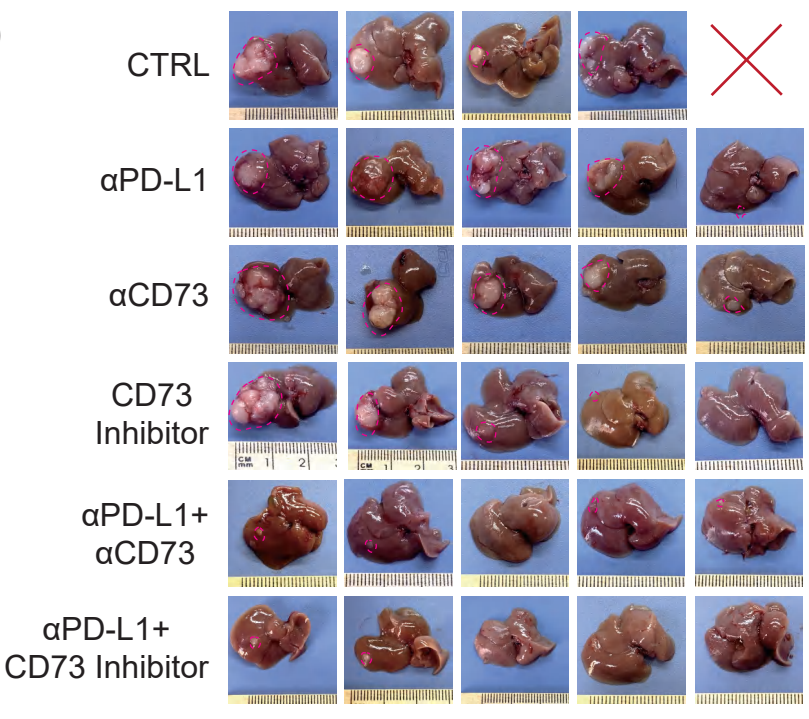
B



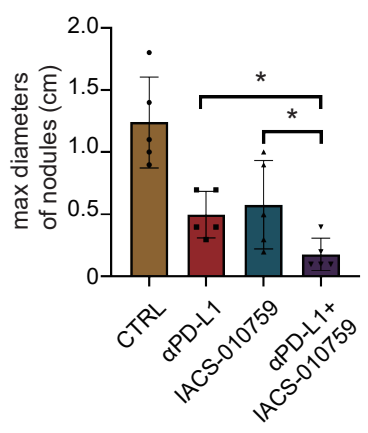
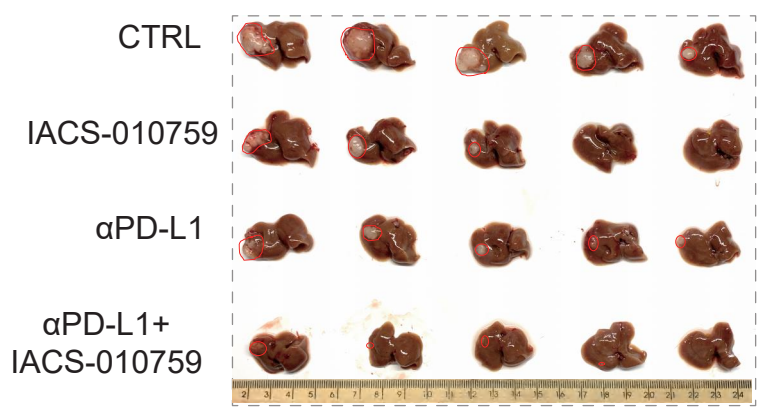
C



D



E



**Tumor-associated CD19⁺ macrophages induce immunosuppressive
microenvironment in hepatocellular carcinoma**

Inventory of Supplemental Information

- **Supplementary Methods**
- **Figures S1-S12 and Figure S legends.**
- **Supplementary Table S1-8.**

Supplementary Table S1. Patients' clinical information, related to **Figure 1**, **Figure 2**, and **Figure S2**.

Supplementary Table S2. Sequences of primer for transgenic mice genotyping, related to **Figure 5**. and **Figure S8**.

Supplementary Table S3. CyTOF antibody panel, related to **Figure 1** and **Figure S2**.

Supplementary Table S4. CD19 CAR sequences, related to **Figure 2** and **Figure S3**.

Supplementary Table S5. qRT-PCR Primer sequences, related to **Figure 4** and **Figure 6**.

Supplementary Table S6. Differentially expressed genes (DEGs) in CD19⁺ TAMs, CD19⁻TAMs, and B cells (data from sc-RNA seq), related to **Figure 3**.

Supplementary Table S7. Classical M1 and M2 macrophage marker genes expression in CD19⁺ TAMs and CD19⁻ TAMs, related to **Figure 3**.

Supplementary table 8. Key resources table.

Supplementary Methods

Human specimens

Tumors (without necrotic foci) and matched adjacent normal tissues, along with peripheral and portal vein blood, were obtained from patients who were diagnosed with HCC or other specific cancers by pathology and underwent curative surgical resection between 2019 and 2024. Normal tissues were resected from a macroscopically normal part that was at least 2 cm away from the tumor tissue. Specifically, for flow cytometry analyses in Figure 1F, tumor samples with paired non-tumor tissues and peripheral blood of 81 patients were collected, including 28 patients with HCC, 13 patients with pancreatic ductal adenocarcinoma, 12 patients with breast carcinoma, 6 patients with gastric carcinoma, 11 patients with renal carcinoma, 11 patients with colorectal carcinoma (**Supplementary Table 1**). The HCC tissue microarray contains 289 paired paraffin-embedded tumor and para-tumor tissue in our department between 2017 to 2021, by Wuha Servicebio Technology (Wuhan, China) (**Supplementary Table 1**). Clinical stages were classified according to the guidelines of the American Joint Committee on Cancer (AJCC), 8th edition. For survival analysis, patients of HCC received follow up every month for the first year and every 3–6 months thereafter. Survival time was calculated from the date of surgery to the date when death was confirmed. The prospective cohort of HCC patients with anti-PD-1 antibody treatment (**Figure 2E**) was a phase II clinical trial, patients were collected from our department and all diagnosed with HCC through pathology. Patients had not received any other treatment before enrollment (NCT03732547).

Sample processing and single cell harvest

Fresh tumor and adjacent normal tissues from surgical resections or mice were washed three times with PBS and cut into 1-3 mm³ pieces using sterile scalpel blades. The minced pieces were incubated with a digestion solution comprising DMEM, 2% fetal bovine serum (FBS; Gibco), type IV collagenase (1 mg/ml, Worthington, Lakewood, NJ, USA), DNase (15 µg/ml, Sigma-Aldrich, Saint Louis, MO, USA), and hyaluronidase (0.002 mg/ml, Sigma-Aldrich) at 37 °C for 1 hour

under constant shaking. The digested mixture was filtered through a 70 μm nylon mesh (Corning, Teterboro, NJ, USA) and washed with PBS supplemented with 2% FBS. Immune cells were enriched using a 36% Percoll (GE Healthcare, Logan, UT, USA) density gradient medium (Gibco). Peripheral and portal vein blood lymphocytes were isolated using standard Ficoll gradient centrifugation with Lymphocyte Separation Medium (Solarbio, Beijing, China), according to the manufacturer's instructions, to harvest immune cells. Mouse spleens were ground with the flat end of a syringe in RPMI (Gibco) to collect single-cell suspensions. Red blood cells were removed using ACK Lysing Buffer (Sigma-Aldrich). The dissociated cells were used for subsequent experiments.

Transgenic mouse genotyping

To determine the genotype of transgenic mice, genomic DNA was isolated from tail tissues¹ and subjected to PCR using the corresponding primers (**Supplementary Table 2**). The PCR conditions for the *Pax5-floxP* fragment were as follows: 95°C for 10 min, 40 cycles of 95°C for 10s, 60°C for 60s, followed by 95°C for 10s, 60°C for 60s, and 95°C for 15s. The *Cre^{Lyz}* fragment was amplified using PCR conditions of 94°C for 10 min, 38 cycles of 94°C for 10s, 68°C for 30s, 72°C for 35s, followed by 72°C for 10 min. The PCR conditions for the *CD19-floxP* fragment were 94°C for 3 min, 35 cycles of 94°C for 30s, 62°C for 35s, 72°C for 35s, followed by 72°C for 5 min. PCR products were analyzed by electrophoresis in a 1% agarose gel. The *Lyz-Cre (+)* and *Lyz-Cre (-)* loci were identified as 700 bp and 350 bp, respectively. The *Pax5* FloxP-flanking exon (MT) and null loci (WT) were confirmed by two paired primers: primer 4 identified at 219 bp and 152 bp, and primer 5 identified at 212 bp and 156 bp. The *CD19* FloxP-flanking exon (MT) and null loci (WT) were recognized at 208 bp and 140 bp, respectively. Mice certified as *Floxp+/+-Lyz-Cre (+)* phenotypes were considered *Pax5 ^{Δ M ϕ}* or *CD19 ^{Δ M ϕ}* mice for subsequent experiments.

Macrophage depletion and iBMDMs adoptive transfer

To deplete macrophages, C57BL/6 mice were injected intraperitoneally with a standard suspension of clodronate liposomes (10 ml/kg, Vrije Universiteit, Amsterdam, Netherlands) every other day for four times². Control animals received a

control liposomal solution. iBMDMs with or without *Pax5* overexpression (1×10^7 cells in 100 μ L PBS) were injected into the tail veins of C57BL/6 recipient mice 7 days after the in situ model formed.

Transfection of lentiviral vectors and siRNA

THP-1 cells and iBMDMs were seeded in 6-well plates at a density of 2×10^5 cells/ml and infected with lenti-*PAX5* or lenti-*TFEB*, lenti-*NC* (Jikai, Shanghai, China). The medium containing lentiviral vectors was removed and replaced with a maintenance medium after 16 hours. Infection efficiency was observed using a fluorescence microscope (Leica, Wetzlar, Germany) and verified by immunoblotting for PAX5 after 72 hours of culture. Stably transduced cells were purified using fluorescence activated cell sorting for further experiments. For siRNA transfection, 1.5×10^5 per well THP-1 cells were seeded in 24-well plates and transfected with human *TFEB* siRNA (Santa Cruz Biotechnology, Santa Cruz, CA) using lipofectamine RNAiMax (ThermoFisher Scientific, Waltham, MA) for 48 hours according to manufacturer's protocols³.

Mass cytometry staining

Mass cytometry was performed by PLTTech Inc. (Hangzhou, China). The protocol has been described previously. Cells isolated from human liver tissues were blocked and stained for 30 min with a surface antibody mix panel (**Supplementary Table 3**) developed in-house, followed by fixation overnight. Permeabilization buffer was applied, and the cells were incubated in an intracellular antibody mix. The immuno-labeled samples were finally "barcoded" with a unique barcode isotope combination for 30 min, re-suspended in deionized (DI) water, and run through a CyTOF instrument (Helios, FLUIDIGM, Shanghai, China).

Flow cytometry and fluorescence-activated cell sorting (FACS)

Single-cell suspensions were generated and cells were stained with specific antibodies (**Supplementary Table 8**) for flow cytometry or FACS according to the manufacturer's instructions. To exclude dead cells, the cells were firstly stained using Live/Dead Fixable Viability Stain 700 or Fixable Viability Stain 780 or 7-AAD (BD Bioscience) in PBS for 30 min at 4 °C. For surface marker staining, cells were blocked

with Fc block for 30 min and stained for 30 min at 4 °C with fluorescence-conjugated antibodies. For intracellular staining of transcription factors, we followed the manufacturer's protocol using a Transcription Factor Staining Buffer set (Thermo Fisher Scientific, Waltham, MA, USA). For staining of secreted cytokines, we fixed and permeabilized the cells using a Fixation/Permeabilization Solution Kit (BD Bioscience, Franklin Lakes, NJ, USA) after activating the cells with a Leukocyte Activation Cocktail with BD GolgiPlugIII (BD Bioscience) for 5 h. Flow cytometry acquisition was carried out on a BD LSRFortessa (BD Biosciences), and analyses were performed using FlowJo V.10.0 software (Tree Star, Ashland, OR, USA). Using specific antibodies (Supplementary Table 8), FACS was performed on a flow cell sorter (Beckman Coulter, Indianapolis, IN, USA) at 4 °C in 15 ml RNase and DNase free tubes (Simport, Saint-Mathieu-de-Beloeil, Canada) pre-filled with 5 ml of PBS with 5% FBS. The purity of the sorted populations was verified (98% pure) and cells were immediately used for further experiments.

CD19-CAR plasmid construction

The chimeric antigen receptor (CAR) was pieced together using murine CD8 α signal peptide, anti-mouse-CD19 scFv, the hinge and transmembrane domains of murine CD8 α , and the cytoplasmic domains of murine CD28 and CD3 ζ . Then CAR was cloned into the pMSCV-IRES-GFP II (pMIGII; Addgene, Watertown, MA, USA) retroviral plasmid backbone through the EcoRI and BamHI site. Nucleotide sequence and amino acid sequence of CD19 CAR were showed in

Supplementary Table 4.

Mouse primary T cell activation and isolation

Spleen cells from 8-week-old C57BL/6 mice were proceed into suspensions and activated using anti-CD3 ϵ (1 μ g/ml; Biolegend, Waltham, MA, USA) and anti-CD28 (0.5 μ g/ml; Biolegend) antibodies for 24 hours. Activated T cells were enriched by Percoll (GE Healthcare) gradient centrifugation. The residual B cells were removed by using biotin anti-mouse-CD19 antibodies and MojoSort™ Streptavidin Nanobeads (Biolegend). Briefly, the enriched activated

spleen cells were resuspended to 1×10^8 /ml in complete T cell medium with 10 μ g/ml biotin anti-mouse-CD19 antibodies (Biolegend) and incubated at 4 °C for 30 min, followed by centrifugation at 500g for 5 min and resuspension in complete T cell medium with 20 μ l/ml MojoSort™ Streptavidin Nanobeads. After another round of incubation at 4 °C for 30 min, the CD19⁺ B cells were labeled with Nanobeads and then removed by MojoSort™ Magnet (Biolegend).

Retrovirus production, transduction and anti-CD19-CAR-T/control CAR-T cell expansion

Retroviral supernatant was produced in the Plat-E cell line. Briefly, the pMIGII plasmids containing CD19-CAR were transfected into Plat-E cells using calcium phosphate-mediated transfection protocol³. The retroviral supernatant was harvested at 48 and 72 hours after transfection respectively, and concentrated by ultrafiltration using Amicon Ultra-15 (Millipore, Billerica, MA, USA). Retrovirus transduction of anti-CD19 CAR-T/control CAR-T cells was performed in 6-well plates with polybrene (1:100). Transduced cells were resuspended after 4 hours and transferred to 10-cm plates for expansion. Mouse primary T cells were maintained in incomplete T cell medium, which was RPMI 1640 Medium (Gibco) supplemented with 10% FBS (NEWZERUM, Christchurch, New Zealand), 100 IU/ml IL-2 (Novoprotein, Suzhou, China) and 0.05 mM 2-mercaptoethanol (Gibco).

Targeted anti-CD19 CAR-T cell therapy

CD19⁺/CD19⁻ macrophages were isolated from the spleens of mice (CD45⁺CD11b⁺F4/80⁺CD19⁺), and were mixed with Hepa1-6 cells to establish subcutaneous xenograft model at the left (CD19⁺ macrophages) or right (CD19⁻ macrophages) flank of C57BL/6 or muMT mice. Anti-CD19 CAR-T cells were prepared and expanded. Mice were randomly assigned into groups for T cell infusion (1×10^7 cells in 100 μ L PBS), and were sacrificed after 14 days. Harvested tumors were processed for subsequent experiments.

ImageStream analysis

Single-cell suspensions were blocked with Fc Block for 30 min on ice, then incubated with fluorescence-conjugated antibodies for 30 min in the dark on ice, including anti-CD45 (Apc-cy7, Biolegend), anti-CD11b (PE-cy7, Biolegend), anti-CD14 (FITC, Biolegend), anti-CD19 (BV421, Biolegend). After washed with PBS-2% FBS, cells were resuspended in 50 μ l PBS and analyzed with ImageStream II system (Amnis Corp, Seattle, WA, USA) for single cell image of CD19⁺ TAMs, CD19⁻ TAMs and B cells. A total of 1×10^5 cells were imaged at 40 \times magnification at low speed for receiving high-quality images with an acquisition time of 30 min per sample. Data were analyzed using IDEAS software version 6.2 (Amnis Corp). The optimal compensation matrix between individual fluorescence channels was established using the same cells, stained with each of the above-mentioned antibodies separately or without stained. The settings for acquisition and analyses were used for all samples.

Multiplex immunohistochemistry (mIHC) image acquisition

We used Opal™ 6-Plex Detection Kits (Akoya Biosciences, MA, USA) to perform mIHC according to the manufacturer's protocol. In brief, HCC and para-tumor tissues were processed to slides with 4- μ m thickness. Tissue slides were baked at 65 °C for 3 hours to remove paraffin, then washed with xylene for 10 min three times, rehydrated in graded ethanol (100%-95%-70%-50%-30%), subsequently washed three with deionized distilled H₂O. The epitope retrieval was performed in microwave heating using AR buffer, and cooled to room temperature at least 15 min, following by washing slides with Tris Buffered Saline with Tween® 20 (TBST) buffer. PAP pen was used to mark around the tissue on the slide. After incubating in blocking solution at room temperature for 15 min, slides were covered with primary antibody for 60 min, corresponding horseradish peroxidase-conjugated secondary antibody for 30 min, opal fluorophore for 10 min, following by 2 minutes TBST wash for three times individually. Repeated epitope retrieval, blocking, primary antibody, secondary antibody, and opal fluorophore for each of the primary antibodies. Finally, tissue slides were counterstained with spectral DAPI for 5 min and coverslipped with fluoromount medium (SouthernBiotech, Birmingham, USA). Acquisition of the

multi-color images was conducted using the Vectra Polaris System (Akoya Biosciences). Spectral unmixing was done in the inForm® software (Akoya Biosciences). The primary antibodies used for identifying CD19⁺ TAMs and B cells, along with their respective fluorescent dyes, were as follows: CD68 (Abcam, Cat. no. ab192874, 1:200)/opal 520, CD14 (CST, Cat. no. 75181S, 1:200)/opal 570, CD19 (Abcam, Cat. no. ab134114, 1:50)/opal 690, CD20 (CST, Cat. no. 48750S, 1:200)/opal 620.

Immunoblotting and immunoprecipitation (IP) analysis

For immunoprecipitation, cells were washed with ice-cold PBS and harvested in a suitable volume of cell lysis buffer (25 mmol/L HEPES pH 7.5, 150 mmol/L NaCl, 0.25% Triton X-100, 0.25% NP-40, 0.25% CHAPS, 10% glycerol, and 1 × protease inhibitor cocktail) on ice for 30 min, and then centrifuged at 13,000 × g for 15 min. The protein concentration was evaluated using the bicinchoninic acid (BCA) method (Pierce, Rockford, IL, USA). For immunoprecipitation analysis, the supernatants were incubated with the indicated primary antibodies or isotype control IgG overnight at 4 °C and then incubated with 40 µl protein A/G-coupled agarose (Santa Cruz) for another 2 h at 4 °C. After three washes with lysis buffer, the immunoprecipitations were boiled in 2 × loading buffer (Thermo Fisher Scientific) for western blotting analysis. In some experiments, the nuclear and cytoplasmic proteins were extracted and isolated using a Nuclear and Cytoplasmic Protein Extraction Kit (Beyotime, Shanghai, China).

Proteins (40 µg per lane for a 10-lane comb and 20 µg for a 15-lane comb) were separated by 10 or 12% sodium dodecyl sulfate–polyacrylamide gel electrophoresis (SDS-PAGE), according to the molecular weight of the target proteins, which were then transferred to polyvinylidene difluoride (PVDF) membranes (Millipore). Membranes were blocked with 10% skim milk (Bio-Rad Laboratories, Hercules, CA, USA) in tris-buffered saline/0.1% Tween 20 (TBST, Applygen, Beijing, China) for 1.5 hours and subsequently incubated overnight at 4 °C with specific primary antibodies (**Supplementary Table 8**) according to the manufacturer's recommendation. The next day, the membranes were washed three times with Tris-buffered saline with 0.1%

Tween® 20 Detergent (TBST) and further incubated with appropriate horseradish peroxidase (HRP)-labeled secondary antibodies for 2h at room temperature. Membranes were washed and the immunoreactive protein bands were visualized using a ChemiDoc XRS System (Bio-Rad). The photodensity of the immunoreactive protein bands was assessed using IPP software (Media Cybernetics, Rockville, MD, USA).

RNA extraction and quantitative real-Time reverse transcription polymerase chain reaction (qRT-PCR)

Tissue and cell RNA was extracted using the Trizol (Thermo Fisher Scientific) reagent⁴, and reverse transcribed into cDNA using a Prime Script^{III} RT reagent Kit (Takara Biotechnology Co., Dalian, China) following the manufacturer's protocol. Then, the cDNA was subjected to quantitative real-time PCR (qPCR), which was performed in duplicate for each sample on a Prism 7900HT instruments (Applied Biosystems) with TB green premix EX Taq^{III} reagent Kit (Takara Biotechnology Co.). The qPCR conditions were: 50 °C for 2 min, 95 °C for 10 min, followed by 40 cycles at 95 °C for 15 s, and 60 °C for 1 min. Amplification of specific transcripts was confirmed by melting curve profiles generated at the end of the PCR program. The expression levels of target genes were normalized to the expression of glyceraldehyde-3-phosphate dehydrogenase (GAPDH, internal control) or corresponding house-keeping protein, and calculated based on the comparative cycle threshold (CT) method ($2^{-\Delta\Delta Ct}$) (PMID: 11846609). All primers were synthesized by Sunya (Hangzhou, China) and listed in **Supplementary Table 5**.

Immunofluorescence and immunohistochemistry

For cell immunofluorescence, cultured cells were fixed using 4% paraformaldehyde (PFA) for 20 min, and then treated with 0.1% Triton X-100 (Sigma-Aldrich) for 20 min. For tissue immunofluorescence, formalin-fixed paraffin-embedded samples were cut into 5 µm thick serial sections and heat-induced antigen retrieval was performed by microwaving in sodium citrate (pH 6.0, 98 °C, 10 min). The slides or cells were blocked in 3% bovine serum albumin (BSA, Sigma-Aldrich) for 1 h at room temperature and then incubated with the indicated primary antibodies

(**Supplementary Table 8**) diluted according to the manufacturer's recommendation in a buffer (PBS plus 1% BSA, 0.3% Triton X-100 at pH 7.4) overnight at 4 °C. After washing three times with PBS, slides or cells were incubated with fluorescent-dye-conjugated secondary antibodies and DAPI (Life Technologies, Invitrogen, and Carlsbad, CA). Immunofluorescent microscopic images were obtained and viewed using a confocal microscope (TSC SP8, Leica).

For tissue immunohistochemistry, formalin-fixed paraffin-embedded samples were cut into 5 µm thick serial sections. After dewaxing, heat-induced antigen retrieval was performed by microwaving in sodium citrate (pH 6.0, 98 °C, 10 min). The slides were blocked in 3% BSA for 1 hat room temperature and then incubated with the indicated primary antibodies (**Supplementary Table 8**), diluted according to the manufacturer's recommendation, overnight at 4 °C. The next day, slides were washed three times with PBS and then incubated with the corresponding horseradish peroxidase-conjugated secondary antibodies. Subsequently, the slides were stained using a Histostain-Plus Kit (ZSGB-BIO, Beijing, China) and then further counterstained with hematoxylin. Images were obtained and viewed using an inverted microscope (DMI8, Leica).

Single-cell RNA sequencing (scRNA-seq) and analysis

Based on FACS analysis, we first sorted CD19+ TAMs, CD19- TAMs and B cells from HCC samples. Single cells were counted and assessed for viability with Trypan blue using a Countess II automated counter (Thermo Fisher Scientific), subsequently processed for 10x Genomics when viability of > 90%. Individually, CD19+ TAMs and CD19- TAMs were mixed with B cells at a ratio of 3:1, numbers of 1×10^4 cells for each sample were then encapsulated into emulsion droplets using Chromium Single Cell Controller (10 x Genomics, Pleasanton, CA, USA). Reverse transcription and library preparation was performed on aVeriti Thermal Cycler with 96-Deep Well Reaction Module (Thermo Fisher Scientific). Amplified cDNA was purified using SPRIselect beads (Beckman Coulter) and sheared to 200-300 bp. ScRNA-seq libraries were constructed using a Chromium Single Cell 3' Library and Gel Bead Kit v3.1 (10 x Genomics) according to the manufacturer's protocol. Qualification was

performed using a Qubit 3.0 Fluorometer (Thermo Fisher Scientific). Libraries were sequenced on an Illumina HiSeq PE150 system (Illumina). Raw reads were demultiplexed and mapped to the reference genome using the 10× Genomics Cell Ranger pipeline using default parameters. All downstream single-cell analysis were performed using Cell Ranger⁵, Seurat⁶, and Monocle⁷, unless mentioned specifically. In brief, for each gene and each cell barcode (filtered by Cell Ranger), unique molecule identifiers were counted to construct digital expression matrices. For secondary filtration in Seurat analysis, a gene with expression in more than three cells was considered as expressed and each cell was required to have at least 200 expressed genes, but below 5000. Cells with unique molecular identifier (UMI) numbers < 1000, or with > 10% mitochondrial-derived UMI counts were considered low-quality cells and removed.

Principal component analysis (PCA) was performed to reduce the dimensionality of scRNA-seq data through the prcomp package of the R software (Version 4.0.5)⁸. The number of principal components was determined from a scree plot. Uniform Manifold Approximation and Projection (UMAP) or t-distributed stochastic neighbor embedding (t-SNE) analysis was then performed on the principal components with default parameters to visualize cells in a two-dimensional space. Conventional markers were used to categorize cells into a known biological cell type, including macrophages: CD11b, CD14, CD68; B cells: CD45, CD19, CD79a. Combined FACS and PCA analyses, we recognized three clusters of all samples, the differentially expressed genes (DEGs, Supplementary Table 6) were calculated in the one cluster in comparison with other two clusters. The false-positive result was corrected by Benjamini–Hochberg adjustment (adjusted p value; adj.p value). The “adj. p value < 0.05” and “|logFC| > 0.25” were considered as statistically significant. Particularly, we used pheatmap R package (Version:1.0.12) to construct the DEGs, and ComplexHeatmap R package (Version: 2.13.1) to picture the M1 and M2 macrophage markers gene expression heatmap with the scaled gene expression value (**Supplementary Table 7**). Furthermore, DEGs were applied to pathway enrichment analysis through Web-based Gene Set Analysis Tool Kit

(WebGestalt), with KEGG gene sets (c2.cp.kegg.v7.5.1). To define mitochondria score in CD19⁺ TAMs and CD19⁻ TAMs, the mean expression of "MT-ND1", "MT-ND2", "MT-CO1", "MT-CO2", "MT-ATP8", "MT-ATP6", "MT-CO3", "MT-ND3", "MT-ND4L", "MT-ND4", "MT-ND5", "MT-ND6", "MT-CYB" were individually calculated through Percentage FeatureSet Function (Seurat package).

RNA-seq and gene expression analysis

RNA-seq was performed using the Illumina HiSeq XTEN platform (Illumina, San Diego, CA, USA) at Novogene Co. Ltd (Beijing, China). In brief, total RNA was extracted and its purity were checked using a NanoPhotometer® spectrophotometer (IMPLEN, Westlake Village, CA, USA). mRNA was isolated using Oligo Magnetic Beads and cut into small fragments for cDNA synthesis. Libraries were generated using the NEBNext UltraIII RNA Library Prep Kit for the Illumina system (New England Biolabs, Ipswich, MA, USA) following the manufacturer's instructions, and index codes were added to attribute sequences to each sample. After cluster generation, the library preparations were sequenced on an Illumina HiSeqXTEN platform. Raw data were processed through quality control steps to obtain clean data with high quality. After reads mapping, HTSeq was used to count the reads numbers mapped to each gene⁹. Then, the Fragments Per Kilobase of transcript per Million mapped reads (FPKM) value was calculated based on the gene length and reads count mapped to this gene. The list of ranked genes was based on the normalized enrichment score (NES).

Untargeted metabolomics by Liquid chromatography tandem mass spectrometry (LC-MS/MS)

Tumor tissues were individually grounded with liquid nitrogen and 100 µL of the homogenates was resuspend with precooled 100% methanol (-20 °C) followed by vortexing, and then incubated at -20 °C for 60 min, centrifuged at 14,000 g, 4°C for 15 min. The supernatants were then transferred to a fresh microcentrifuge tube and dried under vacuum in a centrifugal evaporator. The dried metabolite pellets were redissolved by 80% methanol and analyzed by LC-MS/MS. LC-MS/MS analysis was performed using a Vanquish UHPLC system (Thermo Fisher Scientific)

coupled with an Orbitrap Q Exactive HF-X mass spectrometer (Thermo Fisher Scientific) by Novogene Co. Ltd. Samples were injected onto an Accucore HILIC column (100×2.1 mm, 2.6 μm) using a 20-min linear gradient at a flow rate of 0.3 mL/min. Eluent A (95% ACN, 10 mM ammonium acetate, pH 9.0) and eluent B (50% ACN, 10 mM ammonium acetate, pH 9.0) were mixed for negative polarity mode. The solvent gradient was set as follows: 2% B, 1 min; 2-50% B, 16.5 min; 50-2% B, 2.5 min. Q-Exactive HF-X mass spectrometer was operated in positive/negative polarity mode with spray voltage of 3.2 kV, capillary temperature of 320°C, sheath gas flow rate of 35 arb and aux gas flow rate of 10 arb. Identification and quantification of metabolites were performed using the mzCloud database by the search engines: Compound Discoverer 3.0 (Thermo Fisher Scientific). Differentially expressed metabolites were screened based on VIP value from PLS-DA analysis and P value from t-test (VIP > 1 and P value < 0.05).

Metabolic extracellular flux analysis (Seahorse XF Cell Mito Stress Test)

Real-time bioenergetic profiles of CD19⁺ macrophages, CD19⁻ macrophages and THP-1 cells were obtained by measuring oxygen consumption rate (OCR) using a Seahorse XF24 Flux Analyzer (Seahorse Bioscience, Inc, North Billerica, MA, USA). Briefly, cells were seeded into a Cell-Tak (Corning) coated Seahorse 24-well plate (Agilent Technologies, Santa Clara, CA, USA) at a density of 5× 10⁵ cells per well and allowed to adhere for 2h. Cells were then washed and the medium was replaced with Seahorse XF RPMI Medium supplemented with 10 mM glucose, 2 mM glutamine, and 1 mM pyruvate (Agilent). Following incubation in an incubator without CO₂ at 37 °C for 60 min, the basal OCR and ECAR were recorded. A Mito Stress assay was performed by sequential addition of 1 μM oligomycin (Cayman, Ann Arbor, MI, USA), 1 μM carbonyl cyanide 4- (trifluoromethoxy) phenylhydrazone (FCCP, Cayman), and 0.5 μM rotenone/antimycin A (Cayman). Parameters such as ATP-linked OCR, maximal OCR, reserve capacity, and proton leak were calculated from Mito Stress assays of three independent experiments as previously described¹⁰.

Phagocytosis assay

Cells were seeded into 96-well plates and allowed to adhere for 2 h at a density of 5×10^5 , then media were removed and replaced with 200 $\mu\text{g/ml}$ pHrodo™ Red SE or pHrodo red Escherichia coli bioparticles (Thermo Fisher Scientific) labeled dead cells as per the manufacturer's instruction for 0.5, 1, 2, or 24 h before flow cytometry analyses.

In vitro co-culture experiments

T cells (CD3, CD4, CD8) generated by sorting ($\text{CD45}^+\text{CD3}^+/\text{CD45}^+\text{CD3}^+\text{CD4}^+/\text{CD45}^+\text{CD3}^+\text{CD8}^+$) were collected and co-cultured with target macrophages (1×10^4) for 72 h at different ratios in a 96-well plate. The plate was centrifuged at $500 \times g$ for 1 min at 4°C to initiate cell-cell contact and transferred to a 37°C water bath immediately. Thereafter, T cells were analyzed using flow cytometry.

Electronic microscopy

Cells were fixed with 2.5% glutaraldehyde in phosphate buffer (0.1 M, PH 7.0) for 4 h at 4°C . The samples were then washed three times for 15 min each in 0.1 M phosphate buffer (0.1 M, PH 7.0), postfixed with ice-cold 1% osmium tetroxide in 0.1 M phosphate buffer for 1 h, and washed three times for 15 min each in phosphate buffer (0.1 M, PH 7.0). Then, all samples were dehydrated for 15 min using a graded ethanol series (30%, 50%, 70%, 80%, 90%, 95% and 100%) and then transferred to absolute acetone for 20 min. Subsequently, the sample was placed in a mixture of 1:1 absolute acetone and the final Spurr resin, left at room temperature for 1 h, transferred to 1:3 absolute acetone and final resin mixture for 3 h, transferred to the final Spurr resin mixture, and left overnight. Next, the specimen was placed in Eppendorf container sprayed with resin and heated for more than 9 h at 70°C . The specimens were sliced on a Leica EM UC7 slicing machine and stained with uranyl acetate and basic lead citrate for 5-10 min before observation on a Hitachi Model H-7650 TEM (Tokyo, Japan).

Mitochondrion assessment

Cells (5×10^5) were incubated with 50 nM MitotrackerIII probe (Thermo Fisher Scientific) for 30 min at 37 °C in the indicated dilutions before washing away the probe. Then cells were used for flow cytometry analyses.

MitoSox assay

To determine mitochondrial ROS production, cells (5×10^5) were stained with 2 μ m of MitoSox (Thermo Fisher Scientific) for 10 min at the end of the experiment, followed by flow cytometry analyses.

Adenosine measurements

Cells (5×10^5) were seeded in 6-well plates in triplicate. When culture plates reached 80-90% confluence, the media were replaced with 2 ml of serum-free phenol red free RPMI (Gibco) with inhibitors (erythro-9-(2-hydroxy-3-nonyl) adenine (EHNA) 100 μ mol/L, Nitrobenzylthioinosine (NBMPR) 100 μ mol/L, Dipyridamole 40 μ mol/L). Conditioned media were collected and centrifuged at 10,000 \times g for 10 min at 4 °C to remove insoluble particles after 16 h incubation. Cells were harvested and cell counts were recorded for back calculations. For adenosine measurements, conditioned media were added in 96- well fluorescence black microtiter plates using an adenosine assay kit (Cell Biolabs, Inc. USA) according to a modified manufacturer's protocol. The plates were read using a SpectraMax i3x multi-Model Microplate Reader (Molecular Devices LLC.) for excitation in the 530-570 nm range and for emission in the 590–600 nm range.

CD73 activity assay

CD73 activity was measured using a 5' nucleotidase (CD73) activity assay kit (Abcam, Cambridge, MA, USA). Briefly, samples and a standard curve were prepared, and then added into 96 wells plates along with reaction mix at 37 °C for 20 min. Next, stop solution added, and then developer solution I and II. After incubating at room temperature for 20 min, the absorbance was recorded at 670 nm by a SpectraMax i3x multi-Model Microplate Reader (Molecular Devices, LLC., San Jose, CA, USA).

Cut & Tag (cleavage under targets and tagmentation) sequencing

THP-1 cells with or without *PAX5* overexpression were harvested and dead cells were removed. After incubation with the indicated primary *PAX5* antibodies (Abcam, Cambridge, MA, USA), the corresponding secondary antibody, and hyperactive PG/PA-Tn5 transposase, cells were fragmented and DNA was extracted for further library construction. Then, paired-end Illumina sequencing was performed on the barcoded libraries by OE BioLab Co. Ltd. (Shanghai, China), following the manufacturer's instructions.

Proliferation analysis

For short-term in vivo proliferation assay, mice were intraperitoneally injected with 50 mg/kg EdU (Beyotime), cells were obtained at 6 h post-injection and detected by using the Click-iTTM Plus EdU Flow Cytometry Assay Kits, then analyzed using flow cytometry.

Lysosome labeling

For LysoTracker staining, cells (5×10^5) were incubated with 50 nM of the LysoTrackerIII probe (Beyotime) diluted in serum-free RPMI for 5 min at 37 °C before washing away the probe. For LysoSensor staining, cells (5×10^5) were incubated with 1 μ M LysoTrackerIII probe (Invitrogen) diluted in serum-free RPMI before washing away the probe. The cells were then used for confocal imaging or flow cytometrical analyses.

Measurements of [Ca²⁺]

For the measurement of [Ca²⁺]_{cyt} and [Ca²⁺]_{mito}, 5×10^4 THP-1 cells with or without *Pax5* overexpressing were collected and incubated with Calbryte 630^{AM} (2 μ M, 37 °C, 60 min, ABD Bioquest, Sunnyvale, CA) or Rhod2 (2 μ M, 37 °C, 60 min, specific expression in mitochondria with a low concentration, ABD Bioquest) in HBSS (Cienry, supplemented with CaCl₂ and MgCl₂). Cells were detected at indicated excitation and emission wavelengths with Microplate Reader every 30s for 30 mins. In some experiments, cells were pretreated with IASC-010759 (100 nM) and ionomycin (1 μ M) for 20 min at 37 °C for next calcium fluorophore procedure.

Statistical analyses

Statistical tests were selected based on the appropriate assumptions with respect to data distribution and variance characteristics using Prism8 (Graphpad). Student's t-test or the Mann–Whitney test was used to compare the data from two groups. For comparison of data from more than two groups, one-way analysis of variance (ANOVA) was performed. Two-way ANOVA with the Bonferroni multiple comparison test was used for co-culture analysis. Categorical variables were compared using a chi-squared test or Fisher's exact test. Survival analysis was conducted using the Kaplan–Meier method and compared using the log-rank test. Details were indicated in Figure legends. The number of animals used per group is indicated in the figure legends as 'n'. The data are shown as mean \pm standard error of mean (SEM). NS, not significant, *P < 0.05; **P < 0.01; ***P < 0.001; ****P < 0.0001.

Reference

1. Truett GE, Heeger P, Mynatt RL, Truett AA, Walker JA, Warman ML: (2000).Preparation of PCR-quality mouse genomic DNA with hot sodium hydroxide and tris (HotSHOT). *BioTechniques* 29(1):52, 54.
2. Toda G, Yamauchi T, Kadowaki T, Ueki K: (2021).Preparation and culture of bone marrow-derived macrophages from mice for functional analysis. *STAR protocols* 2(1):100246.
3. Kumar P, NagarajanA, Uchil PD: (2019).Calcium Phosphate-Mediated Transfection of Adherent Cells or Cells Growing in Suspension: Variations on the Basic Method. *Cold Spring Harbor protocols* 2019(10).
4. Rio DC, Ares M, Jr., Hannon GJ, Nilsen TW: (2010).Purification of RNA using TRIzol (TRI reagent). *Cold Spring Harbor protocols* 2010(6):pdb.prot5439.
5. Zheng GX, Terry JM, Belgrader P, Ryvkin P, Bent ZW, Wilson R, Ziraldo SB, Wheeler TD, McDermott GP, Zhu J et al: (2017).Massively parallel digital transcriptional profiling of single cells. *Nature communications* 8:14049.
6. Butler A, Hoffman P, Smibert P, Papalexi E, Satija R: (2018).Integrating single-cell transcriptomic data across different conditions, technologies, and species. *Nature biotechnology* 36(5):411-420.
7. Qiu X, Mao Q, Tang Y, Wang L, Chawla R, Pliner HA, Trapnell C: (2017).Reversed graph embedding resolves complex single-cell trajectories. *Nature methods* 14(10):979-982.
8. Dessau RB, Pipper CB: (2008).["R"--project for statistical computing]. *Ugeskrift for laeger* 170(5):328-330.
9. Putri GH, Anders S, Pyl PT, Pimanda JE, Zanini F: (2022).Analysing high-throughput sequencing data in Python with HTSeq 2.0. *Bioinformatics (Oxford, England)* 38(10):2943-2945.
10. Leung DTH, Chu S: (2018).Measurement of Oxidative Stress: Mitochondrial Function Using the Seahorse System. *Methods in molecular biology (Clifton, NJ)* 1710:285- 293.

Fig. S1

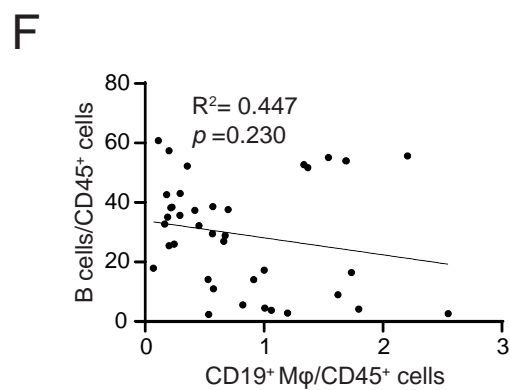
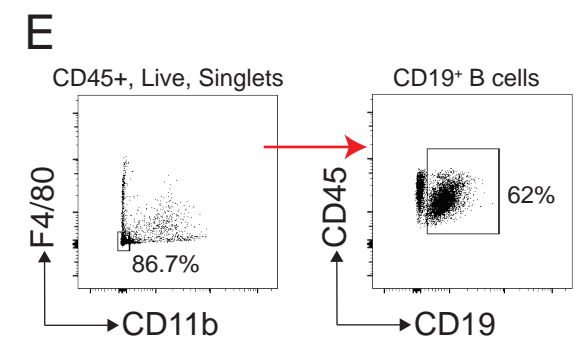
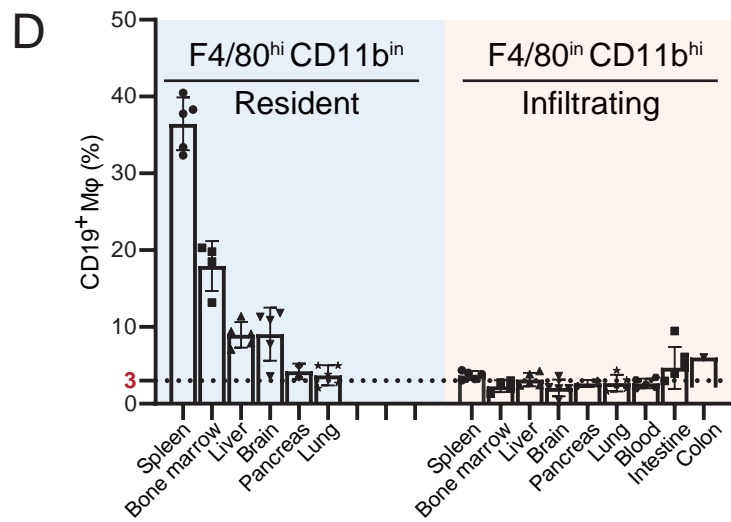
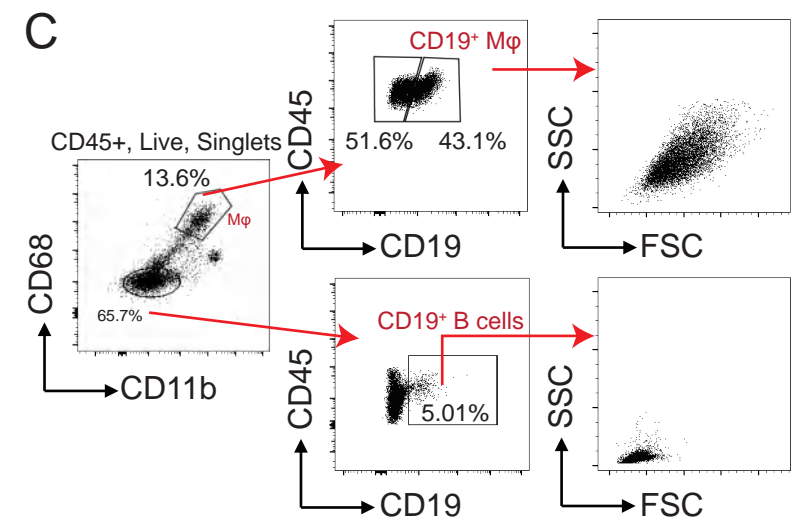
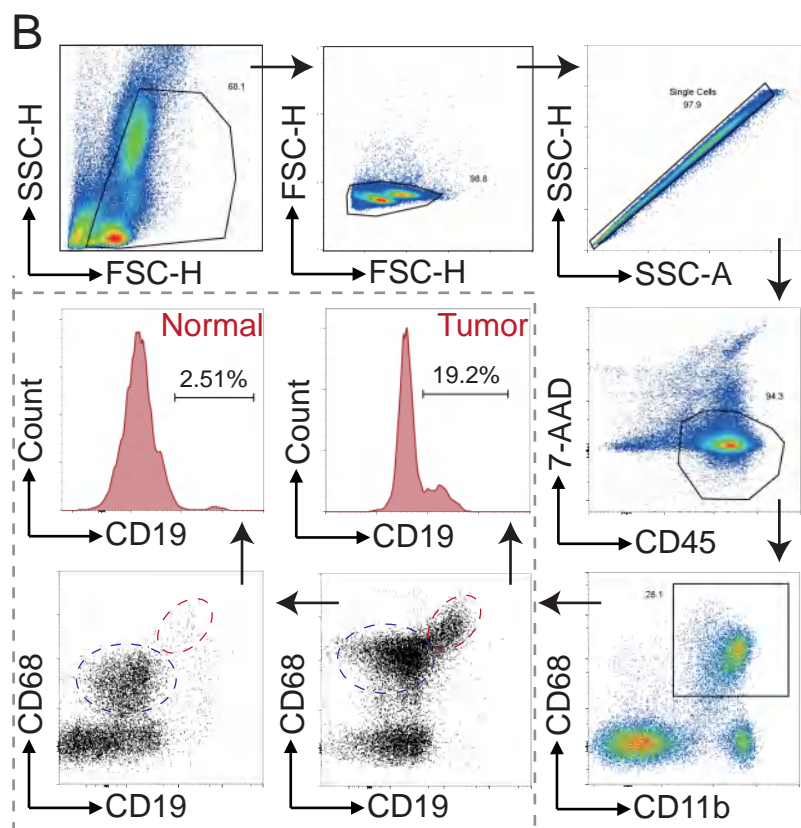
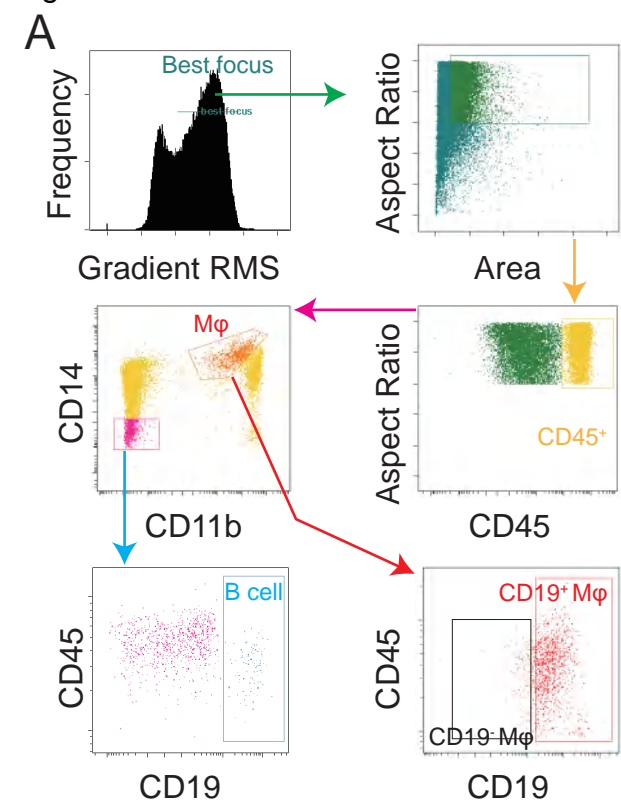


Fig. S1. CD19⁺ macrophages are enriched in HCC (Related to Fig. 1).

(A) ImageStream gating strategy for identifying CD19⁺ TAMs, CD19⁻ TAMs, and B cells in HCC. CD19⁺ TAMs are defined as CD45⁺CD11b⁺CD14⁺CD19⁺, CD19⁻ TAMs are defined as CD45⁺CD11b⁺CD14⁺CD19⁻, and B cells are defined as CD45⁺CD11b⁻CD14⁻CD19⁺. **(B)** Flow cytometry gating strategy for identifying CD19⁺ TAMs and CD19⁻ TAMs in HCC. CD19⁺ TAMs are defined as CD45⁺CD11b⁺CD68⁺CD19⁺, and CD19⁻ TAMs are defined as CD45⁺CD11b⁺CD68⁺CD19⁻. **(C)** Back-gating flow cytometry plots of CD19⁺ TAMs and B cells to FSC and SSC values. **(D)** Quantification of CD19⁺ macrophages proportion in normal tissues of C57 BL/6 mice. Resident macrophages are identified as F4/80^{high}CD11b^{intermediate}, while infiltrating macrophages are identified as F4/80^{intermediate}CD11b^{high}. Data were detected by flow cytometry. n = 5. **(E)** Flow cytometry gating strategy for identifying B cells in mice **(F)** Correlation analysis between CD19⁺ macrophages and B cells in mice tissues. n = 17. Data are presented as the mean ± SEM. Pearson correlation test was used in **(F)**.

Fig. S2

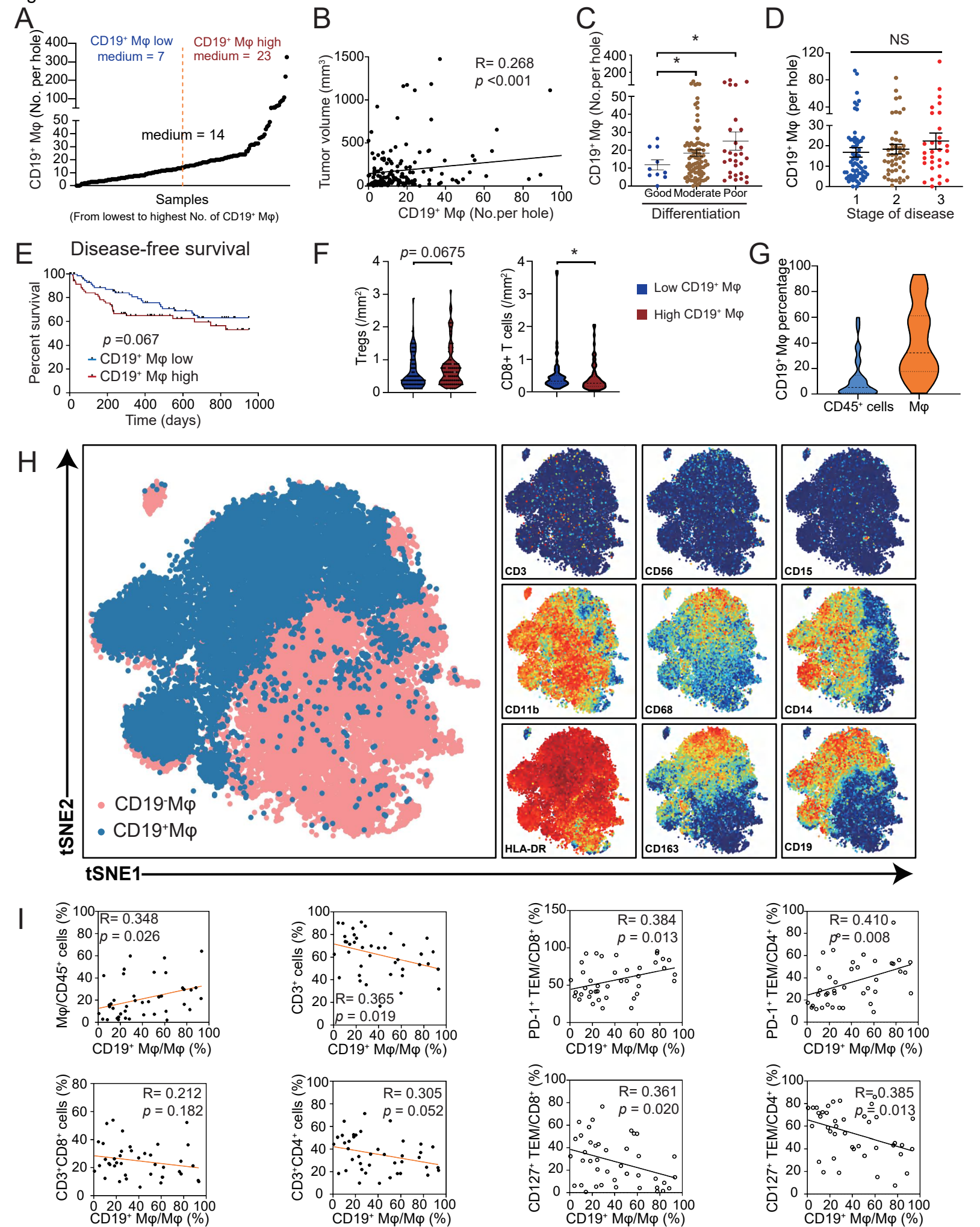


Fig. S2. CD19⁺ TAMs are associated with poor clinical outcome and immunotherapy response (Related to Fig. 2).

(A) Densities of CD19⁺ TAMs in HCC tissues included in an HCC tissue microarray. n = 156. (B) Correlation analysis between tumor volume and the density of CD19⁺ TAMs in the tumor. Data are derived from immunofluorescence analysis of the HCC tissue microarray. n = 156. (C) Tumor differentiation status is correlated with the density of CD19⁺ TAMs in the tumor. Data are derived from immunofluorescence of HCC tissue microarray. n = 145. (D) Disease stage of HCC is not correlated with the density of CD19⁺ TAMs in the tumor. Data are derived from immunofluorescence analysis of the HCC tissue microarray. n = 145. (E) Kaplan-Meier curves showing disease-free survival (DFS) of HCC patients with a high (> median) or low (< median) ratio of CD19⁺ TAMs. Data are derived from immunofluorescence analysis of the HCC tissue microarray. n = 149. (F) Violin plot showing the proportions of Tregs and CD8⁺ T cells in HCC patients with a high (> median) or low (< median) ratio of CD19⁺ TAMs. Data are derived from the human HCC tissue microarray. n = 156. (G) Violin plot showing the proportion of CD19⁺ TAMs in CD45⁺ cells or total macrophages in human HCC samples. Data are derived from CyTOF. n = 41. (H) Visualized *t*-SNE map showing CD19⁺ TAMs, CD19⁻ TAMs, and cell subpopulations with specific markers. Data are derived from CyTOF. (I) Correlation between percentage of CD19⁺ TAMs and percentage of other types of immune cells as indicated, including macrophages, $\gamma\delta$ T cells, NK cells, T cells, CD8⁺ T cells, CD4⁺ T cells, PD-1⁺ TEMs and CD127⁺ TEMs. Data are derived from CyTOF. n = 41. Data are presented as the mean \pm SEM. Pearson correlation test (B, I), unpaired one-way ANOVA with Welch's correction (C, D), log-rank test (E), or unpaired two-tailed *t*-test (F) was used. **P* < 0.05; NS, not significant.

Fig. S3

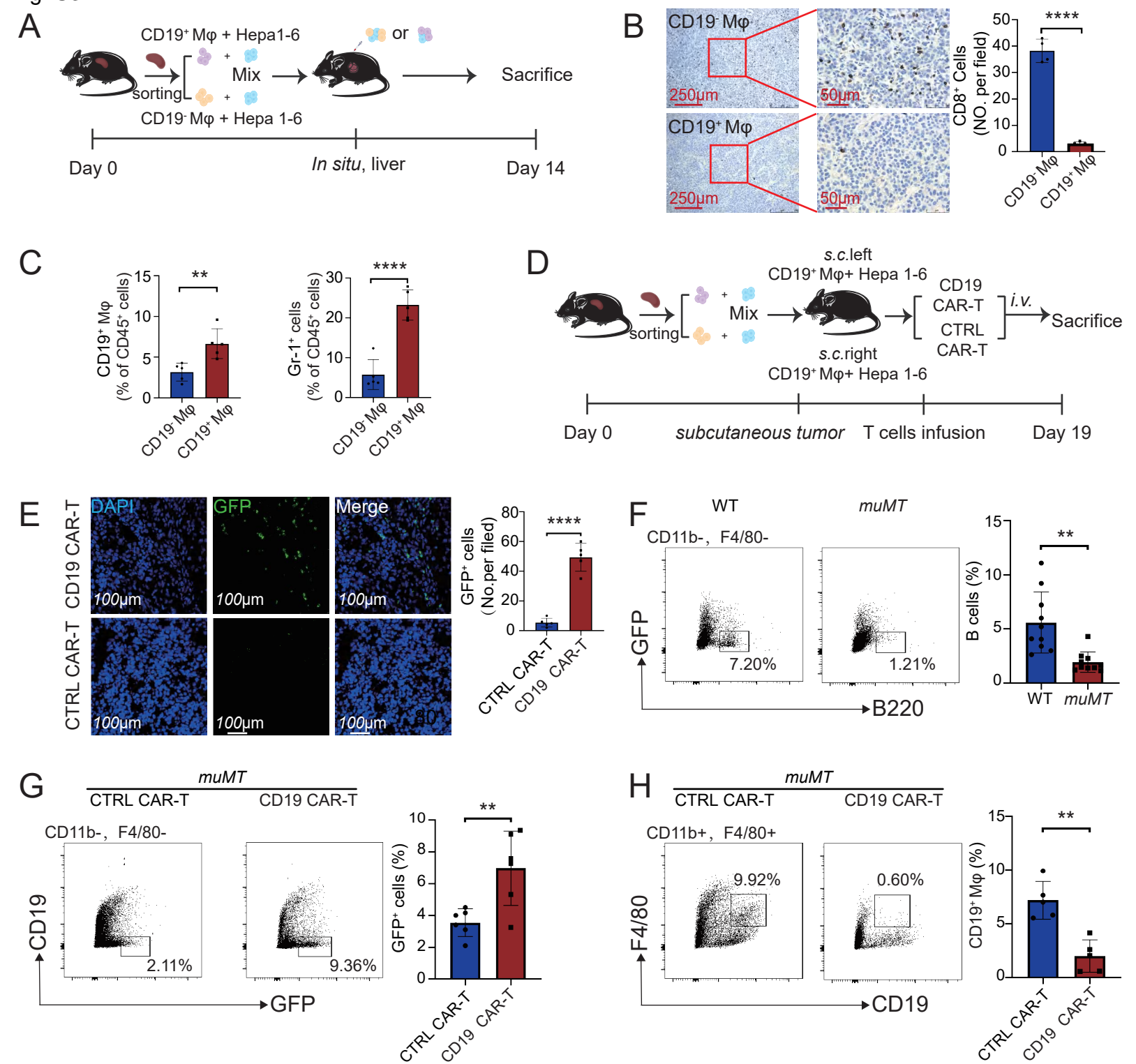


Fig. S3. CD19⁺ TAMs promote HCC tumor progression in mice (Related to Fig. 2).

(A) Schematic illustration of in vivo experiment for testing the role of CD19⁺

macrophages on tumor progression. Splenic CD19⁺ and CD19⁻ macrophages were sorted and separately mixed with 5×10^5 Hepa1-6 cells at a ratio of 1:5, and then injected

into the liver of mice. **(B)** Flow cytometrical quantification of CD19⁺ macrophages and

Gr-1⁺ cells in tumors in **Fig. 2F**. n = 5 per group. **(C)** Representative

immunohistochemical images and quantification of CD8⁺ T cells in **Fig. 2F**. **(D)**

Schematic illustration of anti-CD19 CAR-T cell targeted therapy on HCC. Splenic CD19⁺ and CD19⁻ macrophages were sorted and separately mixed with 5×10^5 Hepa1-6 cells at

a ratio of 1:5, and then inoculated subcutaneously (*s.c.*) into the left and right flanks of

mice. When tumors reached 35 to 45 mm², mice received intravenous injection (*i.v.*) with

GFP⁺ control CAR-T cells or GFP⁺ anti-CD19 CAR-T cells (1×10^7 cells in 100 μ L of

PBS). **(E)** Representative immunofluorescence images and quantification of control

GFP⁺ CAR-T cells or GFP⁺ anti-CD19 CAR-T infiltration in tumors (**Fig. 2G**). n = 5 per

group. **(F)** Representative flow cytometry plots showing B cells quantification in *muMT*

and wild-type mice. n = 10 per group. **(G)** Representative flow cytometry plots and

quantification of control GFP⁺ CAR-T cells and GFP⁺ anti-CD19 CAR-T infiltration in

tumors from *muMT* mice. n = 5 per group. **(H)** Representative flow cytometry plots and

quantification of the after percentage of CD19⁺ TAMs in *muMT* mice with control CAR-T

cells or anti-CD19 CAR-T treatment. n = 5 per group. Data are presented as the

mean \pm SEM. An unpaired two-tailed *t*-test (**B, C, E, F, G, H**) was used. ***P* < 0.01;

****P* < 0.0001.

Fig. S4

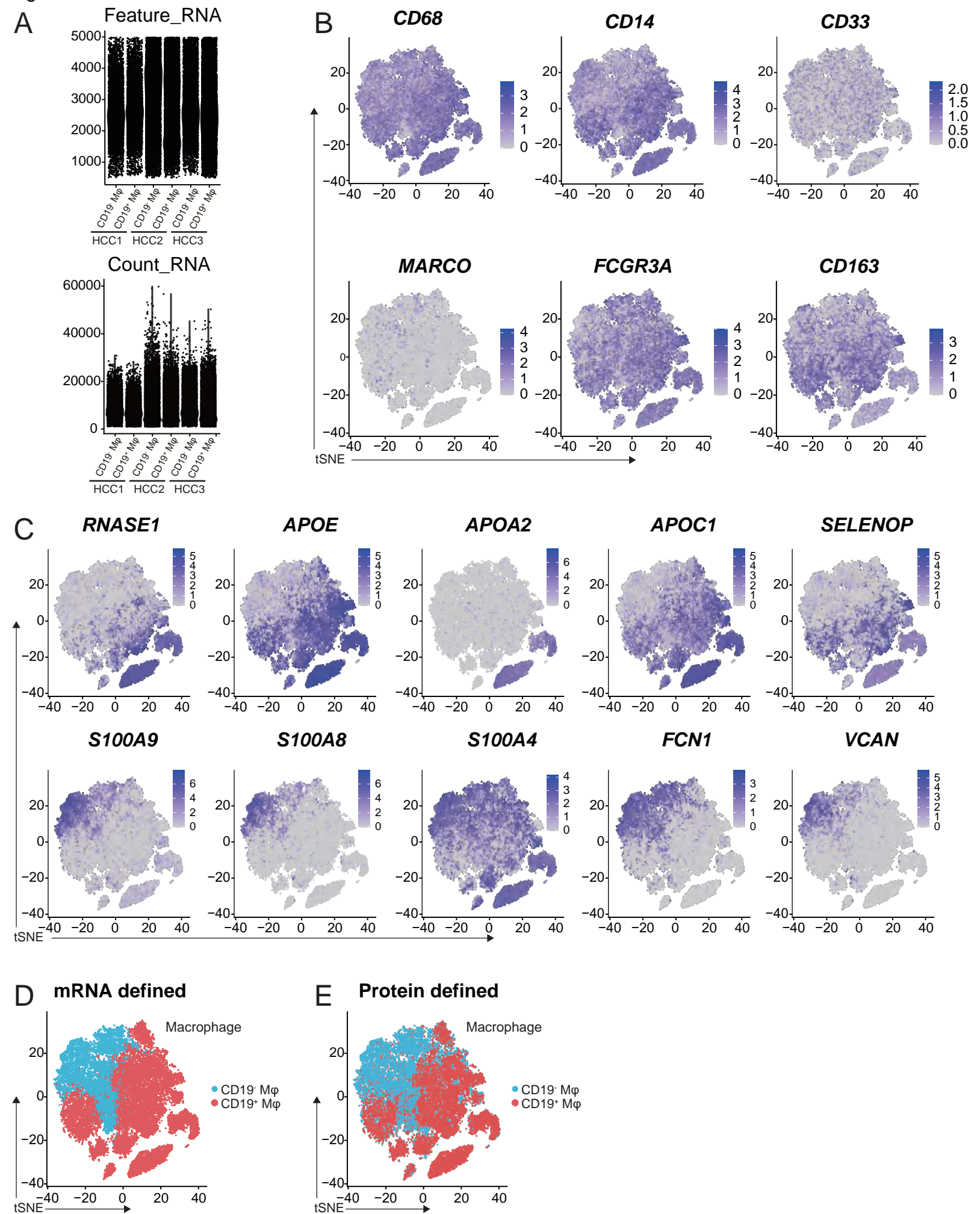


Fig. S4. CD19⁺ TAMs exhibit a distinct gene expression profile (Related to Fig. 3).

(A) VlnPlot analysis of sc-RNAs in three HCC samples after quality control. (B) UMAP plot showing *CD19* mRNA expression levels in CD19⁺ TAMs, CD19⁻ TAMs, and B cells. Macrophages were labelled with red dotted lines, B cells were labelled with orange dotted lines. (C) t-SNE plots showing expression levels of classical macrophage markers in CD19⁺ TAMs and CD19⁻ TAMs, including *CD68*, *CD14*, *CD33*, *MARCO*, *FCGR3A*, *CD163*. (D) t-SNE plots showing the expression levels of five feature genes in CD19⁺ TAMs (*RNASE1*, *APOE*, *APOA2*, *APOC1*, and *SELENOP*) and CD19⁻ TAMs (*S100A9*, *S100A8*, *S100A4*, *FCN1*, *VCAN*), respectively. (E) t-SNE plot showing CD19⁺ TAMs and CD19⁻ TAMs distribution based on the protein levels of the above 10 feature genes. (F) t-SNE plot showing CD19⁺ TAMs and CD19⁻ TAMs distribution based on the mRNA expression levels of the above 10 feature genes.

Fig. S5

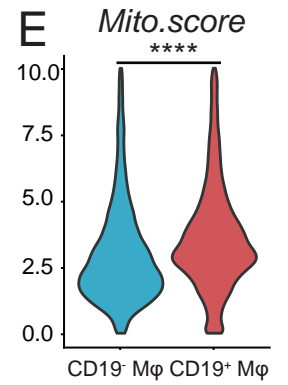
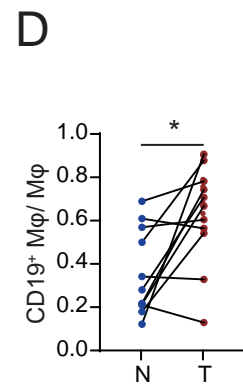
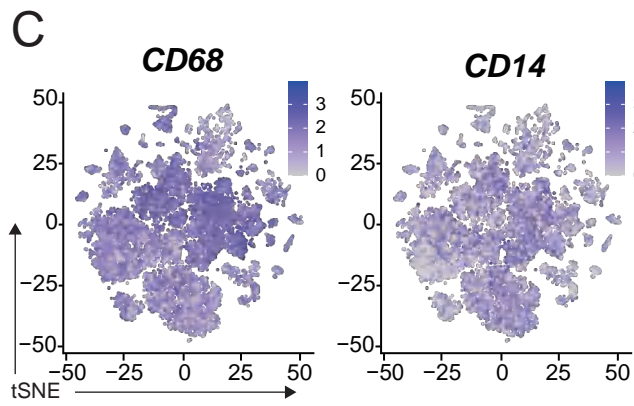
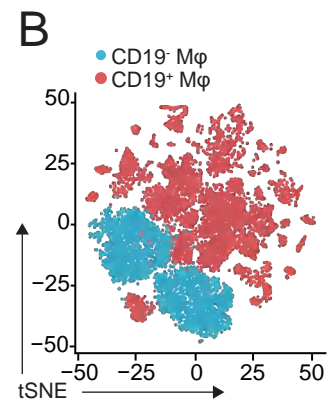
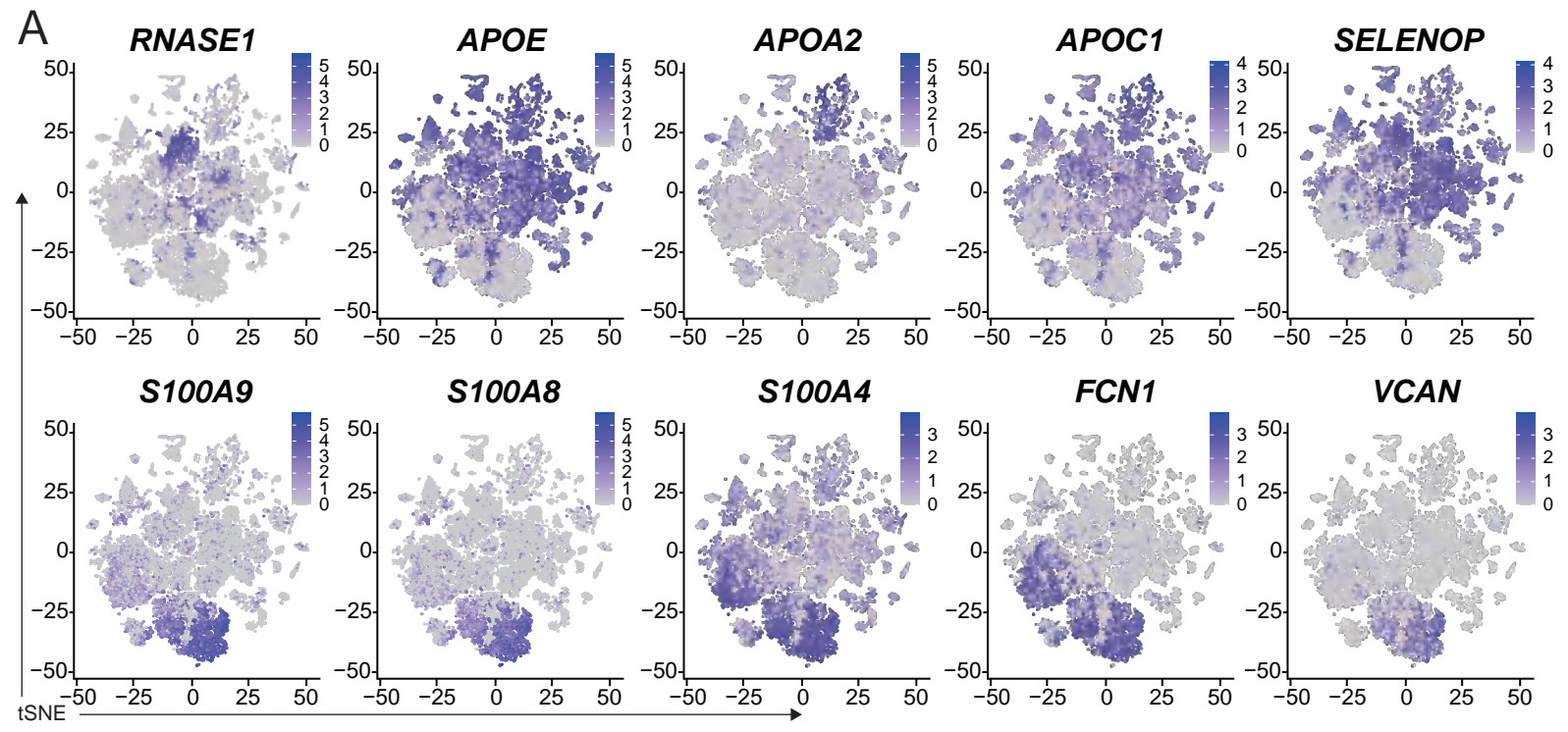


Fig. S5. CD19⁺ TAMs exhibit a distinct gene expression profile (Public dataset: Bioproject, PRJCA010606) (Related to Fig. 3).

(A) t-SNE plot showing mRNA expression levels of the 10 feature genes in CD19⁺ TAMs and CD19⁻ TAMs. (B) t-SNE plot showing the distribution of CD19⁺ TAMs and CD19⁻ TAMs defined by the expression of the 10 feature genes. (C) t-SNE plot showing mRNA expression levels of *CD68*, *CD14*, and *CD19* in CD19⁺ TAMs and CD19⁻ TAMs. (D) Quantification of CD19⁺ TAMs proportion in tumors and matched adjacent normal tissues. n = 11. (E) Violin plot showing the expression levels of mitochondrion-related genes in CD19⁺ TAMs and CD19⁻ TAMs. Data are presented as the mean ± SEM. A paired two-tailed *t*-test (D) or an unpaired two-tailed *t*-test (E) was used. **P* < 0.05.

Fig. S6

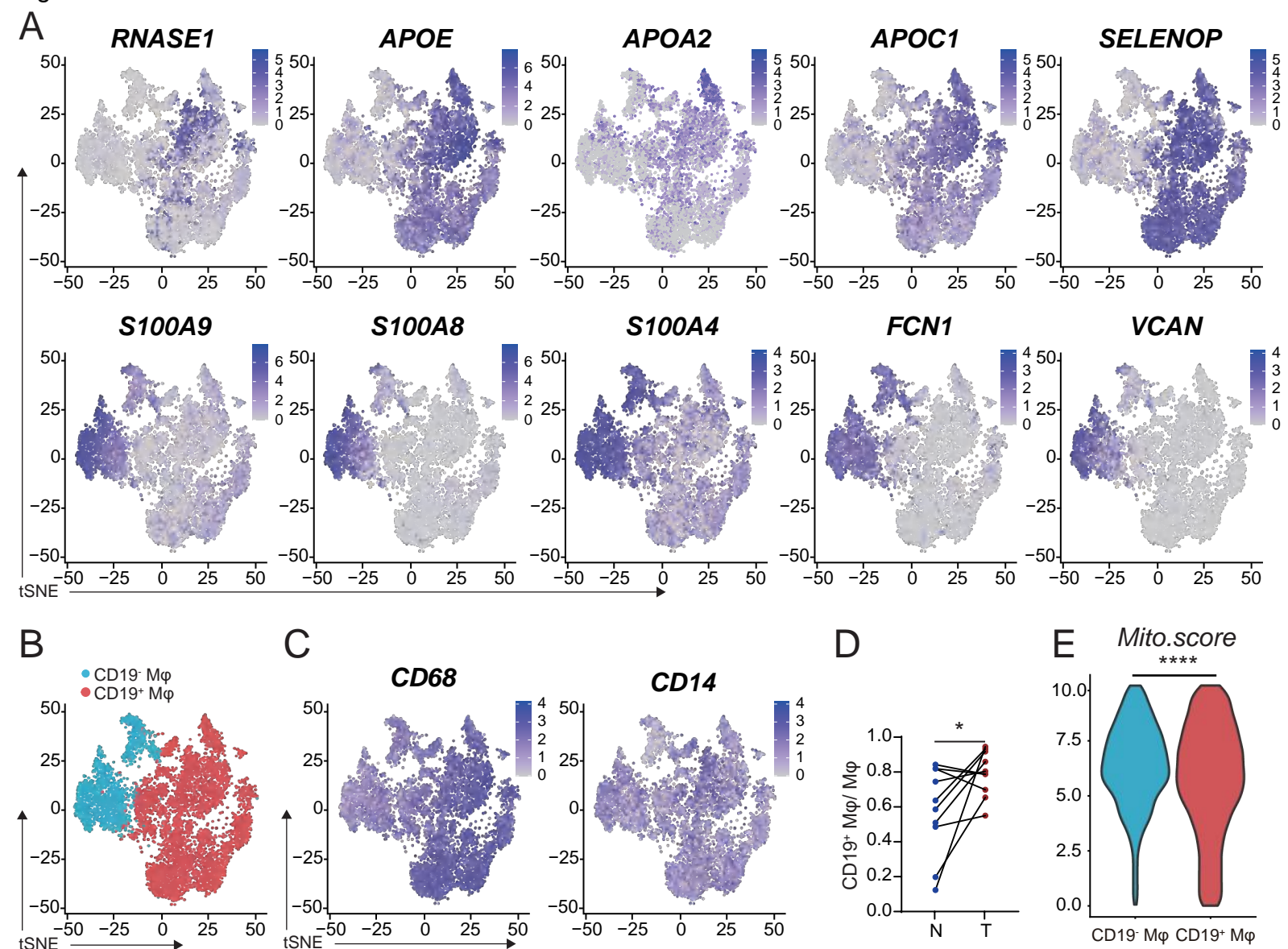


Fig. S6. CD19⁺ TAMs exhibit a distinct gene expression profile (Public dataset: Bioproject, PRJCA007744) (Related to Fig. 3).

(A) t-SNE plot showing mRNA expression levels of the 10 feature genes in CD19⁺ TAMs and CD19⁻ TAMs. (B) t-SNE plot showing the distribution of CD19⁺ TAMs and CD19⁻ TAMs defined by the expression of the 10 feature genes. (C) t-SNE plot showing mRNA expression levels of *CD68*, *CD14*, and *CD19* in CD19⁺ TAMs and CD19⁻ TAMs. (D) Quantification of CD19⁺ TAMs proportion in tumors and matched adjacent normal tissues. n = 11. (E) Violin plot showing the expression levels of mitochondrion-related genes in CD19⁺ TAMs and CD19⁻ TAMs. Data are presented as the mean ± SEM. A paired two-tailed *t*-test (D) or an unpaired two-tailed *t*-test (E) was used. **P* < 0.05.

Fig. S7

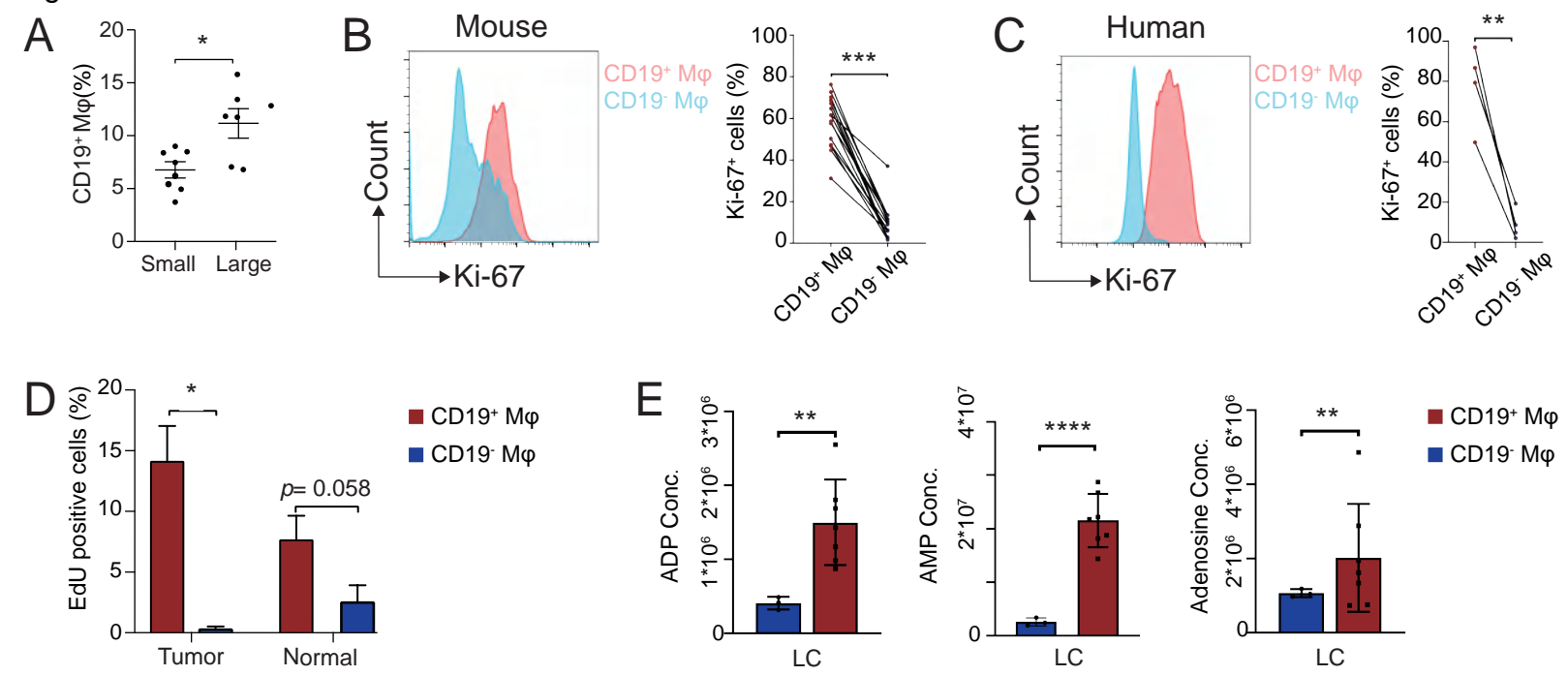


Fig. S7. CD19⁺ TAMs are highly proliferative and immunosuppressive (Related to Fig. 4).

(A) Flow cytometry quantification of CD19⁺ TAM proportions in small or large tumors of syngeneic HCC mouse model. n = 15. (B) Representative flow cytometry histogram and quantification of Ki-67⁺ cells in CD19⁺ TAMs and CD19⁻ TAMs from the tumors in (A). (C) Representative flow cytometry histogram and quantification of Ki-67⁺ cells in CD19⁺ TAMs and CD19⁻ TAMs from human HCC tissues. n = 4. (D) Quantification of Edu⁺ cells in CD19⁺ TAMs and CD19⁻ TAMs of HCC tumors in orthotopic HCC mouse model. n = 10. (E) High Performance Liquid Chromatography (HPLC) analysis showing ADP, AMP, and adenosine concentrations in HCC samples with high (> median) or low (< median) CD19⁺ TAM proportions. Data are presented as the mean ± SEM. Unpaired Wilcoxon test (A), paired two-tailed *t*-test (B, C, D), or unpaired two-tailed *t*-test (E) was used.

P* < 0.05; *P* < 0.01; ****P* < 0.001; *****P* < 0.0001.

Fig. S8

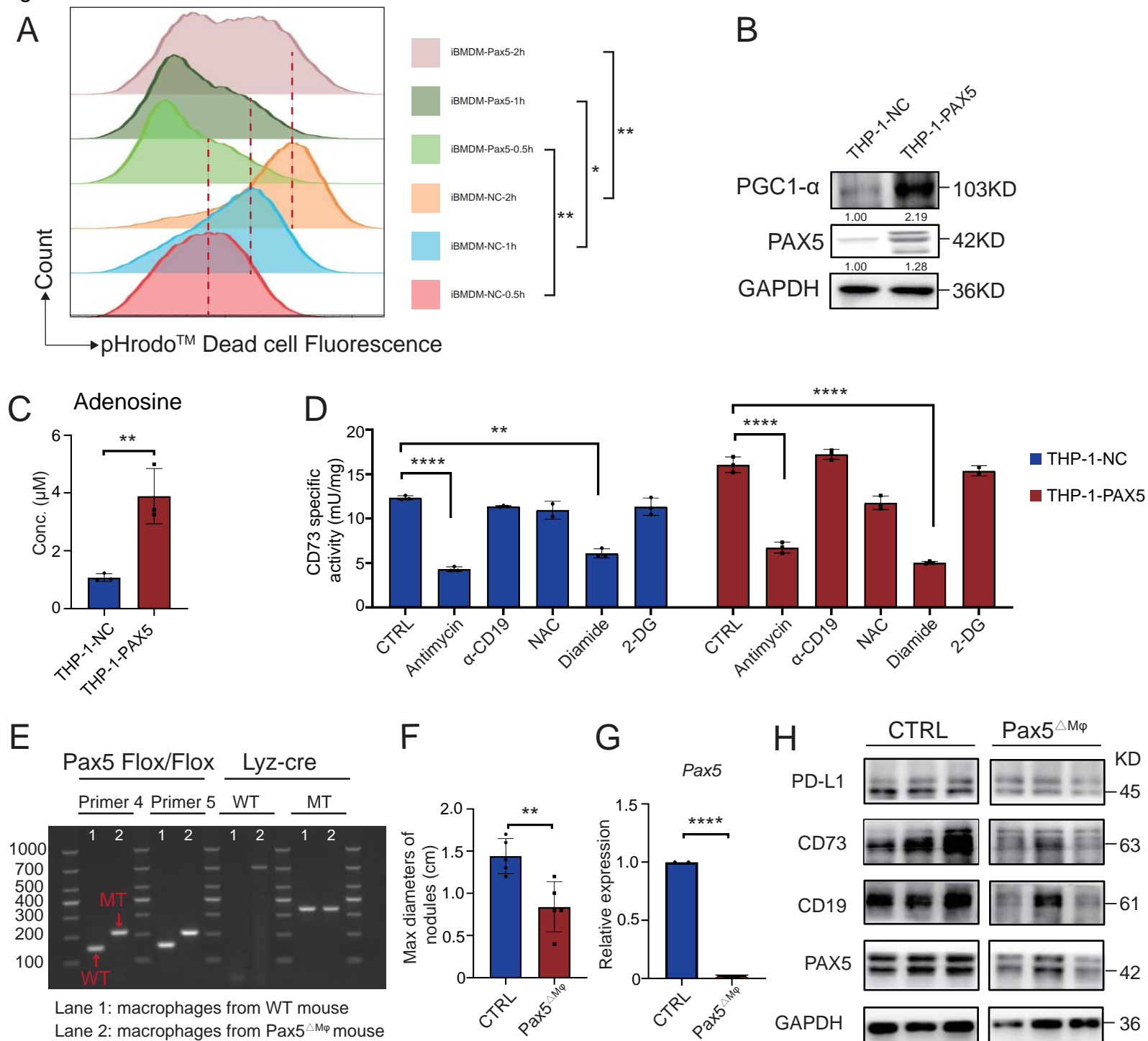


Fig. S8. PAX5 is a master regulator for CD19+ macrophages (Related to Fig. 5).

(A) Flow cytometry histogram showing the phagocytosis of pHydroTM Red SE labelled dead cells by iBMDM cells with or without *Pax5* overexpression. (B) Western blotting analysis of PGC1- α and PAX5 in THP-1 cells with or without *PAX5* overexpression. (C) Quantification of normalized adenosine concentration in conditioned media of THP-1 cells with or without *PAX5* overexpression. n = 3 independent experiments. (D) Quantification of normalized 5'-nucleotidase (CD73) specific activity in THP-1 cells with or without *PAX5* overexpression, or treated with antimycin (mitochondrial respiration inhibitor, 0.5 μ M), anti-CD19 neutralizing antibody (10g/ml), NAC (ROS inhibitor, 2mM), diamide (ROS inducer, 1mM), or 2-DG (glycolysis inhibitor, 20 μ M). n = 3 independent experiments. (E) Macrophages were sorted from the spleens of wild-type mice and *Pax5* ^{Δ M ϕ} mice. Genomic DNA was extracted and subject to Southern blotting analysis to verify *Pax5* gene DNA deletion. Primer 4 and Primer 5 were used for *Pax5* floxed allele. WT: wild type allele; MT: floxed/Cre allele. Lane 1: macrophages from littermate control mice.; Lane 2: macrophages from *Pax5* ^{Δ M ϕ} mice. (F) Maximum diameter quantification of tumors in Figure 5i. (G) Macrophages were sorted from the spleens of littermate control mice and *Pax5* ^{Δ M ϕ} mice. Total RNA was extracted and subjected to RT-PCR for *Pax5* mRNA levels. (H) Macrophages were differentiated from the bone marrow cells of littermate control mice and *Pax5* ^{Δ M ϕ} mice. Proteins were extracted and subjected to western blotting analysis for PAX5, CD19, CD73, and PD-L1 levels. Data are presented as the mean \pm SEM. Two-way ANOVA test (A), unpaired two-tailed *t*-test is used (C, D, G), or unpaired One-way ANOVA with Welch's correction (F) was used. **P* < 0.05; ***P* < 0.01; *****P* < 0.0001.

Fig. S9

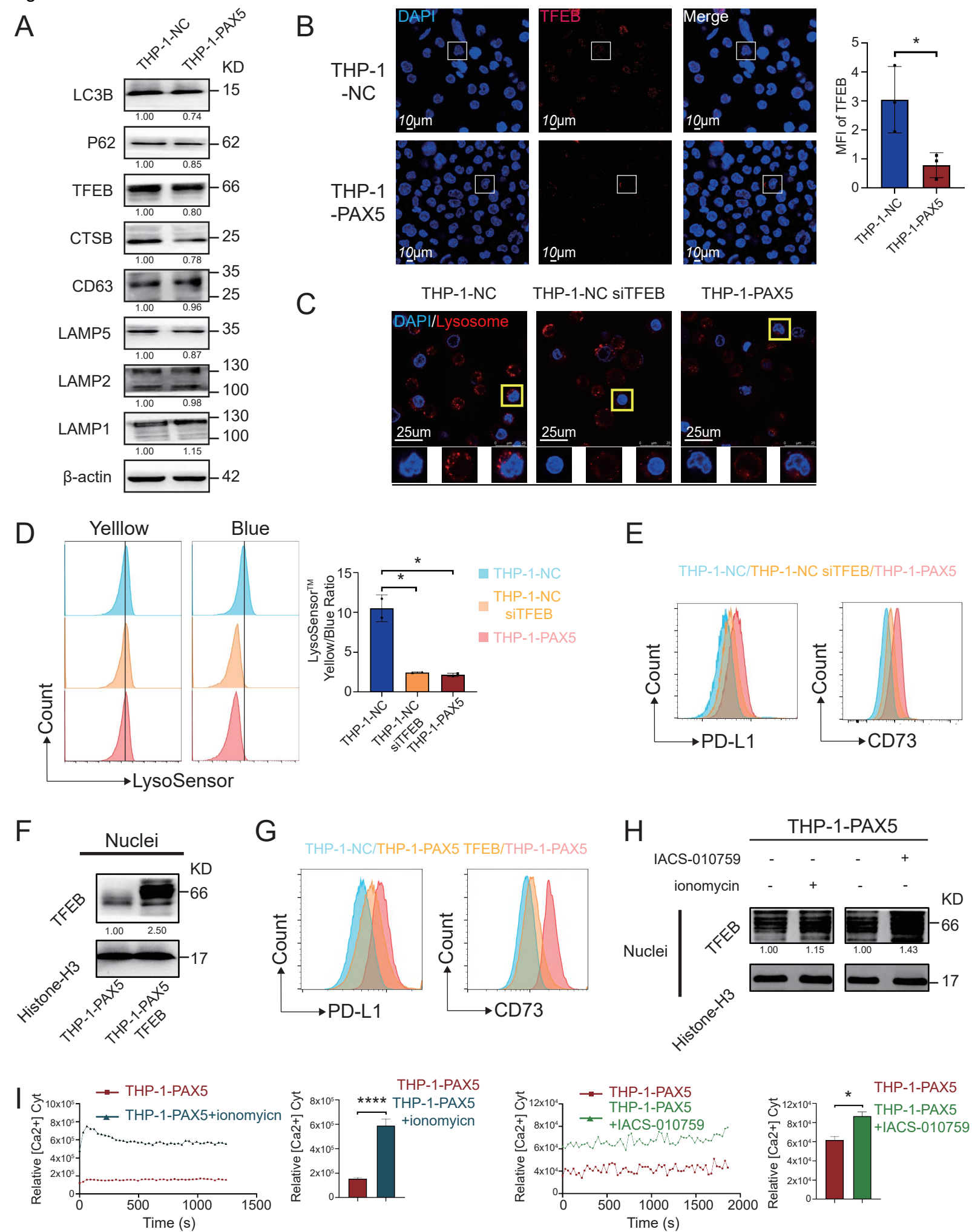


Fig. S9. PAX5 induces PD-L1 and CD73 in a post-transcriptional manner (Related to Fig. 6).

(A) Western blotting analysis of lysosome-associated proteins in THP-1 cells with or without *PAX5* overexpression. (B) Representative immunofluorescence images and quantification of TFEB (red) in THP-1 cells with or without *PAX5* overexpression. Blue, DAPI; scale bar, 10 μ m. (C) Representative immunofluorescence showing LysoTracker (red) and DAPI (blue) in THP-1 cells with or without *PAX5* overexpression or *TFEB* knockdown. (D) Representative immunofluorescence images and quantification of LysoTracker (red) in THP-1 cells with or without *PAX5* overexpression or *TFEB* knockdown. Blue, DAPI. (E) Representative flow cytometry histograms showing CD19, CD73, and PD-L1 expression in THP-1 cells with or without *PAX5* overexpression or *TFEB* knockdown. (F) Western blotting analysis of nuclear TFEB in *PAX5*-overexpressing THP-1 cells. (G) Representative flow cytometry histograms showing CD19, CD73, and PD-L1 levels in *PAX5*-overexpressing THP-1 cells with or without *TFEB* overexpression. (H) Western blotting analysis of nuclear TFEB levels in *PAX5*-overexpressing THP-1 cells pretreated with ionomycin (a Ca^{2+} ionophore, 1 μ M, 24 h), or oxidative phosphorylation inhibitor IACS-010759 (100 nM, 24 h). (I) Fluorescent probe indicating relative Ca^{2+} levels in the cytoplasm of *PAX5*-overexpressing THP-1 cells pretreated with ionomycin or IACS-010759. Data are presented as the mean \pm SEM. Unpaired two-tailed *t*-test (B, D), or two-way ANOVA test (I) was used. **P* < 0.05; *****P* < 0.0001.

Fig. S10

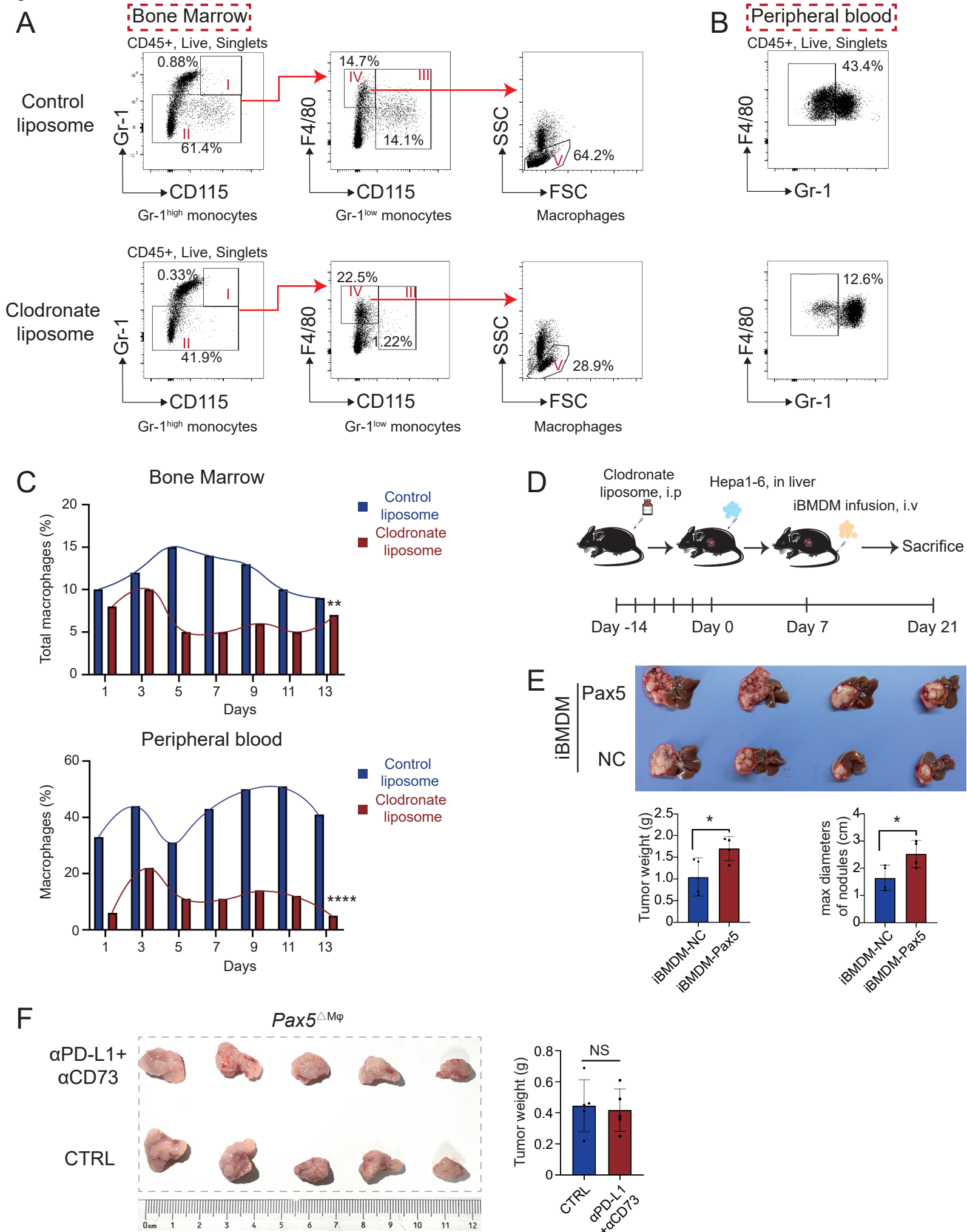


Fig. S10. Blocking CD19⁺ TAMs enhances the efficacy of immune checkpoint blockade therapy (Related to Fig. 7).

(A) Representative flow cytometry plots showing gating strategy for bone marrow mononuclear phagocytes. Part I indicates Gr-1^{high} monocytes (Gr-1^{high}CD115⁺), Part II indicates Gr-1^{low} fraction, which was further divided into Part III (Gr-1^{low} monocytes, Gr-1^{low}CD115⁺) and Part IV (F4/80⁺CD115⁻) populations. Part IV fraction was further subdivided into Part V (SSC^{low} macrophages). (B) Representative flow cytometry plots showing gating strategy of peripheral blood mononuclear phagocytes F4/80⁺Gr- population. (C) Quantification of macrophages depletion efficiency by clodronate liposome or control liposome. Mice received clodronate liposome or control liposome every other day for four times, then bone marrow and peripheral macrophages were subjected to flow cytometrical analysis (gating as in A and B). (D) Schematic illustration showing the experiment for testing CD19⁺ TAMs function in vivo in case of macrophage elimination. C57 BL/6 mice received clodronate liposomes every other day for four times, then were inoculated with Hepa 1-6 cells *in situ*, following by intravenous injection (*i.v.*) with iBMDMs with or without *Pax5* overexpression. (E) Images and sizes of the tumors in (D). n = 4 per group. (F) Images and sizes of the tumors treated with a combined therapy (anti-CD73/anti-PD-L1 neutralizing antibodies) or control IgG antibodies in orthotopic HCC model using *Pax5*^{ΔMφ} (*Pax5*^{flox/flox}; *Lyz-Cre*) mice. n = 5 per group. Data are presented as mean ± SEM; Two-way ANOVA test (C), or unpaired one-way ANOVA with Welch's correction (D, E, F) was used. **P* < 0.05; ***P* < 0.01; *****P* < 0.0001.

Fig. S11

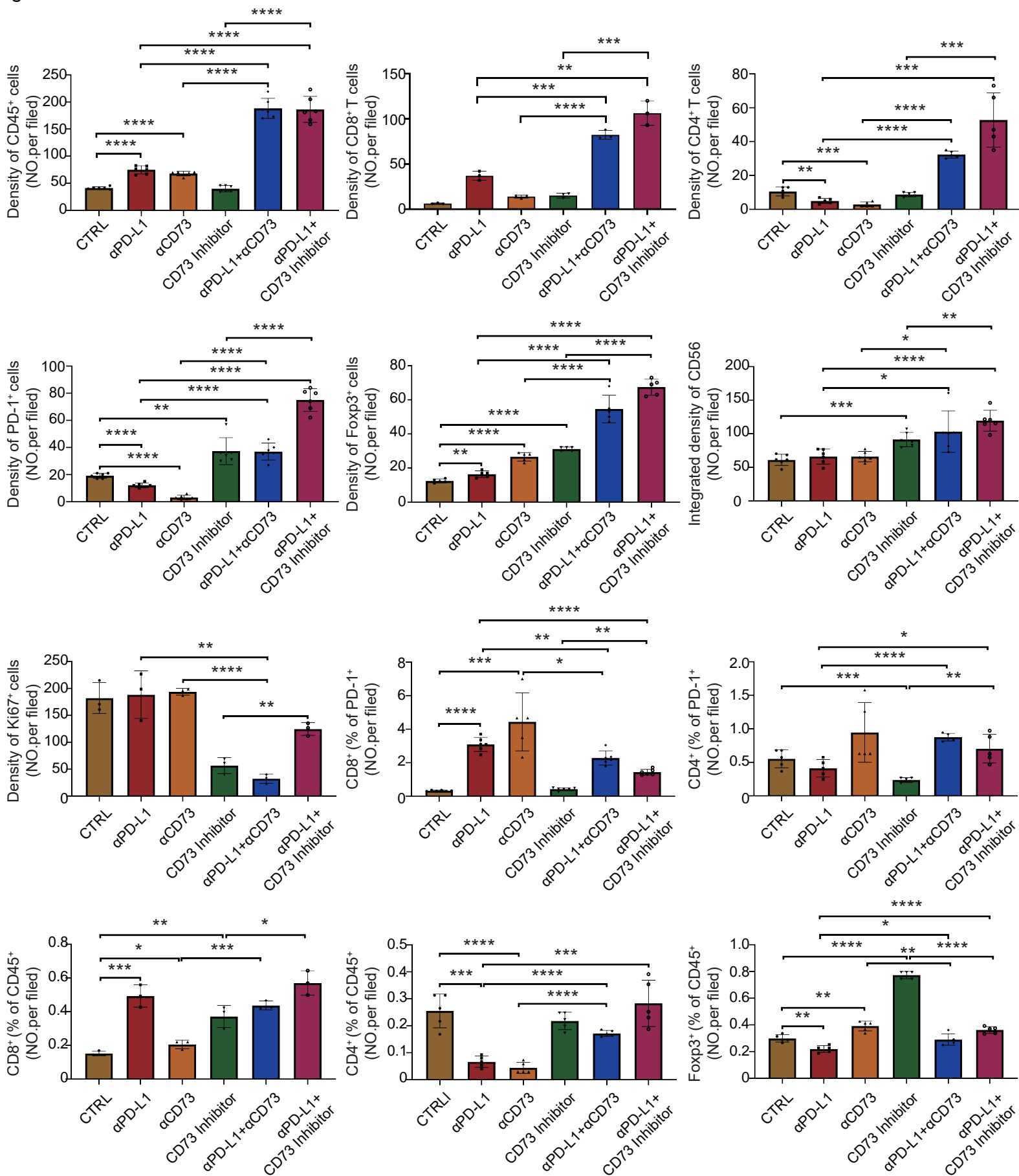


Fig. S11. Blocking CD73 of CD19⁺ TAMs enhances the efficacy of immune checkpoint blockade therapy (Related to Fig. 7).

Tumor Immune microenvironment analysis of the HCC tumors with targeted therapy of CD73 and PD-L1 in CD19⁺ TAM. Analyzed immune cells include CD45⁺ cells, CD8⁺ T cells, CD4⁺ T cells, PD-1⁺ cells, Foxp3⁺ cells, CD56⁺ cells, Ki67⁺ cells, CD8⁺/PD-1⁺ T cells, CD4⁺/PD-1⁺ T cells, CD8⁺ T/CD45⁺ cells, CD4⁺ T/CD45⁺ cells, and Foxp3⁺ T/CD45⁺ cells. Statistical analyses were performed using an unpaired One-way ANOVA with Welch's correction. Data are presented as the mean \pm SEM. * $P < 0.05$; ** $P < 0.01$; *** $P < 0.001$, **** $P < 0.0001$.

Fig. S12

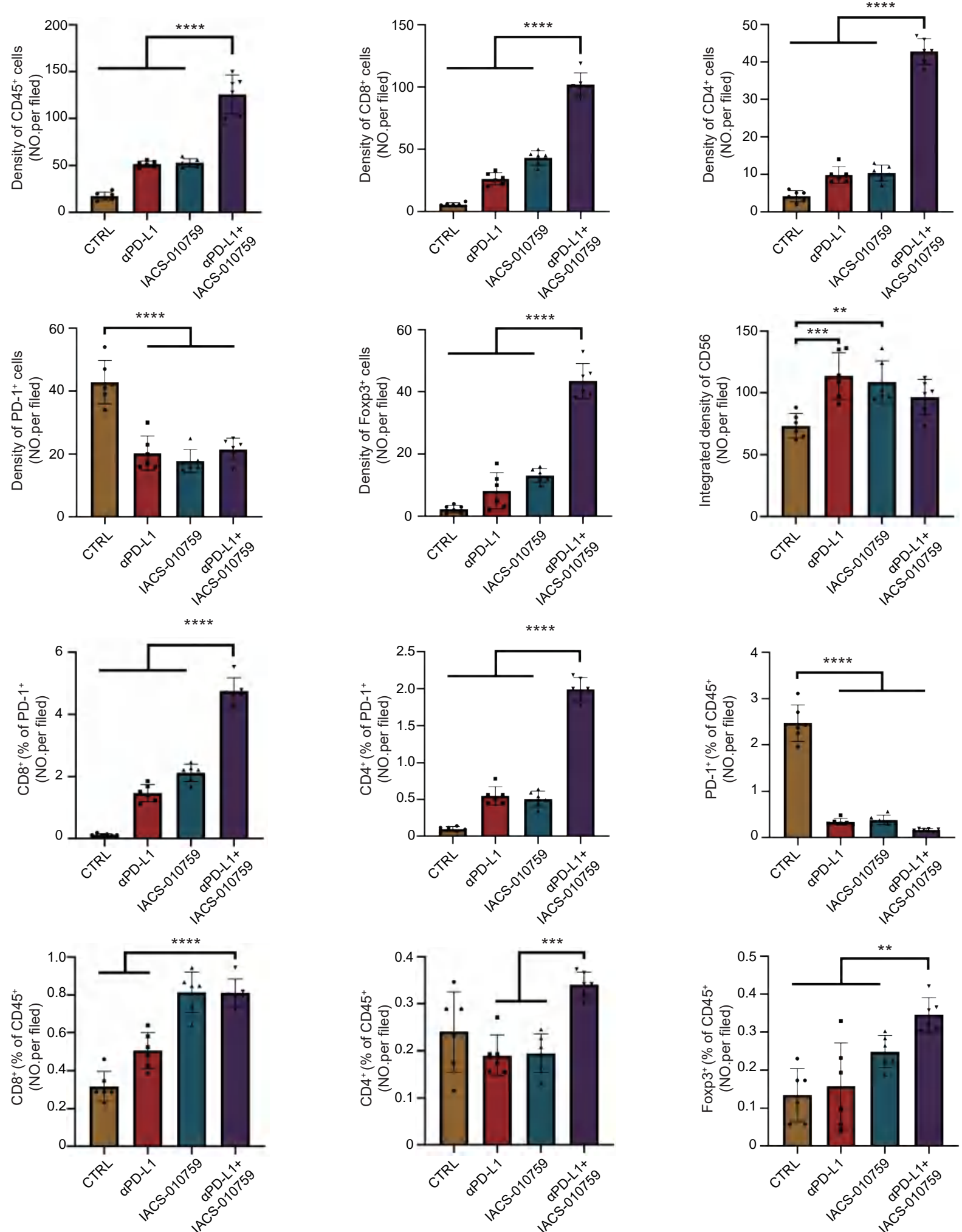


Fig. S12. Blocking OXPPOS activity of CD19⁺ TAMs enhances the efficacy of immune checkpoint blockade therapy (Related to Fig. 7).

Tumor Immune microenvironment analysis of the HCC tumors with targeted therapy of OXPPOS and PD-L1 in CD19⁺ TAM. Analyzed immune cells include CD45⁺ cells, CD8⁺ T cells, CD4⁺ T cells, PD-1⁺ cells, Foxp3⁺ cells, CD56⁺ cells, CD8⁺/PD-1⁺ T cells, CD4⁺/PD-1⁺ T cells, PD-1⁺/CD45⁺ cells, CD8⁺ T/CD45⁺ cells, CD4⁺ T/CD45⁺ cells, and Foxp3⁺ T/CD45⁺ cells. Statistical analyses were performed using unpaired One-way ANOVA with Welch's correction. Data are presented as the mean \pm SEM. * $P < 0.05$; ** $P < 0.01$; *** $P < 0.001$, **** $P < 0.0001$.

Supplementary Table 1. Patients' clinical information, related to Fig. 1, Fig. 2, and Fig. S2.

HCC

Patient	Age	Gender	Tumor size (cm)	Histopathology	Grade	TNM Stage
Patient 1	62	Male	<5	HCC	III	T1aN0M0
Patient 2	67	Male	<5	HCC	III	T1aN0M0
Patient 3	55	Female	<5	HCC	III	T1aN0M0
Patient 4	46	Male	<5	HCC	I	T2N0M0
Patient 5	57	Male	>=5	HCC	II	T3aN0M0
Patient 6	52	Male	<5	HCC	II	T1aN0M0
Patient 7	80	Female	<5	HCC	III	T2N0M0
Patient 8	71	Male	<5	HCC	II	T1aN0M0
Patient 9	52	Male	>=5	HCC	III	T1bN0M0
Patient 10	53	Male	>=5	HCC	III	T1bN0M0
Patient 11	68	Female	<5	HCC	I	T1aN0M0
Patient 12	54	Male	<5	HCC	I	T1aN0M0
Patient 13	64	Male	>=5	HCC	II	T1bN0M0
Patient 14	62	Male	<5	HCC	II	T1aN0M0
Patient 15	65	Male	>=5	HCC	II	T1bN0M0
Patient 16	64	Male	>=5	HCC	III	T3N1M0
Patient 17	66	Female	<5	HCC	III	T1aN0M0

Patient 18	60	Female	<5	HCC	III	T1aN0M0
Patient 19	47	Male	<5	HCC	II	T1aN0M0
Patient 20	63	Male	>=5	HCC	II	T1bN0M0
Patient 21	68	Male	>=5	HCC	II	T1bN0M0
Patient 22	45	Male	<5	HCC	I	T1aN0M0
Patient 23	74	Male	<5	HCC	II	T2N0M0
Patient 24	63	Male	<5	HCC	II	T2N0M0
Patient 25	71	Female	>=5	HCC	II	T2N0M0
Patient 26	77	Male	<5	HCC	II	T1aN0M0
Patient 27	78	Female	>=5	HCC	II	T2N0M0
Patient 28	74	Female	<5	HCC	II	T1aN0M0

PDAC

Patient	Age	Gender	Tumor size (cm)	Histopathology	Grade	TNM Stage
Patient 1	74	Female	>=5	Adenocarcinoma	Poorly-moderate	T3N0M0
Patient 2	68	Male	>=5	Adenocarcinoma	Moderate	T3N0M0
Patient 3	59	Female	>=5	Adenocarcinoma	Moderate	T3N0M0
Patient 4	61	Female	>=2, <5	Adenocarcinoma	Poorly-moderate	T3N1M1
Patient 5	71	Male	<2	Adenocarcinoma	Moderate	T1cN1M0
Patient 6	66	Female	>=2, <5	Adenocarcinoma	Moderate-highly	T2N1M0
Patient 7	55	Male	>=2, <5	Adenocarcinoma	Poorly-moderate	T2N0M0

Patient 8	72	Female	>=2, <5	Adenocarcinoma	Moderate	T2N0M0
Patient 9	48	Female	>=2, <5	Adenocarcinoma	Moderate	T2N0M0
Patient 10	69	Female	>=2, <5	Adenocarcinoma	Moderate	T2N0M0
Patient 11	55	Male	>=2, <5	Adenocarcinoma	Moderate	T1cN0M0
Patient 12	67	Female	>=2, <5	Adenocarcinoma	Poorly-moderate	T2N1M0
Patient 13	48	Male	>=2, <5	Adenocarcinoma	Poorly	T2N0M0

Breast carcinoma

Patient	Age	Gender	Tumor size (cm)	Histopathology	Grade	TNM Stage
Patient 1	53	Female	>=2, <5	Invasive ductal carcinoma	III	T2N1aM0
Patient 2	62	Female	>=2, <5	Invasive carcinoma (micropapillary + mucinous)	II	T2N3aM0
Patient 3	55	Female	>=2, <5	Invasive ductal carcinoma	III	T2N0M0
Patient 4	56	Female	>=2, <5	Invasive ductal carcinoma	III	T2N1aM0
Patient 5	30	Female	>=2, <5	Invasive ductal carcinoma	III	T2N1aM0
Patient 6	49	Female	>=2, <5	Invasive lobular carcinoma	I	T2N0M0
Patient 7	45	Female	>=2, <5	Invasive ductal carcinoma	III	T2N0M0
Patient 8	40	Female	<2	Invasive ductal carcinoma	II	T1cN0M0
Patient 9	51	Female	>=2, <5	Invasive ductal carcinoma	II	T2N2M0
Patient 10	53	Female	<2	Invasive ductal carcinoma	III	T1cN3M0
Patient 11	48	Female	>=2, <5	Invasive ductal carcinoma	III	T1cN0M0

Patient 12	57	Female	<2	Invasive ductal carcinoma	II	T1cN2M0
------------	----	--------	----	---------------------------	----	---------

Gastric carcinoma

Patient	Age	Gender	Tumor size (cm)	Histopathology	Grade	TNM Stage
Patient 1	38	Female	<5	Adenocarcinoma	I	T1N0M0
Patient 2	62	Female	<5	Adenocarcinoma	I	T1N1M0
Patient 3	74	Male	>=5	Adenocarcinoma	II	T3N0M0
Patient 4	57	Male	<5	Adenocarcinoma	II	T1N0M0
Patient 5	71	Female	>=5	Adenocarcinoma	I	T3N0M0
Patient 6	63	Female	<5	Adenocarcinoma	II	T1N0M0

Renal carcinoma

Patient	Age	Gender	Tumor size (cm)	Histopathology	Grade	TNM Stage
Patient 1	60	Female	>7, <=10	No classification	NA	T2aN0M0
Patient 2	60	Male	>4, <=7	Clear cell carcinomma	NA	T1bN0M0
Patient 3	63	Male	<=4	Clear cell carcinomma	NA	T1aN0M0
Patient 4	53	Female	>4, <=7	Clear cell carcinomma	NA	T1bN0M0
Patient 5	69	Male	<=4	Clear cell carcinomma	NA	T1aN0M0
Patient 6	51	Female	<=4	No classification	NA	T1aN0M0
Patient 7	56	Male	<=4	Clear cell carcinomma	NA	T1aN0M0
Patient 8	70	Female	>4, <=7	Clear cell carcinomma	NA	T1bN0M0

Patient 9	53	Male	<=4	Clear cell carcinomma	NA	T1aN0M0
Patient 10	45	Male	<=4	Clear cell carcinomma	NA	T1aN0M0
Patient 11	54	Female	>4, <=7	Clear cell carcinomma	NA	T1bN0M0

Colorectal carcinoma

Patient	Age	Gender	Tumor size (cm)	Histopathology	Grade	TNM Stage	OS (m)
Patient 1	68	Male	>=5cm	Adenocarcinoma	Poorly-moderate	T3N1M0	
Patient 2	61	Female	<5	Adenocarcinoma	Moderate	T1N0M0	
Patient 3	74	Female	<5	Adenocarcinoma	Moderate	T3N0M0	
Patient 4	67	Male	<5	Adenocarcinoma	Poorly	T3N1M0	
Patient 5	62	Male	<5	Adenocarcinoma	Moderate	T3N0M0	
Patient 6	62	Female	>=5cm	Adenocarcinoma	Moderate	T3N1M0	
Patient 7	67	Male	<5	Adenocarcinoma	Poorly-moderate	T3N0M0	
Patient 8	70	Male	>=5cm	Adenocarcinoma	Highly	T1N0M0	
Patient 9	82	Female	>=5cm	Adenocarcinoma	Poorly-moderate	T4aN1M0	
Patient 10	68	Female	<5	Adenocarcinoma	Moderate	T1N1M0	
Patient 11	69	Male	<5	Adenocarcinoma	Moderate	T1N0M0	
Patient 1	58	Male	<5	HCC	II	T4N1M1	13
Patient 2	65	Male	<5	HCC	III	T1aN0M0	14

Patient 3	18	Male	<5	HCC	I	T2N0M0	15
Patient 4	72	Male	>=5	HCC	II	T1bN0M0	15
Patient 5	49	Female	>=5	HCC	II	T4N1M1	7
Patient 6	61	Male	<5	HCC	II	T3N0M0	20
Patient 7	46	Male	>=5	HCC	II	T3N0M0	24
Patient 8	58	Male	<5	HCC	II	T2N0M0	25
Patient 9	59	Male	<5	HCC	II	T1aN0M0	25
Patient 10	65	Male	<5	HCC	III	T1aN0M0	26
Patient 11	62	Female	<5	HCC	III	T1aN0M0	26
Patient 12	59	Male	<5	HCC	III	T1aN0M0	43
Patient 13	35	Male	>=5	HCC	II	T2N0M0	19
Patient 14	61	Male	>=5	HCC	II	T3N0M0	32
Patient 15	46	Male	<5	HCC	II	T2N0M0	34
Patient 16	63	Male	<5	HCC	II	T2N0M0	35
Patient 17	58	Male	<5	HCC	II	T2N0M0	35
Patient 18	69	Male	<5	HCC	II	T2N0M0	47
Patient 19	79	Male	<5	HCC	III	T2N0M0	43
Patient 20	43	Female	<5	HCC	III	T1aN0M0	45
Patient 21	49	Male	<5	HCC	II	T1aN0M0	45
Patient 22	55	Male	<5	HCC	I	T2N0M0	6

Patient 23	64	Male	<5	HCC	II	T2N0M0	46
Patient 24	47	Male	<5	HCC	III	T1aN0M0	48
Patient 25	81	Male	<5	HCC	II	T1aN0M0	38
Patient 26	59	Male	<5	HCC	II	T1aN0M0	50
Patient 27	53	Male	<5	HCC	II	T1aN0M0	51
Patient 28	58	Male	<5	HCC	II	T2N0M0	63
Patient 29	39	Male	>=5	HCC	II	T1bN0M0	12
Patient 30	47	Male	>=5	HCC	II	T3N0M0	39
Patient 31	58	Male	<5	HCC	II	T1aN0M0	51
Patient 32	67	Male	<5	HCC	II	T1aN0M0	52
Patient 33	45	Female	<5	HCC	II	T1aN0M0	53
Patient 34	64	Male	>=5	HCC	I	T4N1M1	25
Patient 35	53	Male	>=5	HCC	II	T2N0M0	26
Patient 36	22	Male	<5	HCC	II	T1aN0M0	54
Patient 37	64	Male	>=5	HCC	II	T1bN0M0	54
Patient 38	73	Male	>=5	HCC	I	T3N0M0	55
Patient 39	52	Male	>=5	HCC	II	T4N1M0	55
Patient 40	69	Male	<5	HCC	II	T1aN0M0	55
Patient 41	74	Male	<5	HCC	II	T4N1M1	56
Patient 42	84	Male	<5	HCC	II	T1aN0M0	43

Patient 43	57	Male	>=5	HCC	III	T1bN0M0	56
Patient 44	54	Male	>=5	HCC	I	T1bN0M0	56
Patient 45	67	Female	<5	HCC	II	T1aN0M0	57
Patient 46	60	Male	<5	HCC	II	T1aN0M0	58
Patient 47	66	Male	<5	HCC	II	T1aN0M0	61
Patient 48	67	Female	>=5	HCC	II	T1bN0M0	62
Patient 49	46	Male	<5	HCC	II	T1aN0M0	63
Patient 50	84	Male	<5	HCC	III	T1aN0M0	27
Patient 51	54	Male	<5	HCC	II	T1aN0M0	51
Patient 52	60	Female	>=5	HCC	II	T1bN0M0	64
Patient 53	63	Male	<5	HCC	II	T2N0M0	65
Patient 54	75	Male	<5	HCC	II	T4N1M1	64
Patient 55	58	Female	<5	HCC	II	T1aN0M0	66
Patient 56	51	Male	>=5	HCC	II	T4N1M1	34
Patient 57	60	Female	<5	HCC	III	T1aN0M0	66
Patient 58	44	Male	<5	HCC	II	T1aN0M0	67
Patient 59	41	Female	<5	HCC	II	T1aN0M0	67
Patient 60	46	Male	<5	HCC	II	T1aN0M0	61
Patient 61	68	Male	>=5	HCC	I	T3N0M0	17
Patient 62	59	Male	>=5	HCC	II	T3N0M0	68

Patient 63	59	Female	<5	HCC	III	T1aN0M0	62
Patient 64	76	Male	<5	HCC	III	T1aN0M0	71
Patient 65	52	Male	<5	HCC	I	T1aN0M0	64
Patient 66	62	Male	<5	HCC	II	T1aN0M0	19
Patient 67	79	Male	>=5	HCC	II	T1bN0M0	10
Patient 68	65	Male	<5	HCC	II	T1aN0M0	72
Patient 69	69	Male	<5	HCC	II	T1aN0M0	25
Patient 70	65	Male	<5	HCC	II	T2N0M0	67
Patient 71	48	Male	<5	HCC	II	T2N0M0	67
Patient 72	80	Male	<5	HCC	II	T1aN0M0	35
Patient 73	48	Male	<5	HCC	III	T2N0M0	67
Patient 74	66	Male	>=5	HCC	II	T1bN0M0	20
Patient 75	60	Male	<5	HCC	II	T4N1M0	66
Patient 76	50	Male	<5	HCC	II	T1aN0M0	11
Patient 77	43	Male	>=5	HCC	I	T2N0M0	64
Patient 78	81	Male	>=5	HCC	III	T1bN0M0	62
Patient 79	75	Male	<5	HCC	II	T2N0M0	17
Patient 80	78	Male	>=5	HCC	II	T2N0M0	48
Patient 81	54	Male	>=5	HCC	II	T2N0M0	8
Patient 82	52	Male	>=5	HCC	I	T3N0M0	44

Patient 83	77	Male	<5	HCC	II	T2N0M0	9
Patient 84	61	Male	>=5	HCC	II	T1bN0M0	44
Patient 85	73	Female	>=5	HCC	II	T3N0M0	38
Patient 86	70	Male	>=5	HCC	II	T1bN0M0	33
Patient 87	67	Male	<5	HCC	III	T2N0M0	12
Patient 88	39	Female	<5	HCC	II	T1aN0M0	9
Patient 89	62	Male	<5	HCC	II	T2N0M0	37
Patient 90	66	Male	<5	HCC	II	T1aN0M0	10
Patient 91	58	Male	>=5	HCC	II	T2N0M0	12
Patient 92	55	Female	<5	HCC	I	T2N0M0	19
Patient 93	63	Male	<5	HCC	I	T2N0M0	21
Patient 94	65	Male	<5	HCC	II	T1aN0M0	22
Patient 95	69	Male	<5	HCC	II	T1aN0M0	21
Patient 96	69	Male	>=5	HCC	I	T2N0M0	19
Patient 97	57	Female	>=5	HCC	II	T3N0M0	14
Patient 98	73	Male	>=5	HCC	II	T1bN0M0	27
Patient 99	58	Male	>=5	HCC	II	T1bN0M0	30
Patient 100	58	Male	<5	HCC	II	T1aN0M0	30
Patient 101	57	Female	<5	HCC	II	T1aN0M0	30
Patient 102	53	Male	<5	HCC	I	T1aN0M0	32

Patient 103	56	Male	>=5	HCC	II	T1aN0M0	33
Patient 104	72	Male	<5	HCC	II	T2N0M0	35
Patient 105	46	Male	<5	HCC	III	T1aN0M0	37
Patient 106	69	Male	<5	HCC	I	T2N0M0	37
Patient 107	55	Male	<5	HCC	II	T2N0M0	38
Patient 108	63	Male	<5	HCC	II	T1aN0M0	41
Patient 109	48	Male	<5	HCC	II	T2N0M0	42
Patient 110	63	Male	<5	HCC	III	T2N0M0	43
Patient 111	64	Male	<5	HCC	II	T1aN0M0	45
Patient 112	74	Male	<5	HCC	III	T1aN0M0	45
Patient 113	77	Male	<5	HCC	III	T1aN0M0	47
Patient 114	68	Male	<5	HCC	III	T1aN0M0	48
Patient 115	61	Male	<5	HCC	II	T1aN0M0	49
Patient 116	57	Male	<5	HCC	III	T1aN0M0	53
Patient 117	64	Male	<5	HCC	III	T1aN0M0	54
Patient 118	45	Male	<5	HCC	II	T1aN0M0	52
Patient 119	63	Male	<5	HCC	III	T1aN0M0	52
Patient 120	61	Male	<5	HCC	I	T1aN0M0	48
Patient 121	65	Male	<5	HCC	II	T1aN0M0	11
Patient 122	67	Female	<5	HCC	II	T1aN0M0	44

Patient 123	58	Female	<5	HCC	II	T1aN0M0	36
Patient 124	36	Male	<5	HCC	III	T2N0M0	15
Patient 125	55	Male	>=5	HCC	II	T2N0M0	15
Patient 126	59	Male	<5	HCC	III	T1aN0M0	29
Patient 127	54	Male	<5	HCC	II	T1aN0M0	26
Patient 128	63	Male	>=5	HCC	II	T1bN0M0	24
Patient 129	75	Male	>=5	HCC	II	T3N0M0	23
Patient 130	53	Male	<5	HCC	II	T1aN0M0	23
Patient 131	63	Male	>=5	HCC	II	T1bN0M0	54
Patient 132	76	Female	<5	HCC	III	T1aN0M0	32
Patient 133	62	Male	>=5	HCC	II	T1bN0M0	8
Patient 134	55	Male	<5	HCC	I	T2N0M0	11
Patient 135	56	Male	>=5	HCC	II	T1bN0M0	11
Patient 136	69	Male	<5	HCC	III	T1aN0M0	11
Patient 137	53	Male	<5	HCC	III	T1aN0M0	47
Patient 138	55	Female	<5	HCC	I	T1aN0M0	40
Patient 139	76	Female	>=5	HCC	II	T2N0M0	36
Patient 140	69	Male	>=5	HCC	II	T1bN0M0	29
Patient 141	63	Male	>=5	HCC	I	T2N0M0	25
Patient 142	62	Male	<5	HCC	II	T1aN0M0	22

Patient 143	67	Male	<5	HCC	III	T1aN0M0	19
Patient 144	75	Male	<5	HCC	II	T2N0M0	19
Patient 145	32	Female	>=5	HCC	II	T1aN0M0	17
Patient 146	38	Male	>=5	HCC	II	T2N0M0	16
Patient 147	55	Male	>=5	HCC	II	T1bN0M0	17
Patient 148	66	Male	<5	HCC	II	T2N0M0	17
Patient 149	48	Male	<5	HCC	I	T2N0M0	16
Patient 150	59	Female	<5	HCC	II	T2N0M0	16
Patient 151	49	Male	>=5	HCC	II	T2N0M0	17
Patient 152	50	Male	>=5	HCC	I	T2N0M0	16
Patient 153	66	Male	<5	HCC	II	T1aN0M0	16
Patient 154	71	Male	>=5	HCC	II	T2N0M0	15
Patient 155	68	Male	<5	HCC	II	T2N0M0	7
Patient 156	65	Male	<5	HCC	II	T1aN0M0	14
Patient 157	50	Male	>=5	HCC	I	T1bN0M0	12
Patient 158	62	Male	<5	HCC	II	T1aN0M0	10
Patient 159	64	Female	<5	HCC	II	T1aN0M0	11
Patient 160	70	Male	<5	HCC	II	T2N0M0	10
Patient 161	60	Female	>=5	HCC	II	T2N0M0	6
Patient 162	71	Male	>=5	HCC	II	T1bN0M0	10

Patient 163	52	Male	>=5	HCC	II	T2N0M0	41
Patient 164	47	Male	>=5	HCC	II	T1bN0M0	22
Patient 165	46	Male	>=5	HCC	II	T1bN0M0	12
Patient 166	49	Male	>=5	HCC	II	T1bN0M0	35
Patient 167	71	Male	>=5	HCC	I	T2N0M0	10
Patient 168	56	Male	<5	HCC	II	T2N0M0	19
Patient 169	55	Male	<5	HCC	II	T2N0M0	50
Patient 170	69	Male	>=5	HCC	II	T2N0M0	10
Patient 171	57	Male	<5	HCC	III	T2N0M0	15
Patient 172	70	Male	<5	HCC	II	T1aN0M0	16
Patient 173	80	Male	<5	HCC	I	T2N0M0	20
Patient 174	44	Male	>=5	HCC	I	T2N0M0	20
Patient 175	47	Male	>=5	HCC	II	T1bN0M0	20
Patient 176	48	Male	>=5	HCC	II	T2N0M0	20
Patient 177	52	Male	<5	HCC	II	T2N0M0	26
Patient 178	59	Female	<5	HCC	II	T1aN0M0	28
Patient 179	56	Male	<5	HCC	II	T1aN0M0	29
Patient 180	72	Male	<5	HCC	II	T1aN0M0	33
Patient 181	65	Male	<5	HCC	II	T1aN0M0	25
Patient 182	64	Male	<5	HCC	III	T2N0M0	35

Patient 183	67	Male	<5	HCC	I	T1aN0M0	44
Patient 184	57	Male	<5	HCC	II	T1aN0M0	48
Patient 185	44	Male	>=5	HCC	II	T2N0M0	48
Patient 186	48	Male	<5	HCC	II	T1aN0M0	49
Patient 187	76	Male	<5	HCC	II	T1aN0M0	53
Patient 188	65	Male	<5	HCC	I	T4N1M1	55
Patient 189	66	Male	<5	HCC	II	T1aN0M0	11
Patient 190	75	Male	>=5	HCC	III	T1bN0M0	54
Patient 191	69	Male	<5	HCC	II	T1aN0M0	55
Patient 192	59	Male	<5	HCC	II	T2N0M0	10
Patient 193	65	Male	<5	HCC	II	T1aN0M0	8
Patient 194	71	Male	>=5	HCC	II	T2N0M0	9
Patient 195	62	Male	>=5	HCC	I	T1bN0M0	9
Patient 196	71	Male	>=5	HCC	I	T2N0M0	10
Patient 197	52	Male	>=5	HCC	I	T2N0M0	10
Patient 198	60	Male	<5	HCC	II	T1aN0M0	13
Patient 199	63	Male	<5	HCC	II	T1aN0M0	18
Patient 200	68	Male	<5	HCC	II	T2N0M0	22
Patient 201	68	Male	<5	HCC	II	T1aN0M0	24
Patient 202	45	Male	>=5	HCC	II	T3N0M0	30

Patient 203	53	Male	<5	HCC	II	T2N1M0	30
Patient 204	55	Male	<5	HCC	III	T2N1M0	31
Patient 205	84	Male	<5	HCC	I	T1aN0M0	31
Patient 206	58	Male	>=5	HCC	II	T2N0M0	32
Patient 207	67	Male	<5	HCC	I	T2N0M0	32
Patient 208	68	Male	<5	HCC	I	T2N0M0	95
Patient 209	61	Male	>=5	HCC	II	T2N0M0	31
Patient 210	64	Male	<5	HCC	III	T1aN0M0	95
Patient 211	73	Male	<5	HCC	II	T1aN0M0	41
Patient 212	67	Female	>=5	HCC	II	T2N0M0	16
Patient 213	58	Male	<5	HCC	II	T1aN0M0	12
Patient 214	65	Male	>=5	HCC	II	T1bN0M0	43
Patient 215	78	Male	<5	HCC	II	T2N0M0	43
Patient 216	45	Male	>=5	HCC	II	T2N0M0	43
Patient 217	69	Male	>=5	HCC	III	T1bN0M0	44
Patient 218	52	Female	>=5	HCC	I	T3N0M0	45
Patient 219	66	Male	<5	HCC	II	T1aN0M0	21
Patient 220	75	Female	<5	HCC	II	T3N0M0	60
Patient 221	58	Male	<5	HCC	II	T4N1M1	59
Patient 222	44	Male	<5	HCC	I	T1aN0M0	50

Patient 223	79	Male	<5	HCC	II	T1aN0M0	56
Patient 224	69	Male	>=5	HCC	II	T3N0M0	55
Patient 225	58	Male	>=5	HCC	II	T2N0M0	36
Patient 226	49	Male	>=5	HCC	I	T3N0M0	53
Patient 227	46	Male	>=5	HCC		T1bN0M0	52
Patient 228	47	Male	<5	HCC	II	T3N0M0	48
Patient 229	63	Male	<5	HCC	III	T1aN0M0	48
Patient 230	59	Female	>=5	HCC	II	T1bN0M0	47
Patient 231	50	Male	>=5	HCC	III	T2N0M0	45
Patient 232	59	Male	>=5	HCC	II	T1bN0M0	43
Patient 233	62	Male	>=5	HCC	II	T3N0M0	41
Patient 234	67	Male	>=5	HCC	II	T2N0M0	16
Patient 235	57	Male	<5	HCC	III	T2N0M0	40
Patient 236	70	Male	<5	HCC	II	T1aN0M0	40
Patient 237	52	Female	>=5	HCC	II	T1bN0M0	57
Patient 238	77	Male	>=5	HCC	II	T2N0M0	14
Patient 239	52	Female	<5	HCC	I	T3N0M0	28
Patient 240	55	Male	<5	HCC	II	T1aN0M0	37
Patient 241	66	Male	<5	HCC	I	T2N0M0	35
Patient 242	60	Male	<5	HCC	II	T1aN0M0	34

Patient 243	74	Male	<5	HCC	III	T4N1M1	30
Patient 244	61	Male	>=5	HCC	II	T2N0M0	22
Patient 245	62	Male	>=5	HCC	I	T2N0M0	28
Patient 246	52	Male	<5	HCC	II	T1aN0M0	9
Patient 247	77	Male	<5	HCC	II	T1aN0M0	28
Patient 248	81	Male	>=5	HCC	II	T1bN0M0	28
Patient 249	62	Male	>=5	HCC	II	T1bN0M0	28
Patient 250	52	Female	>=5	HCC	II	T3N0M0	23
Patient 251	50	Male	>=5	HCC	II	T1bN0M0	18
Patient 252	57	Male	<5	HCC	I	T2N0M0	15
Patient 253	58	Female	>=5	HCC	II	T2N0M0	14
Patient 254	68	Female	>=5	HCC	II	T2N0M0	23
Patient 255	67	Male	<5	HCC	II	T2N0M0	15
Patient 256	70	Male	<5	HCC	III	T2N0M0	47
Patient 257	50	Male	<5	HCC	II	T1aN0M0	45
Patient 258	66	Male	>=5	HCC	II	T2N0M0	8
Patient 259	71	Male	<5	HCC	I	T2N0M0	8
Patient 260	60	Female	>=5	HCC	II	T3N0M0	7
Patient 261	88	Male	<5	HCC	II	T2N0M0	35
Patient 262	48	Male	>=5	HCC	II	T3N0M0	19

Patient 263	70	Male	<5	HCC	I	T2N0M0	17
Patient 264	55	Male	>=5	HCC	II	T3N0M0	34
Patient 265	64	Male	>=5	HCC	II	T2N0M0	19
Patient 266	58	Female	>=5	HCC	II	T4N1M1	31
Patient 267	70	Male	>=5	HCC	II	T1bN0M0	29
Patient 268	64	Male	<5	HCC	III	T3N0M0	17
Patient 269	70	Male	>=5	HCC	II	T2N0M0	22
Patient 270	58	Male	>=5	HCC	II	T3N0M0	22
Patient 271	43	Male	<5	HCC	II	T2N0M0	18
Patient 272	53	Male	>=5	HCC	II	T1bN0M0	16
Patient 273	57	Male	>=5	HCC	II	T2N0M0	16
Patient 274	49	Male	<5	HCC	I	T3N0M0	15
Patient 275	69	Male	>=5	HCC	II	T2N0M0	14
Patient 276	50	Male	>=5	HCC	II	T3N0M0	9
Patient 277	64	Male	>=5	HCC	II	T2N0M0	14
Patient 278	65	Female	>=5	HCC	II	T3N0M0	12
Patient 279	63	Male	<5	HCC	II	T2N0M0	12
Patient 280	52	Male	<5	HCC	I	T2N0M0	12
Patient 281	66	Male	<5	HCC		T2N0M0	11
Patient 282	75	Male	>=5	HCC	II	T3N0M0	10

Patient 283	59	Female	<5	HCC	II	T2N0M0	10
Patient 284	55	Male	>=5	HCC	I	T3N0M0	10
Patient 285	47	Male	>=5	HCC	I	T3N0M0	9
Patient 286	64	Male	>=5	HCC	II	T3N0M0	9
Patient 287	63	Male	>=5	HCC	II	T3N0M0	9
Patient 288	55	Male	>=5	HCC	I	T3N0M0	9
Patient 289	40	Female	>=5	HCC	I	T2N0M0	9

Supplementary Table 2. Sequence of primer for Transgenic mice genotyping, related to Fig. 5, and Fig. S8.

Primers' name	Primers' sequence	Amplified band size
Lyz-cre common	CTTGGGCTGCCAGAATTTCTC	Mutan allele: 700bp
Lyz-cre MT	CCCAGAAATGCCAGATTACG	Wildtype allele: 350bp
Lyz-cre WT	TTACAGTCGGCCAGGCTGAC	
Pax5 flox forward primer (primer 4)	TGCTCATGCACAGAAAAGTGAAAAG	Mutan allele: 219bp
Pax5 flox reverse primer (primer 4)	GTGGATTCCGACCAGTCTGA	Wildtype allele: 152bp
Pax5 flox forward primer (primer 5)	ACGTAAACGGCCACAAGTTC	Mutan allele: 212bp
Pax5 flox reverse primer (primer 5)	AGGAGAGTGAGAAAGGATGAGGTG	Wildtype allele: 156bp
CD19 flox forward primer	AAGCGGATGCCAGACATTGTGG	Mutan allele: 208bp
CD19 flox forward primer	TTCAGATGAGTGGGTGCAGGCTT	Wildtype allele: 140bp

Supplementary Table 3. CytoF antibody panel, related to Fig. 1 and Fig. S2.

Antibodies	Metal	Clone	Source
CD45	89Y	HI30	BioLegend
CD3	115In	UCHT1	BioXcell
CD68	139La	Y1/82A	BioLegend
CD56	141Pr	NCAM16.2	BD Biosciences
CD19	142Nd	HIB19	BioLegend
CD27	143Nd	O323	BioLegend
CD14	144Nd	M5E2	BioLegend
IgD	145Nd	IA6-2	BioLegend
CD123	146Nd	6H6	BioLegend
CD15	147Sm	W6D3	BioLegend
CD33	148Nd	WM53	BioLegend
CD25	149Sm	24212	R&D Systems
CD7	150Nd	CD7-6B7	BioLegend
CD38	151Eu	HIT2	BioLegend
CD103	152Sm	B-Ly7	Ebioscience
CD274 (PD-L1)	153Eu	29E.2A3	BioLegend
CD163	154Sm	GHI/61	BioLegend
CD45RA	155Gd	HI100	BioLegend
CD24	156Gd	ML5	BioLegend
CD172a/b	157Gd	SE5A5	BioLegend
CD197 (CCR7)	158Gd	G043H7	BioLegend
CD11c	159Tb	BU15	BioLegend
CD28	160Gd	CD28.2	BioLegend
CTLA-4	161Dy	14D3	Ebioscience
FoxP3	162Dy	PCH101	BioLegend
CD137 (4-1BB)	163Dy	4B4-1	BioLegend
CD95	164Dy	DX2	BioLegend
IL-1beta	165Ho	8516	R&D Systems
CX3CR1	166Er	K0124E1	BioLegend
CD278(ICOS)	167Er	C398.4A	BioLegend
Tbet	168Er	4B10	BioLegend
Ki-67	169Tm	SolA15	Ebioscience
IL-7Ra(CD127)	170Er	A019D5	BioLegend
Eomes	171Yb	644730	R&D Systems
Tim3	172Yb	F38-2E2	BioLegend
CD154(CD40L)	173Yb	24-31	BioLegend

CD279 (PD-1)	174Yb	EH12.2H7	BioLegend
CD16	175Lu	3G8	BioLegend
HLA-DR	176Yb	L243	BioLegend
CD4	197gd	RPA-T4	BioLegend
CD8a	198pt	RPA-T8	BioLegend
CD11b	209Bi	ICRF44	BioLegend

Supplementary Table 4. CD19 CAR sequences, related to Fig. 2 and Fig. S3.

Nucleotide sequence

ATGGCCTCACCGTTGACCCGCTTTCTGTCGCTGAACCTGCTGCTGCTGGGTGA
GTCGATTATCCTGGGGAGTGGAGAAGCTGAAGTCCAGCTGCAGCAGTCTGGG
GCTGAGCTTGTGAGACCTGGGACCTCTGTGAAGTTATCTTGCAAAGTTTCTGG
CGATACCATTACATTTTACTACATGCACTTTGTGAAGCAAAGGCCTGGACAGGG
TCTGGAATGGATAGGAAGGATTGATCCTGAGGATGAAAGTACTAAATATTCTGA
GAAGTTCAAAAACAAGGCGACACTCACTGCAGATACATCTTCCAACACAGCCTA
CCTGAAGCTCAGCAGCCTGACCTCTGAGGACACTGCAACCTATTTTTGTATCTA
CGGAGGATACTACTTTGATTACTGGGGCCAAGGGGTCATGGTCACAGTCTCCT
CAGGTGGAGGTGGATCAGGTGGAGGTGGATCTGGTGGAGGTGGATCTGACAT
CCAGATGACACAGTCTCCAGCTTCCCTGTCTACATCTCTGGGAGAAACTGTCA
CCATCCAATGTCAAGCAAGTGAGGACATTTACAGTGTTTTAGCGTGGTATCAG
CAGAAGCCAGGGAAATCTCCTCAGCTCCTGATCTATGGTGCAAGTGACTTACA
AGACGGCGTCCATCACGATTCAGTGGCAGTGGATCTGGCACACAGTATTCTC
TCAAGATCACCAGCATGCAAAGTGAAGATGAAGGGGTTTTATTTCTGTCAACAGG
GTTTAACGTATCCTCGGACGTTTCGGTGGCGGCACCAAGCTGGAATTGAAACGG
GCGGCCGCATCTACTACTACCAAGCCAGTGCTGCGAACTCCCTCACCTGTGCA
CCCTACCGGGACATCTCAGCCCCAGAGACCAGAAGATTGTCGGCCCCGTGGC
TCAGTGAAGGGGACCGGATTGGACTTCGCCTGTGATATTTACATCTGGGCACC
CTTGGCCGGAATCTGCGTGGCCCTTCTGCTGTCCTTGATCATCACTCTCATCT
GCTACAATAGTAGAAGGAACAGACTCCTTCAAAGTGACTACATGAACATGACTC
CCCGGAGGCCTGGGCTCACTCGAAAGCCTTACCAGCCCTACGCCCTGCCAG
AGACTTTGCAGCGTACCGCCCCAGAGCAAATTCAGCAGGAGTGCAAGAGACT
GCTGCCAACCTGCAGGACCCCAACCAGCTCTACAATGAGCTCAATCTAGGGCG
AAGAGAGGAATATGACGTCTTGGAGAAGAAGCGGGCTCGCGATCCAGAGATG
GGAGGCAAACAGCAGAGGAGGAGGAACCCCAAGGCGTATACAATGCAC
TGCAGAAAGACAAGATGGCAGAAGCCTACAGTGAGATCGGCACAAAAGGCGA
GAGGCGGAGAGGCAAGGGGCACGATGGCCTTTACCAGGGTCTCAGCACTGCC
ACCAAGGACACCTATGATGCCCTGCATATGCAGACCCTGGCCCCCTCGCTAA

Amino acid sequence

MASPLTRFSLNLLLLGESIILGSGEAEVQLQQSGAELVRPGTSVKLSCKVS
GDTITFYMHFVKQRPGGLEWIGRIDPEDESTKYSEKFNKATLTADTSS
NTAYLKLSSLTSEDATYFCIYGGYFDYWGQGVMVTVSSGGGGSGGGG
SGGGGSDIQMTQSPASLSTSLGETVTIQCQASEDIYSGLAWYQQKPGKSP
QLLIYGASDLQDGVPSRFSGSGSGTQYSLKITSMQTEDEGVYFCQQGLTY
PRTFGGGTKLELKRAAASTTTKPVLRTPSPVHPTGTSQPQRPEDCRPRGS
VKGTGLDFACDIYIWAPLAGICVALLSLIITLICYNRRNRLLQSDYMNMT
RRPGLTRKPYQPYAPARDFAAAYRPAKFSRSAETAANLQDPNQLYNELNL
GRREEYDVLEKKRARDPEMGGKQRRRRNPQEGVYNALQKDKMAEAYSEI
GTKGERRRGKGGHDGLYQGLSTATKDTYDALHMQLAPR

Supplementary Table 5. qRT-PCR Primer sequences, related to Fig. 4 and Fig. 6.

Genes	Species	Forward primer (5'-3')	Reverse primer (5'-3')
<i>NDUFS</i> 8	Human	TCGACATGACCAAGTGCAT C	CCCGTTGTTGAGCAACTTCT
<i>NDUFA</i> 4	Human	AGCAGCACTGTATGTGATG CGC	TGTAGTCCACATTCACAGAG TAGA
<i>NDUFA</i> 9	Human	GCCTATCGATGGGTAGCAA GA	CTTCTAAGCCAGGCAGGTG A
<i>NDUFA</i> 1	Human	TTTTGGCCTAGGTAACGGG G	TGTGGATGTACGCAGTAGC C
<i>NDUFB</i> 2	Human	AGCGGACTCATGTGGTTCT GGA	AGAGTGAGGCTGAGTCTAC ACC
<i>SDHA</i>	Human	GAGATGTGGTGTCTCGGTC CAT	GCTGTCTCTGAAATGCCAG GCA
<i>SDHB</i>	Human	CAATGGAGGCAACACTCTA GCTT	GGAAGAGGGTAGATTTTTG AGACCTT
<i>SDHD</i>	Human	GACTAGCGAGAGGGTTGTC AGTGT	CATCGCAGAGCAAGGATTC A
<i>CYC1</i>	Human	CTACGGACACCTCAGGCAG T	CAGGTCACTGGCACTCACA G
<i>CYCS</i>	Human	GAGGCAAGCATAAGACTGG ACC	ACTCCATCAGGGTATCCTCT CC
<i>UQCR</i> C2	Human	GTGGCATGTAAGAACCAGC A	TCCAACACAGATGTCCAAG C
<i>COX5A</i>	Human	GGGAATTGCGTAAAGGGAT AA	TCCTGCTTTGTCTTAACAA CC
<i>COX5B</i>	Human	AGTCGCCTGCTCTTCATCAG	TGGCTTCAAGGTTACTTCGC
<i>COX6A</i> 1	Human	AGCCAGTTGGAAGTGGATT C	TGTACCTGAAGTCGCACCA C
<i>ATP5G</i> 1	Human	TGAGACCAAGGGCTAAAGC TG	TCAGTCTGCACTCCTACTAC CC
<i>ATP5A</i> 1	Human	AAGACACGCCAGTTTCTTC	TTTGGGTTTCATCTTTCATTG C
<i>ATP5B</i>	Human	CAAGTCATCAGCAGGCACA T	GTGGGCTATCAGCCTACCC T
<i>ATP5E</i>	Human	CTTCAGTGCATCTCTCACTG C	TACAGCATGGTGGCCTACT G
<i>ND1</i>	Human	GGCTATATACTACTACGCAA AGGC	GGTAGATGTGGCGGGTTTT AGG

<i>ND2</i>	Human	CTTCTGAGTCCCAGAGGTTA CC	GAGAGTGAGGAGAAGGCTT ACG
<i>ND3</i>	Human	TTGATCTAGAAATTGCCCTC C	GGCAGGTTAGTTGTTTGTA GG
<i>ND4</i>	Human	CCCTCGTAGTAACAGCCATT CTC	CGACTGTGAGTGCGTTCGT AGT
<i>ND4L</i>	Human	CTCATAACCCTCAACACCCA	AGACTAGTATGGCAATAGG CAC
<i>ND6</i>	Human	GCGATGGCTATTGAGGAGT ATCC	CACAGCACCAATCCTACCT CCA
<i>ATP6</i>	Human	TCCCTCTACACTTATCATCT TCAC	GACAGCGATTTCTAGGATA GTC
<i>ATP8</i>	Human	TAAATACTACCGTATGGCCC AC	GTGATGAGGAATAGTGTA GGAG
<i>ND5</i>	Human	TCTTAGTTACCGCTAACAAC C	ATAATTCCTACGCCCTCTCA G
<i>COX2</i>	Human	ACGCATCCTTTACATAACAG AC	GCCAATTGATTTGATGGTAA GG
<i>COX1</i>	Human	ATATTTACCTCCGCTACCA	TCAGCTAAATACTTTGACGC C
<i>COX3</i>	Human	CTCTCAGCCCTCCTAATGAC	GCGTTATGGAGTGGAAGTG
<i>CYTB</i>	Human	ATCACTTTATTGACTCCTAG CC	TGGTTGTCCTCCGATTCAG
<i>12S/M T- RNR1</i>	Human	AAGATTACACATGCAAGCAT CC	TTGATCGTGGTGATTTAGAG G
<i>16S/M T- RNR2</i>	Human	AACTCGGCAAATCTTACCC	AATACTGGTGATGCTAGAG GTG
<i>PAX5</i>	Human	CTTGCTCATCAAGGTGTCAG GC	TGGCGACCTTTGGTTTGG TCC
<i>CD73</i>	Human	AGTCCACTGGAGAGTTCCT GCA	TGAGAGGGTCATAACTGGG CAC
<i>CD19</i>	Human	GGCTATGAGGAACCTGACA GTG	TCATCCTCAGGGTTCTCGTA GC
<i>PD-L1</i>	Human	GCCGACTACAAGCGAATTA C	TCTCAGTGTGCTGGTCACAT

<i>Pax5</i>	Mouse	ACGTAAACGGCCACAAGTT C	AGGAGAGTGAGAAAGGATG AGGTG
<i>Cd73</i>	Mouse	CGCTCAGAAAGTTCGAGGT GTG	CGCAGGCACTTCTTTGGAA GGT
<i>Cd19</i>	Mouse	GGCACCTATTATTGTCTCCG TGCGGACTACAAGCGAATC	GGGTCAGTCATTCGCTTC CTCAGCTTCTGGATAACCCT
<i>Pd-11</i>	Mouse	ACG	CG

Supplementary Table 6. Differentially expressed genes (DEGs) in CD19+ TAMs, CD19-TAMs, and B cells (data from sc-RNA seq), related to Fig. 3.

Cluster	Gene	Avg_log2FC
CD19- TAMs	S100A9	3.340504294
CD19- TAMs	S100A8	2.930711861
CD19- TAMs	FCN1	2.566707976
CD19- TAMs	LYZ	2.131023307
CD19- TAMs	VCAN	2.080575685
CD19- TAMs	EREG	1.940225065
CD19- TAMs	MNDA	1.642424955
CD19- TAMs	COTL1	1.538471379
CD19- TAMs	G0S2	1.466540093
CD19- TAMs	S100A4	1.444668371
CD19- TAMs	IL1B	1.435207909
CD19- TAMs	LGALS2	1.338150614
CD19- TAMs	AREG	1.335322968
CD19- TAMs	SLC8A1	1.282108583
CD19- TAMs	LST1	1.278503463
CD19- TAMs	TIMP1	1.275011214
CD19- TAMs	S100A6	1.251437828
CD19- TAMs	AOAH	1.212618069
CD19- TAMs	DPYD	1.194388645
CD19- TAMs	BCL2A1	1.192443505
CD19- TAMs	CD52	1.189102179
CD19- TAMs	PLXDC2	1.172425514
CD19- TAMs	SERPINA1	1.124294435
CD19- TAMs	CLEC12A	1.119820159
CD19- TAMs	LYST	1.116733768
CD19- TAMs	CD44	1.098460979
CD19- TAMs	BAG3	1.076846334
CD19- TAMs	NEAT1	1.07568367
CD19- TAMs	JAML	1.072806356
CD19- TAMs	RETN	1.065992664
CD19- TAMs	OLR1	1.057102245
CD19- TAMs	HSPH1	1.056390765
CD19- TAMs	MAML3	1.02137655
CD19- TAMs	ZEB2	1.020788305
CD19- TAMs	CSTA	1.016991289
CD19- TAMs	WARS	1.001425195
CD19- TAMs	SLC2A3	0.995337894

CD19- TAMs	LRRFIP1	0.990029128
CD19- TAMs	LCP1	0.985788879
CD19- TAMs	DNAJA4	0.982852734
CD19- TAMs	S100A10	0.979073318
CD19- TAMs	C1orf162	0.974251251
CD19- TAMs	ARHGAP26	0.974194192
CD19- TAMs	GNAQ	0.95056841
CD19- TAMs	MAP2K1	0.947428329
CD19- TAMs	DNAJB1	0.938068425
CD19- TAMs	ZFAND2A	0.92519094
CD19- TAMs	H3F3A	0.91512567
CD19- TAMs	IFI30	0.914823948
CD19- TAMs	CLEC10A	0.912435883
CD19- TAMs	RTN1	0.88349309
CD19- TAMs	FGD4	0.882660782
CD19- TAMs	HSPD1	0.87024431
CD19- TAMs	C15orf48	0.868163747
CD19- TAMs	PLCB1	0.866398668
CD19- TAMs	PTPRE	0.852584503
CD19- TAMs	SAMHD1	0.844902861
CD19- TAMs	HSP90AA1	0.844124589
CD19- TAMs	SH3BGRL3	0.840692954
CD19- TAMs	FYB1	0.838711669
CD19- TAMs	IRAK3	0.837783119
CD19- TAMs	SLC11A1	0.836157407
CD19- TAMs	SNHG5	0.833479835
CD19- TAMs	JARID2	0.832968847
CD19- TAMs	AIF1	0.828193322
CD19- TAMs	SOD2	0.826088666
CD19- TAMs	ACTB	0.818902612
CD19- TAMs	MXD1	0.818163621
CD19- TAMs	FGR	0.8162538
CD19- TAMs	PLAUR	0.816230435
CD19- TAMs	PTPRC	0.815871218
CD19- TAMs	PTGS2	0.815572563
CD19- TAMs	PLAC8	0.814526183
CD19- TAMs	SLC25A37	0.813378812
CD19- TAMs	FYN	0.812595701
CD19- TAMs	JAK2	0.811804722
CD19- TAMs	TKT	0.810208876
CD19- TAMs	UTRN	0.809378742

CD19- TAMs	GBP1	0.807950619
CD19- TAMs	CORO1A	0.800797112
CD19- TAMs	LRRK2	0.794657026
CD19- TAMs	TYMP	0.791613663
CD19- TAMs	TAOK3	0.789578161
CD19- TAMs	SORL1	0.786968124
CD19- TAMs	RPL39	0.783893524
CD19- TAMs	CSF3R	0.780770778
CD19- TAMs	PPIF	0.779653733
CD19- TAMs	IFITM3	0.778147182
CD19- TAMs	GPCPD1	0.776165165
CD19- TAMs	PSTPIP2	0.776110737
CD19- TAMs	PTMA	0.773133914
CD19- TAMs	ZDHHC20	0.771295364
CD19- TAMs	DOCK8	0.769219503
CD19- TAMs	SSH2	0.769207893
CD19- TAMs	MBNL1	0.766246135
CD19- TAMs	RPS24	0.764929201
CD19- TAMs	AC020916.1	0.760095724
CD19- TAMs	AP1S2	0.755867482
CD19- TAMs	S100A12	0.753151341
CD19- TAMs	PID1	0.751296337
CD19- TAMs	LRMDA	0.750946292
CD19- TAMs	TMSB10	0.750569741
CD19- TAMs	CTSS	0.750144008
CD19- TAMs	TNFSF10	0.749933655
CD19- TAMs	SOCS3	0.742798512
CD19- TAMs	PABPC1	0.741473005
CD19- TAMs	GBP2	0.741089246
CD19- TAMs	ATF3	0.740773983
CD19- TAMs	KYNU	0.738633814
CD19- TAMs	CALHM6	0.733594613
CD19- TAMs	TET2	0.732846447
CD19- TAMs	MYO1F	0.732668426
CD19- TAMs	DENND1A	0.731309165
CD19- TAMs	PPA1	0.725591908
CD19- TAMs	ANXA1	0.72523012
CD19- TAMs	ARL5B	0.719479517
CD19- TAMs	NAP1L1	0.718363661
CD19- TAMs	DOCK5	0.716053775
CD19- TAMs	CFP	0.711703049

CD19- TAMs	SERPINB1	0.711214749
CD19- TAMs	GCH1	0.70698975
CD19- TAMs	FOSL2	0.70589484
CD19- TAMs	FOXP1	0.703475313
CD19- TAMs	SLCO3A1	0.703133546
CD19- TAMs	NCF2	0.702331795
CD19- TAMs	CRIP1	0.698750223
CD19- TAMs	CUX1	0.696713297
CD19- TAMs	TLR2	0.696208661
CD19- TAMs	PRKCB	0.696203778
CD19- TAMs	SMIM25	0.695742541
CD19- TAMs	PSME2	0.688585096
CD19- TAMs	AGTPBP1	0.687591379
CD19- TAMs	CD1C	0.687535002
CD19- TAMs	CHORDC1	0.686965047
CD19- TAMs	UPP1	0.686538669
CD19- TAMs	HSPA1B	0.685883422
CD19- TAMs	TNFRSF1B	0.685020311
CD19- TAMs	S100A11	0.684787866
CD19- TAMs	H2AFY	0.683742274
CD19- TAMs	CFL1	0.682338611
CD19- TAMs	HCK	0.681422849
CD19- TAMs	HSPA8	0.67993017
CD19- TAMs	HSPE1	0.679461891
CD19- TAMs	CD48	0.67933419
CD19- TAMs	CD36	0.678109396
CD19- TAMs	KLF4	0.673971053
CD19- TAMs	TCF7L2	0.673456749
CD19- TAMs	CPPED1	0.67310843
CD19- TAMs	GK	0.668431557
CD19- TAMs	FAM49B	0.667142546
CD19- TAMs	TSPO	0.667118609
CD19- TAMs	NFKBIZ	0.66626754
CD19- TAMs	EFHD2	0.664474704
CD19- TAMs	LYN	0.662491946
CD19- TAMs	PAK1	0.65881822
CD19- TAMs	PLEK	0.656913286
CD19- TAMs	LILRB3	0.656548798
CD19- TAMs	VMP1	0.656118939
CD19- TAMs	TREM1	0.656008696
CD19- TAMs	CMIP	0.655893298

CD19- TAMs	CD300E	0.655407205
CD19- TAMs	RPL23	0.655083512
CD19- TAMs	LIMS1	0.654837901
CD19- TAMs	PRKAG2	0.653754493
CD19- TAMs	MAP3K2	0.650538112
CD19- TAMs	ETV6	0.648961044
CD19- TAMs	CARD16	0.646524565
CD19- TAMs	NR4A1	0.645673748
CD19- TAMs	CLEC7A	0.645508478
CD19- TAMs	SNX10	0.644277936
CD19- TAMs	IL1RN	0.643615361
CD19- TAMs	RPL28	0.643471182
CD19- TAMs	CYBB	0.642319442
CD19- TAMs	FPR1	0.639028408
CD19- TAMs	APBB1IP	0.63862511
CD19- TAMs	DSE	0.637967525
CD19- TAMs	ADGRE2	0.636149846
CD19- TAMs	PTP4A2	0.635029586
CD19- TAMs	DNAJA1	0.634470659
CD19- TAMs	USP15	0.631689736
CD19- TAMs	SLC20A1	0.630571618
CD19- TAMs	VEGFA	0.629590236
CD19- TAMs	PICALM	0.629098201
CD19- TAMs	RIPK2	0.625792528
CD19- TAMs	RPL26	0.623834214
CD19- TAMs	RIPOR2	0.623332642
CD19- TAMs	AQP9	0.619842778
CD19- TAMs	SAT1	0.619377841
CD19- TAMs	UBE2R2	0.616713355
CD19- TAMs	ACTR2	0.616058197
CD19- TAMs	VSIR	0.614779459
CD19- TAMs	ANXA2	0.614692714
CD19- TAMs	RPL37	0.611943772
CD19- TAMs	NUMB	0.611169836
CD19- TAMs	THBS1	0.610680014
CD19- TAMs	STXBP2	0.609931232
CD19- TAMs	DENND5A	0.609836446
CD19- TAMs	DLEU2	0.609187373
CD19- TAMs	RPL36A	0.608676521
CD19- TAMs	LSP1	0.608519808
CD19- TAMs	FBP1	0.607722047

CD19- TAMs	ATP5F1E	0.606704249
CD19- TAMs	TPM3	0.601919071
CD19- TAMs	MEGF9	0.601132637
CD19- TAMs	NLRP3	0.599716798
CD19- TAMs	RPL7	0.59827094
CD19- TAMs	CST3	0.598178698
CD19- TAMs	ENO1	0.598029301
CD19- TAMs	ARPC2	0.597732523
CD19- TAMs	FKBP1A	0.597405114
CD19- TAMs	PLIN2	0.597165714
CD19- TAMs	OSBPL8	0.5968208
CD19- TAMs	ACTR3	0.596252675
CD19- TAMs	ALDH2	0.594965865
CD19- TAMs	DNAJB6	0.592126317
CD19- TAMs	RPL37A	0.59194264
CD19- TAMs	LILRB2	0.589319997
CD19- TAMs	CACYBP	0.589130934
CD19- TAMs	STK38L	0.58778445
CD19- TAMs	IRF1	0.587653568
CD19- TAMs	PFN1	0.587067424
CD19- TAMs	CDC42EP3	0.585443103
CD19- TAMs	PRKCA	0.585328079
CD19- TAMs	CHD1	0.58241754
CD19- TAMs	MCTP1	0.582302031
CD19- TAMs	VIM	0.581882718
CD19- TAMs	SERPINB9	0.58178442
CD19- TAMs	HSPA1A	0.581631525
CD19- TAMs	IL17RA	0.578778933
CD19- TAMs	PTPRJ	0.578164508
CD19- TAMs	FRY	0.577276758
CD19- TAMs	PLSCR1	0.576871251
CD19- TAMs	EMILIN2	0.576621865
CD19- TAMs	CELF2	0.575215209
CD19- TAMs	XYLT1	0.574437035
CD19- TAMs	VASP	0.574321722
CD19- TAMs	BTG1	0.573461281
CD19- TAMs	COP1	0.572231694
CD19- TAMs	GNAI2	0.570741157
CD19- TAMs	HMGN2	0.569578118
CD19- TAMs	TNFSF13B	0.569167049
CD19- TAMs	ZSWIM6	0.568200721

CD19- TAMs	KDM6B	0.568058466
CD19- TAMs	RPS17	0.565380338
CD19- TAMs	SBF2	0.565104081
CD19- TAMs	DDX21	0.564361003
CD19- TAMs	DISC1	0.563277819
CD19- TAMs	RPL4	0.561916849
CD19- TAMs	LINC00278	0.561165868
CD19- TAMs	KDM7A	0.56085421
CD19- TAMs	SULF2	0.560213828
CD19- TAMs	PTEN	0.560086427
CD19- TAMs	TIAM1	0.559339245
CD19- TAMs	CREB5	0.558834397
CD19- TAMs	DIAPH2	0.555819411
CD19- TAMs	LTA4H	0.55447753
CD19- TAMs	YBX1	0.551458813
CD19- TAMs	ARL4A	0.551439951
CD19- TAMs	PTK2B	0.550315231
CD19- TAMs	RPS8	0.548475562
CD19- TAMs	ALOX5	0.547655674
CD19- TAMs	RIN3	0.544888566
CD19- TAMs	RAB11FIP1	0.542917962
CD19- TAMs	TNFSF14	0.542228313
CD19- TAMs	LGALS1	0.542158967
CD19- TAMs	SPTLC2	0.541703254
CD19- TAMs	MSN	0.539305415
CD19- TAMs	ITGAL	0.539016593
CD19- TAMs	TRPS1	0.538172025
CD19- TAMs	PTPN12	0.538128355
CD19- TAMs	TES	0.536849448
CD19- TAMs	LCP2	0.535768481
CD19- TAMs	MBP	0.535473323
CD19- TAMs	EIF4A1	0.535410665
CD19- TAMs	BAZ1A	0.534714436
CD19- TAMs	FBXL5	0.533690596
CD19- TAMs	RPS16	0.533275578
CD19- TAMs	DUSP6	0.533134469
CD19- TAMs	CAST	0.532577999
CD19- TAMs	SRGN	0.53234394
CD19- TAMs	RPS9	0.53224439
CD19- TAMs	ATG3	0.529616394
CD19- TAMs	AHR	0.528794822

CD19- TAMs	RBM3	0.527920123
CD19- TAMs	JMJD1C	0.52724378
CD19- TAMs	GIMAP4	0.526874141
CD19- TAMs	ITGB2	0.526772605
CD19- TAMs	BACH1	0.526334237
CD19- TAMs	DOCK2	0.526320249
CD19- TAMs	GAS7	0.52585517
CD19- TAMs	B4GALT5	0.524488449
CD19- TAMs	UBA52	0.524124138
CD19- TAMs	RGS18	0.523958644
CD19- TAMs	RNF149	0.523315006
CD19- TAMs	ARPC1B	0.521134344
CD19- TAMs	WSB1	0.521104027
CD19- TAMs	SPECC1	0.519928615
CD19- TAMs	FLNA	0.519876283
CD19- TAMs	ARHGDIB	0.519203834
CD19- TAMs	CX3CR1	0.517694221
CD19- TAMs	DIAPH1	0.517313266
CD19- TAMs	MYOF	0.517252489
CD19- TAMs	CKLF	0.516424304
CD19- TAMs	LPCAT2	0.516136451
CD19- TAMs	DMXL2	0.515721399
CD19- TAMs	HNRNPA1	0.515064173
CD19- TAMs	PELI2	0.513718439
CD19- TAMs	CDC42	0.513503966
CD19- TAMs	CGAS	0.513260801
CD19- TAMs	BID	0.513078554
CD19- TAMs	CEBPB	0.512753424
CD19- TAMs	SLC43A2	0.511895907
CD19- TAMs	NOTCH2	0.51125959
CD19- TAMs	CD1E	0.511124549
CD19- TAMs	CD55	0.510785979
CD19- TAMs	RAB31	0.510649582
CD19- TAMs	ACSL4	0.510357907
CD19- TAMs	LITAF	0.509428779
CD19- TAMs	IFITM2	0.509310803
CD19- TAMs	GDI2	0.509190066
CD19- TAMs	TMTC2	0.508563115
CD19- TAMs	CSF2RA	0.506941281
CD19- TAMs	CASP1	0.506101901
CD19- TAMs	AC009093.2	0.505772992

CD19- TAMs	STK17B	0.504399124
CD19- TAMs	HIPK3	0.504275475
CD19- TAMs	C9orf72	0.504211902
CD19- TAMs	JAZF1	0.503989591
CD19- TAMs	CTNND1	0.503891304
CD19- TAMs	HCST	0.503431773
CD19- TAMs	PRAM1	0.502768543
CD19- TAMs	RPLP2	0.502456507
CD19- TAMs	ATP5MC2	0.501871874
CD19- TAMs	PRELID1	0.500708567
CD19- TAMs	RPS13	0.500518235
CD19- TAMs	MYADM	0.500498868
CD19- TAMs	RPS2	0.49949985
CD19- TAMs	ACTG1	0.498846454
CD19- TAMs	UBE2D1	0.498176233
CD19- TAMs	RCOR1	0.497693068
CD19- TAMs	B3GNT5	0.497500457
CD19- TAMs	GABARAPL1	0.497125983
CD19- TAMs	ITGAX	0.496880942
CD19- TAMs	SLC25A5	0.496574904
CD19- TAMs	GLIPR2	0.496036799
CD19- TAMs	KCNE1	0.495921253
CD19- TAMs	CTSH	0.494177615
CD19- TAMs	MRPL18	0.492778904
CD19- TAMs	USP3	0.491877217
CD19- TAMs	USP32	0.491862682
CD19- TAMs	STX11	0.491378846
CD19- TAMs	HNRNPU	0.490655727
CD19- TAMs	TUT7	0.490549614
CD19- TAMs	MED13L	0.490243724
CD19- TAMs	DOK2	0.488374472
CD19- TAMs	ELF2	0.487282345
CD19- TAMs	LDLR	0.486523953
CD19- TAMs	CTBP2	0.485869465
CD19- TAMs	APOBEC3A	0.485545692
CD19- TAMs	LAP3	0.485270992
CD19- TAMs	RPL38	0.485058697
CD19- TAMs	STAT1	0.483268956
CD19- TAMs	RPL34	0.482586873
CD19- TAMs	USP25	0.482334879
CD19- TAMs	ABR	0.482207314

CD19- TAMs	TBXAS1	0.481482125
CD19- TAMs	SPI1	0.480600288
CD19- TAMs	PSMA4	0.478856696
CD19- TAMs	YBX3	0.477438897
CD19- TAMs	TNFAIP6	0.475757908
CD19- TAMs	LMO2	0.474984479
CD19- TAMs	IFNGR1	0.47460676
CD19- TAMs	RHOA	0.47416232
CD19- TAMs	RPS29	0.473783013
CD19- TAMs	WAS	0.47256834
CD19- TAMs	ANXA5	0.470889337
CD19- TAMs	ATP11A	0.470885033
CD19- TAMs	GPAT3	0.470572528
CD19- TAMs	RPS11	0.470566689
CD19- TAMs	POU2F2	0.470446453
CD19- TAMs	RYBP	0.470299999
CD19- TAMs	MTPN	0.469096365
CD19- TAMs	ATP13A3	0.466979548
CD19- TAMs	HRH2	0.466927381
CD19- TAMs	NKRF	0.466785607
CD19- TAMs	COMMD6	0.464410243
CD19- TAMs	ALAS1	0.464277706
CD19- TAMs	SPAG9	0.464233179
CD19- TAMs	TPI1	0.463933251
CD19- TAMs	RPL31	0.462542233
CD19- TAMs	RPL27	0.462248123
CD19- TAMs	RPL12	0.460837501
CD19- TAMs	RPL32	0.460597357
CD19- TAMs	RILPL2	0.458164856
CD19- TAMs	PCBP1	0.457723588
CD19- TAMs	ARPC5	0.457600655
CD19- TAMs	PKM	0.457555084
CD19- TAMs	GAPT	0.456608073
CD19- TAMs	LDLRAD3	0.456557162
CD19- TAMs	EVI2B	0.456271502
CD19- TAMs	GAPDH	0.455827192
CD19- TAMs	STK10	0.45581856
CD19- TAMs	ZNF710	0.455066809
CD19- TAMs	COX7B	0.455064234
CD19- TAMs	HMGB2	0.454547357
CD19- TAMs	RPS6KA3	0.452776197

CD19- TAMs	DEK	0.452580493
CD19- TAMs	SNAP23	0.450902537
CD19- TAMs	RPL18A	0.450826599
CD19- TAMs	ACAP2	0.450162233
CD19- TAMs	OGFRL1	0.449411807
CD19- TAMs	LILRB1	0.449309576
CD19- TAMs	EIF3L	0.448977884
CD19- TAMs	PYCARD	0.447456137
CD19- TAMs	TET3	0.4469606
CD19- TAMs	TCP1	0.446492966
CD19- TAMs	SH3KBP1	0.446212239
CD19- TAMs	RPL6	0.444162817
CD19- TAMs	GPBP1	0.444027922
CD19- TAMs	RAB10	0.442712418
CD19- TAMs	PSME1	0.441156405
CD19- TAMs	RPL27A	0.440352062
CD19- TAMs	MAPK14	0.439870402
CD19- TAMs	YWHAB	0.439786393
CD19- TAMs	COX8A	0.438660102
CD19- TAMs	PGK1	0.438138835
CD19- TAMs	SRSF3	0.437923589
CD19- TAMs	CMTM6	0.437806426
CD19- TAMs	KIF13A	0.436188013
CD19- TAMs	UBAC2	0.435319164
CD19- TAMs	TMEM170B	0.43498949
CD19- TAMs	SNAI1	0.434326312
CD19- TAMs	AC090559.1	0.434260514
CD19- TAMs	ADGRE5	0.433561375
CD19- TAMs	PLEKHO1	0.433385563
CD19- TAMs	FTH1	0.432785723
CD19- TAMs	FAM102B	0.432125124
CD19- TAMs	PHACTR2	0.431421212
CD19- TAMs	ANKRD22	0.431018135
CD19- TAMs	SHTN1	0.42976777
CD19- TAMs	BCL10	0.428811129
CD19- TAMs	PLXNC1	0.428705234
CD19- TAMs	ARPC3	0.427276281
CD19- TAMs	SRGAP2	0.427266952
CD19- TAMs	GRK3	0.426867096
CD19- TAMs	TMSB4X	0.425483346
CD19- TAMs	LIMD2	0.425037395

CD19- TAMs	ZFAS1	0.424539898
CD19- TAMs	MBOAT7	0.423792743
CD19- TAMs	MAP3K20	0.423139005
CD19- TAMs	METRNL	0.422674055
CD19- TAMs	LUCAT1	0.421234469
CD19- TAMs	HIF1A	0.421007539
CD19- TAMs	IPCEF1	0.42044749
CD19- TAMs	FMNL1	0.420128609
CD19- TAMs	ATP5MPL	0.420024453
CD19- TAMs	RPL22	0.419805269
CD19- TAMs	EMP3	0.418513372
CD19- TAMs	SPN	0.415697391
CD19- TAMs	ROCK1	0.415387643
CD19- TAMs	SCLT1	0.415306435
CD19- TAMs	WAC	0.415024171
CD19- TAMs	RAP1A	0.415005363
CD19- TAMs	PILRA	0.414955862
CD19- TAMs	PSEN1	0.414542674
CD19- TAMs	GRB2	0.414390945
CD19- TAMs	CCNY	0.413842109
CD19- TAMs	MYO1G	0.412755416
CD19- TAMs	ADAM17	0.41222379
CD19- TAMs	RNF213	0.411943335
CD19- TAMs	EIF3A	0.410959095
CD19- TAMs	FGL2	0.410954447
CD19- TAMs	ANP32B	0.410541663
CD19- TAMs	HK1	0.410472451
CD19- TAMs	STK38	0.408838331
CD19- TAMs	RAP1GAP2	0.407905149
CD19- TAMs	ATAD2B	0.40730907
CD19- TAMs	RAB7A	0.406075273
CD19- TAMs	CAP1	0.405732041
CD19- TAMs	CBL	0.405603968
CD19- TAMs	GIMAP7	0.405163016
CD19- TAMs	IFNGR2	0.404782409
CD19- TAMs	GLIPR1	0.404380843
CD19- TAMs	CD86	0.404051435
CD19- TAMs	LHFPL6	0.404015313
CD19- TAMs	SKAP2	0.404012695
CD19- TAMs	ZYX	0.403657043
CD19- TAMs	PACSIN2	0.402695878

CD19- TAMs	MYD88	0.402624122
CD19- TAMs	CD300A	0.40258566
CD19- TAMs	GPR132	0.402321983
CD19- TAMs	PPP1R12A	0.402001696
CD19- TAMs	DPYSL2	0.401707229
CD19- TAMs	TACC1	0.401542055
CD19- TAMs	PSMB9	0.400934471
CD19- TAMs	PEA15	0.400917827
CD19- TAMs	LINC02432	0.399051634
CD19- TAMs	PFKFB3	0.398132369
CD19- TAMs	CERS6	0.397969789
CD19- TAMs	PIP4K2A	0.397911003
CD19- TAMs	EIF3H	0.3972646
CD19- TAMs	DDX60L	0.396726982
CD19- TAMs	TOM1	0.396202995
CD19- TAMs	PAK2	0.396069438
CD19- TAMs	ANP32A	0.395979291
CD19- TAMs	KCNAB2	0.395884018
CD19- TAMs	CSNK1A1	0.395718737
CD19- TAMs	HNRNPA3	0.395208075
CD19- TAMs	MX2	0.394926101
CD19- TAMs	PIK3CB	0.394911052
CD19- TAMs	RNF19B	0.39486896
CD19- TAMs	ATP1A1	0.394584041
CD19- TAMs	ATP6V0D1	0.394167174
CD19- TAMs	ADD3	0.393558662
CD19- TAMs	CLEC4A	0.393394866
CD19- TAMs	SLC25A6	0.392855019
CD19- TAMs	ATP5MG	0.392308617
CD19- TAMs	SFPQ	0.392046221
CD19- TAMs	ITPR1	0.391494215
CD19- TAMs	CD300LB	0.390637382
CD19- TAMs	RAC1	0.39049483
CD19- TAMs	CSGALNACT2	0.390154843
CD19- TAMs	RNF130	0.390061964
CD19- TAMs	LACTB	0.389648845
CD19- TAMs	GNG5	0.388803053
CD19- TAMs	MIR181A1HG	0.388441255
CD19- TAMs	ARL8B	0.387921158
CD19- TAMs	YWHAZ	0.387631423
CD19- TAMs	HIGD2A	0.387287989

CD19- TAMs	ARRB1	0.386914158
CD19- TAMs	MAP2K3	0.386846227
CD19- TAMs	ETS2	0.386077213
CD19- TAMs	TGFBI	0.385666306
CD19- TAMs	KDM1B	0.385073327
CD19- TAMs	HNRNPC	0.384997729
CD19- TAMs	ATP6V1B2	0.384326996
CD19- TAMs	CCDC88A	0.384192372
CD19- TAMs	SMCO4	0.384058137
CD19- TAMs	HNRNPAB	0.384038798
CD19- TAMs	PNPLA8	0.383733027
CD19- TAMs	MOB1A	0.383378396
CD19- TAMs	ACTN1	0.382948001
CD19- TAMs	HSBP1	0.382923649
CD19- TAMs	RPS15	0.382424687
CD19- TAMs	PLBD1	0.382376277
CD19- TAMs	PREX1	0.381951517
CD19- TAMs	PRR13	0.38105791
CD19- TAMs	ZNF516	0.380695085
CD19- TAMs	XRN2	0.380611409
CD19- TAMs	EIF3M	0.380041562
CD19- TAMs	REL	0.378204555
CD19- TAMs	SESTD1	0.378128438
CD19- TAMs	ABRACL	0.377973699
CD19- TAMs	SLA	0.376864402
CD19- TAMs	SEC11A	0.376261113
CD19- TAMs	CAPZA1	0.376086687
CD19- TAMs	CD1D	0.375675691
CD19- TAMs	VAMP8	0.374636761
CD19- TAMs	GABARAP	0.374306997
CD19- TAMs	RSL1D1	0.373852055
CD19- TAMs	RIOK3	0.373849471
CD19- TAMs	TP53BP2	0.373476655
CD19- TAMs	PFDN5	0.373373616
CD19- TAMs	COX5B	0.372422937
CD19- TAMs	DNAJC7	0.370912597
CD19- TAMs	RPL35A	0.37078677
CD19- TAMs	IL13RA1	0.370764423
CD19- TAMs	ZBTB43	0.370655616
CD19- TAMs	PLK3	0.370314133
CD19- TAMs	RNF144B	0.370220059

CD19- TAMs	HCAR3	0.369986517
CD19- TAMs	COX6B1	0.369607417
CD19- TAMs	RHOG	0.368639224
CD19- TAMs	CPVL	0.368527462
CD19- TAMs	S100Z	0.368379055
CD19- TAMs	RBM47	0.3681617
CD19- TAMs	RAP1B	0.368157052
CD19- TAMs	GNA15	0.368064849
CD19- TAMs	PGLS	0.36769789
CD19- TAMs	KSR1	0.367418241
CD19- TAMs	FAR1	0.367357175
CD19- TAMs	PSMB10	0.366717621
CD19- TAMs	VASH1	0.366607992
CD19- TAMs	NACA	0.366387755
CD19- TAMs	AGO4	0.366322189
CD19- TAMs	FAM120A	0.36631059
CD19- TAMs	OXSR1	0.366274115
CD19- TAMs	EVI2A	0.365951195
CD19- TAMs	CRYBG1	0.365754239
CD19- TAMs	PRRG4	0.365614889
CD19- TAMs	APAF1	0.36542648
CD19- TAMs	CNN2	0.364498651
CD19- TAMs	THAP9-AS1	0.364366597
CD19- TAMs	ZNF385A	0.363265957
CD19- TAMs	SH3BGRL	0.363123566
CD19- TAMs	ETF1	0.362726982
CD19- TAMs	NSA2	0.360535649
CD19- TAMs	GMFG	0.359957628
CD19- TAMs	PDLIM5	0.359668903
CD19- TAMs	BZW1	0.359648651
CD19- TAMs	VCL	0.35912458
CD19- TAMs	PHC2	0.358689371
CD19- TAMs	SPOPL	0.357037596
CD19- TAMs	NAMPT	0.356859088
CD19- TAMs	CDC42EP2	0.354955721
CD19- TAMs	MAP3K3	0.35486751
CD19- TAMs	ZMIZ1	0.354271092
CD19- TAMs	GSTO1	0.354034091
CD19- TAMs	HMGA1	0.353946987
CD19- TAMs	ASGR1	0.353672773
CD19- TAMs	ZNF207	0.353622919

CD19- TAMs	SNTB1	0.35290511
CD19- TAMs	UBE2W	0.352474922
CD19- TAMs	TRERF1	0.351398201
CD19- TAMs	SVIL	0.351363661
CD19- TAMs	CASP4	0.350583919
CD19- TAMs	CLEC4E	0.349596941
CD19- TAMs	RNF24	0.348851266
CD19- TAMs	RHOQ	0.348778195
CD19- TAMs	BCL6	0.348654988
CD19- TAMs	PALLD	0.348243357
CD19- TAMs	ST3GAL6	0.347463573
CD19- TAMs	IGF2BP2	0.347423295
CD19- TAMs	SNRPF	0.347342307
CD19- TAMs	NCOR2	0.346947268
CD19- TAMs	RPL35	0.346499526
CD19- TAMs	GNB1	0.346297937
CD19- TAMs	NUDT16	0.344311862
CD19- TAMs	CPD	0.343979088
CD19- TAMs	SNHG16	0.342968699
CD19- TAMs	HDAC4	0.342915852
CD19- TAMs	ZNF267	0.342134108
CD19- TAMs	OSCAR	0.341748228
CD19- TAMs	AP2S1	0.341202007
CD19- TAMs	CD300LF	0.341060829
CD19- TAMs	HCLS1	0.341034533
CD19- TAMs	LRG1	0.339140506
CD19- TAMs	PHF20L1	0.33901375
CD19- TAMs	GLT1D1	0.338905076
CD19- TAMs	ANPEP	0.338598043
CD19- TAMs	HNRNPD	0.338545039
CD19- TAMs	STX6	0.337143374
CD19- TAMs	LAT2	0.337074748
CD19- TAMs	TRAF3IP3	0.336912304
CD19- TAMs	SLC24A4	0.336535824
CD19- TAMs	CAPNS1	0.336424717
CD19- TAMs	SPATA13	0.335640924
CD19- TAMs	CCT5	0.3354022
CD19- TAMs	POLR1D	0.335330432
CD19- TAMs	FCGR1A	0.333385997
CD19- TAMs	LATS2	0.333244367
CD19- TAMs	MBD2	0.332960025

CD19- TAMs	CRISPLD2	0.332396002
CD19- TAMs	ABI3	0.332333178
CD19- TAMs	RELT	0.331860145
CD19- TAMs	NDRG1	0.331680272
CD19- TAMs	ZNF106	0.331673278
CD19- TAMs	QKI	0.331526113
CD19- TAMs	CD302	0.330938254
CD19- TAMs	TSPAN14	0.330817481
CD19- TAMs	HADHA	0.33048219
CD19- TAMs	IL6R	0.329268926
CD19- TAMs	ELOB	0.32855036
CD19- TAMs	NFIL3	0.327960999
CD19- TAMs	LILRA5	0.327835442
CD19- TAMs	CDA	0.327665299
CD19- TAMs	ITGA5	0.325537255
CD19- TAMs	SCO2	0.325493764
CD19- TAMs	CCT6A	0.324854975
CD19- TAMs	HK2	0.324685996
CD19- TAMs	BIN2	0.323669387
CD19- TAMs	DAZAP2	0.323556132
CD19- TAMs	NMI	0.323496903
CD19- TAMs	BZW2	0.32327998
CD19- TAMs	RCBTB2	0.322632135
CD19- TAMs	RTN4	0.322196463
CD19- TAMs	MCUB	0.321382548
CD19- TAMs	RASSF5	0.320953173
CD19- TAMs	PARVG	0.320245207
CD19- TAMs	AC015871.7	0.319487191
CD19- TAMs	CHMP4B	0.319125954
CD19- TAMs	PLA2G4A	0.318821961
CD19- TAMs	DYNC1LI1	0.318166922
CD19- TAMs	C19orf38	0.317573944
CD19- TAMs	MAPK1	0.316380002
CD19- TAMs	PCSK5	0.316312176
CD19- TAMs	NDUFB1	0.315770375
CD19- TAMs	CYB5R4	0.315723646
CD19- TAMs	ERICH1	0.315470198
CD19- TAMs	ZC3H12A	0.315077666
CD19- TAMs	AL138899.1	0.314842413
CD19- TAMs	VPS35	0.314565447
CD19- TAMs	OAZ1	0.314126126

CD19- TAMs	TMEM71	0.312360584
CD19- TAMs	LAMTOR4	0.311281019
CD19- TAMs	SERF2	0.310678883
CD19- TAMs	CCDC26	0.310163181
CD19- TAMs	MEFV	0.309374257
CD19- TAMs	ACAA1	0.309047484
CD19- TAMs	TMA7	0.308306722
CD19- TAMs	KIAA0513	0.307936172
CD19- TAMs	SIRPB1	0.307498953
CD19- TAMs	RPS28	0.307465037
CD19- TAMs	NUP214	0.306733043
CD19- TAMs	POLE4	0.30383542
CD19- TAMs	SLC2A6	0.303104943
CD19- TAMs	MIS18BP1	0.302888012
CD19- TAMs	ACOT9	0.302696979
CD19- TAMs	ECHDC1	0.301029725
CD19- TAMs	SH3BP2	0.300700626
CD19- TAMs	RAB32	0.299506711
CD19- TAMs	GCA	0.298262411
CD19- TAMs	RASSF2	0.298052399
CD19- TAMs	PTGIR	0.297861641
CD19- TAMs	SGMS2	0.297393317
CD19- TAMs	SNX27	0.295057232
CD19- TAMs	SECTM1	0.294935179
CD19- TAMs	LINC00877	0.294526319
CD19- TAMs	STK26	0.290191062
CD19- TAMs	STMP1	0.288166695
CD19- TAMs	TTC39C	0.286829307
CD19- TAMs	DENND10	0.28591409
CD19- TAMs	AL034397.3	0.285394597
CD19- TAMs	HDGF	0.28494395
CD19- TAMs	GRAMD1B	0.28353345
CD19- TAMs	LYSMD2	0.282283901
CD19- TAMs	VDR	0.279549551
CD19- TAMs	LFNG	0.279376687
CD19- TAMs	STAT6	0.277004236
CD19- TAMs	ZDHHC7	0.276434444
CD19- TAMs	AGTRAP	0.276350086
CD19- TAMs	PKP2	0.276105087
CD19- TAMs	MPP7	0.275726332
CD19- TAMs	LILRA1	0.273949584

CD19- TAMs	PSTPIP1	0.271772001
CD19- TAMs	PGD	0.271145573
CD19- TAMs	ARRB2	0.26653568
CD19- TAMs	FFAR2	0.266522059
CD19- TAMs	MARCO	0.266161035
CD19- TAMs	CAMKK2	0.265401797
CD19- TAMs	IL27RA	0.262745112
CD19- TAMs	NRGN	0.261376001
CD19- TAMs	CYSLTR2	0.260715762
CD19- TAMs	PRKACA	0.258131576
CD19- TAMs	BST1	0.254079936
CD19- TAMs	CCR2	0.252923175
CD19- TAMs	RPS12	0.397686334
CD19- TAMs	SAP30	0.455389975
CD19- TAMs	STIP1	0.340635656
CD19- TAMs	CSK	0.289364389
CD19- TAMs	C20orf27	0.265428633
CD19- TAMs	PADI2	0.360576263
CD19- TAMs	UBAP1	0.409590931
CD19- TAMs	RPL29	0.397254841
CD19- TAMs	SYAP1	0.387948543
CD19- TAMs	VAMP5	0.44504612
CD19- TAMs	TMPO	0.334774986
CD19- TAMs	KHDRBS1	0.329242701
CD19- TAMs	RPS15A	0.354701142
CD19- TAMs	FOXN2	0.335499975
CD19- TAMs	ITGA4	0.407363175
CD19- TAMs	CAPZA2	0.290610637
CD19- TAMs	MYL12B	0.319679451
CD19- TAMs	TMEM165	0.344725027
CD19- TAMs	AL138720.1	0.358288522
CD19- TAMs	CLK1	0.409563733
CD19- TAMs	SLC7A7	0.300227447
CD19- TAMs	RBPJ	0.324156048
CD19- TAMs	TMOD3	0.311615531
CD19- TAMs	PRKAR2B	0.356722451
CD19- TAMs	AZI2	0.284401899
CD19- TAMs	SLC6A6	0.274340678
CD19- TAMs	PSMA6	0.344134708
CD19- TAMs	XPO1	0.341002128
CD19- TAMs	IER5	0.624692148

CD19- TAMs	EIF4G2	0.375254233
CD19- TAMs	CIITA	0.439433492
CD19- TAMs	BRI3	0.2515886
CD19- TAMs	ARHGAP31	0.410379503
CD19- TAMs	UVRAG	0.424579509
CD19- TAMs	ENGASE	0.412974203
CD19- TAMs	PTPN2	0.316964217
CD19- TAMs	RPS14	0.370894473
CD19- TAMs	TBC1D8	0.335121554
CD19- TAMs	ARPC4	0.318745627
CD19- TAMs	PTGES3	0.445246691
CD19- TAMs	SIGLEC10	0.279824328
CD19- TAMs	TNFAIP3	0.392692554
CD19- TAMs	LSM6	0.272977842
CD19- TAMs	FLVCR2	0.274112849
CD19- TAMs	MOB3A	0.310220301
CD19- TAMs	FAM117B	0.292712517
CD19- TAMs	MARCKSL1	0.280701646
CD19- TAMs	MYO9B	0.372199021
CD19- TAMs	ABHD5	0.321449027
CD19- TAMs	C17orf49	0.324184396
CD19- TAMs	1-Mar	0.341480148
CD19- TAMs	SIPA1L1	0.672282129
CD19- TAMs	IRS2	0.351839858
CD19- TAMs	FKBP4	0.522971003
CD19- TAMs	RHOT1	0.279231521
CD19- TAMs	COX7C	0.31513449
CD19- TAMs	MTMR3	0.334562664
CD19- TAMs	RPS27	0.378680518
CD19- TAMs	PTPN18	0.263551762
CD19- TAMs	HSPA6	0.803196892
CD19- TAMs	TRA2B	0.398892699
CD19- TAMs	ASAP1	0.488892965
CD19- TAMs	CUL1	0.369681537
CD19- TAMs	ZFAND3	0.576354311
CD19- TAMs	TBC1D2	0.266724822
CD19- TAMs	PPIA	0.405988077
CD19- TAMs	YWHAG	0.339412838
CD19- TAMs	NFE2L2	0.351629882
CD19- TAMs	SLC8B1	0.366804211
CD19- TAMs	IQGAP1	0.264952262

CD19- TAMs	WNK1	0.33933174
CD19- TAMs	JOSD1	0.336035138
CD19- TAMs	CLEC5A	0.309082359
CD19- TAMs	ADA2	0.309178171
CD19- TAMs	RGS2	0.391424451
CD19- TAMs	BTF3	0.383026245
CD19- TAMs	RPS20	0.382876939
CD19- TAMs	DAPK1	0.302950022
CD19- TAMs	CAMK1	0.282488165
CD19- TAMs	DENND3	0.342551335
CD19- TAMs	SP110	0.294898612
CD19- TAMs	LRRC25	0.278776366
CD19- TAMs	XAF1	0.30347961
CD19- TAMs	LGALS9	0.284754517
CD19- TAMs	CYTH1	0.423102725
CD19- TAMs	RPL30	0.367453217
CD19- TAMs	TPM4	0.355293758
CD19- TAMs	TAX1BP1	0.301378183
CD19- TAMs	MAP3K5	0.409008166
CD19- TAMs	HNRNPK	0.334386477
CD19- TAMs	SYF2	0.299938584
CD19- TAMs	TMEM167A	0.28119852
CD19- TAMs	NFAT5	0.57398145
CD19- TAMs	APOL3	0.259926147
CD19- TAMs	TCIRG1	0.260243514
CD19- TAMs	PSMB3	0.30826652
CD19- TAMs	HES4	0.458668898
CD19- TAMs	TBC1D1	0.340526636
CD19- TAMs	MICU1	0.377828504
CD19- TAMs	ADSS	0.253093186
CD19- TAMs	HBEGF	0.55542621
CD19- TAMs	IL15	0.307099188
CD19- TAMs	MRTFA	0.373190633
CD19- TAMs	PGAM1	0.300290681
CD19- TAMs	CSRNP1	0.305797002
CD19- TAMs	COX4I1	0.325504508
CD19- TAMs	TRIM25	0.265371018
CD19- TAMs	DOCK10	0.58552555
CD19- TAMs	ACER3	0.355188345
CD19- TAMs	LRRFIP2	0.312234998
CD19- TAMs	KMT2C	0.444454417

CD19- TAMs	SCIMP	0.26806365
CD19- TAMs	ARID1A	0.298422171
CD19- TAMs	MARK2	0.251087324
CD19- TAMs	TNFRSF10B	0.409730007
CD19- TAMs	TMEM131L	0.455874311
CD19- TAMs	MT2A	0.262447408
CD19- TAMs	IER3	0.427349991
CD19- TAMs	SLC25A25	0.337261133
CD19- TAMs	SEMA4D	0.295275362
CD19- TAMs	VDAC1	0.341128579
CD19- TAMs	RP2	0.25561748
CD19- TAMs	SET	0.371299997
CD19- TAMs	EIF3K	0.365064233
CD19- TAMs	CPQ	0.337756017
CD19- TAMs	ENY2	0.312881971
CD19- TAMs	ADAM10	0.353180115
CD19- TAMs	BCL11A	0.280757355
CD19- TAMs	TFCP2	0.299437599
CD19- TAMs	MTHFD2	0.326918
CD19- TAMs	YY1	0.303139174
CD19- TAMs	HIVEP3	0.338637694
CD19- TAMs	SLC25A13	0.31400404
CD19- TAMs	ACTN4	0.259114835
CD19- TAMs	SKIL	0.400355519
CD19- TAMs	NFKBIE	0.287719
CD19- TAMs	PPP1R15A	0.52838111
CD19- TAMs	CXCL8	0.827951501
CD19- TAMs	GRASP	0.343187755
CD19- TAMs	LIMK2	0.268814438
CD19- TAMs	SCAF11	0.295087921
CD19- TAMs	PRKCE	0.517725477
CD19- TAMs	FAM49A	0.336624116
CD19- TAMs	SMAD3	0.300359333
CD19- TAMs	FLOT1	0.297919002
CD19- TAMs	LDHA	0.420468894
CD19- TAMs	LDLRAD4	0.341114431
CD19- TAMs	BAZ2B	0.358606494
CD19- TAMs	DUSP1	0.592620584
CD19- TAMs	SKI	0.311673381
CD19- TAMs	PSMA7	0.365719785
CD19- TAMs	RPS26	0.434303506

CD19- TAMs	MIDN	0.353936933
CD19- TAMs	AGPAT3	0.264595454
CD19- TAMs	CBX3	0.28424595
CD19- TAMs	HSPA1L	0.282717756
CD19- TAMs	GBP4	0.339504559
CD19- TAMs	PLEKHB2	0.287225058
CD19- TAMs	TAF15	0.271900555
CD19- TAMs	HNRNPA2B1	0.299503076
CD19- TAMs	LINC01578	0.317928666
CD19- TAMs	RASGEF1B	0.407712283
CD19- TAMs	DYNLT1	0.258378976
CD19- TAMs	USP10	0.251120717
CD19- TAMs	RPL36	0.258751714
CD19- TAMs	DEDD2	0.294537542
CD19- TAMs	STK3	0.35916867
CD19- TAMs	HSD17B11	0.260097461
CD19- TAMs	SRRM1	0.303001858
CD19- TAMs	LRRC8D	0.299988846
CD19- TAMs	PITPNA	0.297467371
CD19- TAMs	EIF3E	0.342517879
CD19- TAMs	GAB2	0.390726518
CD19- TAMs	NIPBL	0.349880606
CD19- TAMs	BANF1	0.286159594
CD19- TAMs	FNIP2	0.28462891
CD19- TAMs	RPL24	0.303738382
CD19- TAMs	ZC3H15	0.291215229
CD19- TAMs	CAMK2D	0.67143355
CD19- TAMs	PAG1	0.350173571
CD19- TAMs	DUSP10	0.293753927
CD19- TAMs	ST6GALNAC3	0.397448673
CD19- TAMs	ZBTB7A	0.298111642
CD19- TAMs	RASSF3	0.356232497
CD19- TAMs	CHP1	0.252419868
CD19- TAMs	LAPTM5	0.257408315
CD19- TAMs	SERBP1	0.340617923
CD19- TAMs	NAA38	0.252223408
CD19- TAMs	ZBTB16	0.655194002
CD19- TAMs	WTAP	0.287026252
CD19- TAMs	FKBP15	0.253024783
CD19- TAMs	UQCRB	0.293893967
CD19- TAMs	GCNT2	0.278855007

CD19- TAMs	TRIM38	0.314057703
CD19- TAMs	ATP5PD	0.287617004
CD19- TAMs	NAAA	0.266159128
CD19- TAMs	PSMB8	0.326597465
CD19- TAMs	DNMT1	0.284474995
CD19- TAMs	HNRNPF	0.286132825
CD19- TAMs	MYH9	0.293356568
CD19- TAMs	EPB41L3	0.264361524
CD19- TAMs	PRPF40A	0.325468282
CD19- TAMs	LPGAT1	0.282692157
CD19- TAMs	EIF3F	0.318647798
CD19- TAMs	JPT1	0.289645932
CD19- TAMs	MICOS10	0.306520326
CD19- TAMs	AMD1	0.334316409
CD19- TAMs	RPS6KC1	0.309022162
CD19- TAMs	PPP2R2A	0.280373475
CD19- TAMs	PHACTR1	0.413881489
CD19- TAMs	DDX5	0.319197093
CD19- TAMs	TSC22D2	0.326925536
CD19- TAMs	SYK	0.349151851
CD19- TAMs	IL10RB	0.254700955
CD19- TAMs	CERT1	0.298619934
CD19- TAMs	EHD1	0.27497228
CD19- TAMs	CALCOCO2	0.25530156
CD19- TAMs	AKAP13	0.29952939
CD19- TAMs	RPS21	0.292192776
CD19- TAMs	MID1IP1	0.315318537
CD19- TAMs	PECAM1	0.344962088
CD19- TAMs	MORF4L1	0.284863952
CD19- TAMs	PHF21A	0.4261191
CD19- TAMs	SNRPE	0.267534642
CD19- TAMs	MIER1	0.260813915
CD19- TAMs	EPSTI1	0.350844347
CD19- TAMs	RPS19	0.304375411
CD19- TAMs	TWISTNB	0.680905968
CD19- TAMs	APP	0.315582578
CD19- TAMs	ATP5PB	0.300016171
CD19- TAMs	LAMTOR2	0.303393062
CD19- TAMs	RGS19	0.265591059
CD19- TAMs	AC016831.5	0.392771359
CD19- TAMs	PPT1	0.264024641

CD19- TAMs	ATP5F1C	0.285720397
CD19- TAMs	CEBPD	0.253504108
CD19- TAMs	RPLP1	0.251482713
CD19- TAMs	TAOK1	0.300824651
CD19- TAMs	ZNF217	0.269316316
CD19- TAMs	RIN2	0.279584821
CD19- TAMs	HSPB1	0.485929063
CD19- TAMs	DRAP1	0.292796249
CD19- TAMs	MARK3	0.311889779
CD19- TAMs	NDUFB2	0.304398408
CD19- TAMs	GPSM3	0.251750171
CD19- TAMs	EEF1A1	0.369544485
CD19- TAMs	SOAT1	0.295654371
CD19- TAMs	NBN	0.273682324
CD19- TAMs	ATP5MF	0.261857084
CD19- TAMs	TENT5A	0.365805093
CD19- TAMs	SLC7A5	0.311744177
CD19- TAMs	PITPNC1	0.343677577
CD19- TAMs	CORO1C	0.285987884
CD19- TAMs	RPL11	0.314788028
CD19- TAMs	PBX3	0.394771408
CD19- TAMs	RPS3A	0.380020955
CD19- TAMs	CCNL1	0.385354265
CD19- TAMs	FAM241A	0.285859835
CD19- TAMs	FAM110A	0.250876144
CD19- TAMs	RUNX3	0.371390826
CD19- TAMs	IPMK	0.253483797
CD19- TAMs	GPR65	0.275143086
CD19- TAMs	MCL1	0.3078787
CD19- TAMs	TLN1	0.290190117
CD19- TAMs	PCBP2	0.275906137
CD19- TAMs	KIF5B	0.250580451
CD19- TAMs	SMURF1	0.276129033
CD19- TAMs	CREBBP	0.299079289
CD19- TAMs	CTNNB1	0.416637378
CD19- TAMs	APEX1	0.306450512
CD19- TAMs	RPS6	0.361140109
CD19- TAMs	PTPN6	0.271522107
CD19- TAMs	SGK3	0.297623104
CD19- TAMs	CDK19	0.304525372
CD19- TAMs	SOX4	0.405988448

CD19- TAMs	PMAIP1	0.526707167
CD19- TAMs	ARID4B	0.328340694
CD19- TAMs	CD58	0.278152697
CD19- TAMs	BRK1	0.265084996
CD19- TAMs	PDE3B	0.330376655
CD19- TAMs	MAP3K1	0.393589882
CD19- TAMs	MAPKAP1	0.337228412
CD19- TAMs	CIB1	0.31501276
CD19- TAMs	OSM	0.3209141
CD19- TAMs	KLF10	0.333301755
CD19- TAMs	SLC25A33	0.303850197
CD19- TAMs	RACK1	0.347090075
CD19- TAMs	PPP1CA	0.28194012
CD19- TAMs	SNHG6	0.274915039
CD19- TAMs	AGFG1	0.266886887
CD19- TAMs	ATP2B1	0.42774248
CD19- TAMs	PDZD8	0.263827738
CD19- TAMs	ZNF281	0.266257366
CD19- TAMs	FKBP5	0.418198053
CD19- TAMs	ZC3HAV1	0.463419469
CD19- TAMs	PNRC2	0.25885721
CD19- TAMs	GATAD2A	0.259302816
CD19- TAMs	MYL6	0.259028486
CD19- TAMs	AZIN1	0.275190183
CD19- TAMs	ZNF804A	0.340296163
CD19- TAMs	CCRL2	0.282810268
CD19- TAMs	HOOK3	0.282700055
CD19- TAMs	KDM2A	0.389576192
CD19- TAMs	PRRC2C	0.275978429
CD19- TAMs	HSP90AB1	0.420510259
CD19- TAMs	HMGB1	0.423726875
CD19- TAMs	WIPF1	0.265669333
CD19- TAMs	THBD	0.383327417
CD19- TAMs	RBX1	0.260325896
CD19- TAMs	APRT	0.30323289
CD19- TAMs	PIK3AP1	0.288087935
CD19- TAMs	ARHGEF3	0.276448093
CD19- TAMs	EIF4G3	0.397668422
CD19- TAMs	CCNI	0.283957858
CD19- TAMs	HAUS2	0.371699932
CD19- TAMs	NLRP1	0.310769212

CD19- TAMs	WWP2	0.272565963
CD19- TAMs	WDFY2	0.342620253
CD19- TAMs	NIN	0.264213597
CD19- TAMs	TRIP12	0.279572949
CD19- TAMs	LSM7	0.252489902
CD19- TAMs	UBE2E2	0.461980431
CD19- TAMs	ZNF131	0.316540131
CD19- TAMs	ATP5F1B	0.299934249
CD19- TAMs	SLTM	0.266660594
CD19- TAMs	RC3H1	0.303531414
CD19- TAMs	YPEL2	0.259757114
CD19- TAMs	NUDC	0.296447803
CD19- TAMs	TENT4B	0.302536694
CD19- TAMs	NEDD9	0.267998946
CD19- TAMs	SEPTIN9	0.259920178
CD19- TAMs	BHLHE40	0.339089773
CD19- TAMs	EP300	0.278117107
CD19- TAMs	CDC37	0.26189178
CD19- TAMs	CPNE8	0.26878241
CD19- TAMs	PSMA1	0.268496498
CD19- TAMs	RAB8B	0.250443773
CD19- TAMs	GBP5	0.425261694
CD19- TAMs	ATG7	0.394009693
CD19- TAMs	HIP1	0.438977947
CD19- TAMs	SNHG15	0.250734541
CD19- TAMs	RPL21	0.341295963
CD19- TAMs	RPL41	0.251318871
CD19- TAMs	RPL10A	0.392282584
CD19- TAMs	PA2G4	0.286873071
CD19- TAMs	RAB1A	0.292559754
CD19- TAMs	MYL12A	0.278728231
CD19- TAMs	PPP2R5A	0.253130503
CD19- TAMs	RPL15	0.383202977
CD19- TAMs	SNRPB	0.285921639
CD19- TAMs	NXF1	0.284187642
CD19- TAMs	PKIB	0.283485225
CD19- TAMs	SETX	0.322852962
CD19- TAMs	MYLIP	0.353129583
CD19- TAMs	RPS25	0.262867756
CD19- TAMs	TAGLN2	0.300830386
CD19- TAMs	GLUD1	0.260032585

CD19- TAMs	CRLF3	0.254824672
CD19- TAMs	HNRNPM	0.284714068
CD19- TAMs	NOCT	0.285838855
CD19- TAMs	PHLPP1	0.361166832
CD19- TAMs	PPFIA1	0.25740294
CD19- TAMs	CD109	0.312629935
CD19- TAMs	MGAT1	0.266259876
CD19- TAMs	STAT3	0.317028824
CD19- TAMs	NR4A3	0.382922349
CD19- TAMs	RBM25	0.269319666
CD19- TAMs	SYNCRIP	0.255759333
CD19- TAMs	KAT6A	0.293722099
CD19- TAMs	ZNF438	0.283328024
CD19- TAMs	FNIP1	0.313920961
CD19- TAMs	PPP2CA	0.264023616
CD19- TAMs	PIAS1	0.326378401
CD19- TAMs	AL163541.1	0.260447971
CD19- TAMs	C5AR1	0.264290454
CD19- TAMs	SPIDR	0.407341357
CD19- TAMs	NUFIP2	0.294699539
CD19- TAMs	FRYL	0.274147601
CD19- TAMs	FAR2	0.256466301
CD19- TAMs	PPM1B	0.278574043
CD19- TAMs	UBE2K	0.256247437
CD19- TAMs	RPS7	0.310850795
CD19- TAMs	ZFR	0.253879122
CD19- TAMs	MOB3B	0.304294641
CD19- TAMs	XRCC5	0.263357785
CD19- TAMs	PTGER4	0.295128019
CD19- TAMs	SH3PXD2B	0.251723088
CD19- TAMs	P2RX7	0.291049986
CD19- TAMs	PNRC1	0.308675897
CD19- TAMs	TTC7A	0.271204173
CD19- TAMs	RPL9	0.306528084
CD19- TAMs	TOP1	0.325746346
CD19- TAMs	IL18	0.294879603
CD19- TAMs	UBE2L3	0.250416798
CD19- TAMs	TBL1X	0.283375981
CD19- TAMs	SPG11	0.271499519
CD19- TAMs	IL1R2	0.385799945
CD19- TAMs	LCOR	0.286747921

CD19- TAMs	NABP1	0.468523821
CD19- TAMs	CA2	0.300193174
CD19- TAMs	DNAJC8	0.250225961
CD19- TAMs	UBE2E1	0.270858891
CD19- TAMs	NDUFA12	0.270544866
CD19- TAMs	DOCK11	0.261672526
CD19- TAMs	ARFGEF1	0.264505904
CD19- TAMs	YWHAH	0.518002513
CD19- TAMs	TLE4	0.265840254
CD19- TAMs	HECA	0.266230143
CD19- TAMs	PCNX1	0.323218139
CD19- TAMs	KDM4B	0.278285746
CD19- TAMs	RGS10	0.271512656
CD19- TAMs	FOSB	0.505990847
CD19- TAMs	AP3B1	0.29100408
CD19- TAMs	ATP2B1-AS1	0.319887342
CD19- TAMs	EVI5	0.274982813
CD19- TAMs	ZNF609	0.323903767
CD19- TAMs	OTULINL	0.251121053
CD19- TAMs	NCOA1	0.351325715
CD19- TAMs	HSPA9	0.266110973
CD19- TAMs	ATP2C1	0.403579713
CD19- TAMs	MED13	0.28324618
CD19- TAMs	SLC39A11	0.375842412
CD19- TAMs	ZFAND6	0.333266706
CD19- TAMs	RPS23	0.288527725
CD19- TAMs	ENTPD1	0.299468315
CD19- TAMs	INSR	0.369018308
CD19- TAMs	CLIC1	0.250423988
CD19- TAMs	TAB2	0.284507475
CD19- TAMs	RPS18	0.316259315
CD19- TAMs	KDM6A	0.29371813
CD19- TAMs	YWHAE	0.252541396
CD19- TAMs	VAV3	0.284644293
CD19- TAMs	SLC25A3	0.292818948
CD19- TAMs	ATP6V1G1	0.302192248
CD19- TAMs	ELOVL5	0.331628518
CD19- TAMs	WDFY3	0.303797632
CD19- TAMs	R3HDM2	0.268382217
CD19- TAMs	VPS13C	0.251769532
CD19- TAMs	GBP3	0.273679993

CD19- TAMs	CALM1	0.342012957
CD19- TAMs	TAGAP	0.314889283
CD19- TAMs	RPSA	0.374062757
CD19- TAMs	KIAA1109	0.260127081
CD19- TAMs	LINC00243	0.278541317
CD19- TAMs	NR3C1	0.251422443
CD19- TAMs	LPIN2	0.25175383
CD19- TAMs	FOXN3	0.441571448
CD19- TAMs	RAP1GDS1	0.298586531
CD19- TAMs	RALA	0.313815548
CD19- TAMs	FAM133B	0.264807351
CD19- TAMs	RPL19	0.258041797
CD19- TAMs	FLT1	0.319447734
CD19- TAMs	UBASH3B	0.26013414
CD19- TAMs	PDIA3	0.289274427
CD19- TAMs	ISG15	0.499774971
CD19- TAMs	ACSL3	0.32503697
CD19- TAMs	VTI1A	0.312196421
CD19- TAMs	SERTAD2	0.2657022
CD19- TAMs	GSK3B	0.308178682
CD19- TAMs	CHST11	0.343314649
CD19- TAMs	WDR70	0.271056343
CD19- TAMs	SENP6	0.258379116
CD19- TAMs	RPL17	0.286530984
CD19- TAMs	PPP4R3A	0.266776093
CD19- TAMs	SIK3	0.514426523
CD19- TAMs	LY6E	0.25121836
CD19- TAMs	TTC19	0.272938541
CD19- TAMs	TFEC	0.251293256
CD19- TAMs	TOB1	0.26370941
CD19- TAMs	RHOB	0.284228074
CD19- TAMs	FAM168A	0.269184831
CD19- TAMs	PPP1R15B	0.272290034
CD19- TAMs	SLC5A3	0.768750137
CD19- TAMs	ZFP36L2	0.274310797
CD19- TAMs	ANKRD44	0.258707478
CD19- TAMs	PLCL2	0.287662784
CD19- TAMs	EIF4E	0.273705362
CD19- TAMs	DYRK1A	0.29646825
CD19- TAMs	HERC1	0.330225391
CD19- TAMs	MYCBP2	0.25984441

CD19- TAMs	NCL	0.252232407
CD19- TAMs	TUBA1A	0.327903579
CD19- TAMs	FLI1	0.254789033
CD19- TAMs	SNHG29	0.270693961
CD19- TAMs	EXT1	0.342821608
CD19- TAMs	ATP5MC3	0.272031779
CD19- TAMs	SUMF1	0.295761909
CD19- TAMs	MAP4K3	0.313254507
CD19- TAMs	LPP	0.305971824
CD19- TAMs	TBC1D22A	0.363602606
CD19- TAMs	COPA	0.270705165
CD19- TAMs	JUND	0.377186154
CD19- TAMs	PIK3R5	0.250311159
CD19- TAMs	FBXO11	0.280832867
CD19- TAMs	CAMK1D	0.390746575
CD19- TAMs	GPRIN3	0.28166197
CD19- TAMs	TNFAIP8	0.299499468
CD19- TAMs	LRRC23	0.659542435
CD19- TAMs	EEF1G	0.294559917
CD19- TAMs	FOS	0.305854951
CD19- TAMs	DDHD1	0.284995981
CD19- TAMs	USPL1	0.351540073
CD19- TAMs	RAN	0.266295312
CD19- TAMs	RPL13A	0.252098731
CD19- TAMs	CDKN1A	0.305206912
CD19- TAMs	MLKL	0.340494994
CD19- TAMs	BIRC6	0.29367826
CD19- TAMs	NR4A2	0.329308544
CD19- TAMs	PPM1L	0.314687987
CD19- TAMs	CHMP1B	0.276260107
CD19- TAMs	PAN3	0.301661021
CD19- TAMs	GPR183	0.502768071
CD19- TAMs	GSN	0.307016553
CD19- TAMs	S100B	0.273125822
CD19- TAMs	ARIH1	0.281547993
CD19- TAMs	NCOA2	0.299731335
CD19- TAMs	TUBB	0.255922341
CD19- TAMs	DNAJB4	0.390835778
CD19- TAMs	FBXL14	0.355406693
CD19- TAMs	H3F3B	0.257316218
CD19- TAMs	MRPS6	0.280920356

CD19- TAMs	SSBP2	0.405519465
CD19- TAMs	BIRC3	0.563287058
CD19- TAMs	ANKRD17	0.268299881
CD19- TAMs	CYLD	0.258147354
CD19- TAMs	ARL15	0.287736895
CD19- TAMs	PAPSS2	0.372422982
CD19- TAMs	AC025164.1	0.315453188
CD19- TAMs	RUNX1	0.357661826
CD19- TAMs	CPEB2	0.286432108
CD19- TAMs	HDAC9	0.526147964
CD19- TAMs	VPS13B	0.295759219
CD19- TAMs	ABHD3	0.275318506
CD19- TAMs	FBXO34	0.293077266
CD19- TAMs	INTS6	0.323638505
CD19- TAMs	MEF2A	0.481725451
CD19- TAMs	PHF20	0.270269648
CD19- TAMs	MAP4K4	0.272395085
CD19- TAMs	ATP8B4	0.286838813
CD19- TAMs	EML4	0.250041445
CD19- TAMs	DLEU1	0.340026928
CD19- TAMs	CKS2	0.289726529
CD19- TAMs	EIF4A3	0.254937567
CD19- TAMs	CXCL9	0.375363255
CD19- TAMs	INSIG1	0.272401522
CD19- TAMs	ALOX5AP	0.475470011
CD19- TAMs	MAML2	0.327287132
CD19- TAMs	CXCL10	0.455922955
CD19- TAMs	BTBD9	0.260978021
CD19- TAMs	TNF	0.356402433
CD19- TAMs	CRADD	0.328739298
CD19- TAMs	IL10	0.284406858
CD19- TAMs	FCGR2B	0.259824914
B cells	IGHG3	5.864420508
B cells	IGHG1	5.548688779
B cells	IGLC2	4.394092929
B cells	IGKC	4.348637947
B cells	JCHAIN	3.980681405
B cells	IGHA1	3.661309444
B cells	IGHM	3.296325392
B cells	IGLC1	3.211330562
B cells	IGKV1-5	3.119942249

B cells	IGHG4	3.115409814
B cells	MZB1	3.052821042
B cells	IGHV3-23	2.99101681
B cells	ANKRD28	2.624137194
B cells	IFNG-AS1	2.508638845
B cells	IGKV3-11	2.502220338
B cells	FKBP11	2.442082241
B cells	IGHG2	2.179163164
B cells	TXNDC5	2.160220924
B cells	SEC11C	2.045149811
B cells	CD79A	1.992744763
B cells	BANK1	1.927636179
B cells	IGHV1-24	1.88675895
B cells	RALGPS2	1.880410439
B cells	DERL3	1.81572439
B cells	XBP1	1.785942815
B cells	TENT5C	1.760493999
B cells	PRDX4	1.629772788
B cells	ITM2C	1.627508491
B cells	ISG20	1.560012468
B cells	TPD52	1.554588814
B cells	RHOH	1.502526591
B cells	FUT8	1.500677675
B cells	CDK14	1.475387451
B cells	PDE4D	1.462643597
B cells	COBLL1	1.396933767
B cells	POU2AF1	1.390483027
B cells	ST6GAL1	1.382446383
B cells	SOX5	1.347594759
B cells	BACH2	1.343561641
B cells	AC008014.1	1.342839521
B cells	MYO1D	1.314309442
B cells	CD69	1.303452708
B cells	CEP128	1.282464483
B cells	MS4A1	1.281096234
B cells	SPCS2	1.265116587
B cells	TMEM156	1.262287477
B cells	CREB3L2	1.23522551
B cells	LARGE1	1.233189104
B cells	CD27	1.201682082
B cells	MSI2	1.197588406

B cells	LTB	1.177969016
B cells	DENND5B	1.17675929
B cells	RAB30	1.175820057
B cells	OSBPL10	1.169235833
B cells	HIPK2	1.154195476
B cells	FCRL5	1.149919528
B cells	SEL1L3	1.144578227
B cells	LINC02362	1.143414842
B cells	PLCG2	1.132062498
B cells	FBXW7	1.127553207
B cells	NDUFAF6	1.094255585
B cells	EBF1	1.08761323
B cells	IKZF3	1.069731437
B cells	CADPS2	1.054974114
B cells	TP53INP1	1.051806057
B cells	TNFRSF17	1.017929704
B cells	RABGAP1L	1.007743383
B cells	CARMIL1	1.004392123
B cells	NCOA3	1.003118192
B cells	AFF3	1.001042507
B cells	NUCB2	1.000448322
B cells	HSH2D	0.977898741
B cells	LIME1	0.969308648
B cells	PDK1	0.966057209
B cells	GLCC1	0.965741411
B cells	CD79B	0.963286784
B cells	EIF2AK3	0.956823419
B cells	STK17A	0.950092066
B cells	RHEX	0.945186669
B cells	SLC38A1	0.939935425
B cells	ERLEC1	0.913550736
B cells	SYNE2	0.908391838
B cells	TNFRSF13C	0.907671987
B cells	LMAN1	0.902949015
B cells	GAB1	0.902262256
B cells	FNDC3A	0.902116827
B cells	STRBP	0.899843635
B cells	GNG7	0.898054255
B cells	PIM2	0.893010069
B cells	BCL2	0.892432665
B cells	ZEB1	0.891399537

B cells	CYTIP	0.88146198
B cells	PRDM2	0.880858033
B cells	AP001011.1	0.865882745
B cells	JSRP1	0.865567564
B cells	DIPK1A	0.848478581
B cells	LINC02384	0.847403921
B cells	SPATS2	0.835250111
B cells	SP140	0.832785467
B cells	BTD	0.828020756
B cells	ARID5B	0.826643241
B cells	FAM214A	0.825261945
B cells	AC120193.1	0.824560622
B cells	C11orf80	0.816397121
B cells	AC007569.1	0.807526255
B cells	RASGRP3	0.80593982
B cells	PLPP5	0.804699947
B cells	UBE2J1	0.804521065
B cells	AC078883.1	0.800956529
B cells	SELENOM	0.792819766
B cells	DNAJC1	0.788950304
B cells	FAM30A	0.788445449
B cells	ADAM28	0.783769621
B cells	PVT1	0.781659439
B cells	PPP1R16B	0.780742051
B cells	AC023424.3	0.773393097
B cells	ZBTB20	0.77238884
B cells	SSPN	0.77158193
B cells	SPAG4	0.768118854
B cells	AL589693.1	0.757639645
B cells	OSBPL3	0.756714794
B cells	ADAM19	0.752683273
B cells	CCDC88C	0.751786787
B cells	ICAM3	0.748883624
B cells	RRAS2	0.747304343
B cells	GMDS	0.744676569
B cells	STAP1	0.739993885
B cells	FAAH2	0.738922194
B cells	IRF4	0.734816096
B cells	PIP5K1B	0.728113753
B cells	SETBP1	0.726161644
B cells	SMCHD1	0.724435255

B cells	PLEKHG1	0.719937116
B cells	UBE2H	0.716270132
B cells	TLE1	0.709275705
B cells	MEI1	0.703814761
B cells	FAM107B	0.700340851
B cells	BICD1	0.695547627
B cells	FCRL1	0.693176255
B cells	LY9	0.683926753
B cells	ZCCHC7	0.67029537
B cells	BLK	0.669476068
B cells	PPP3CC	0.667475461
B cells	DENND4A	0.666193593
B cells	HIST1H1D	0.665493415
B cells	DNAJB9	0.663439154
B cells	PDE7A	0.663335248
B cells	SNX25	0.657565313
B cells	WWOX	0.65109014
B cells	SDC1	0.645218073
B cells	AL050309.1	0.644951525
B cells	PAX5	0.644877019
B cells	MEF2C-AS1	0.634726651
B cells	LINC00926	0.624897733
B cells	ITGA8	0.624749627
B cells	PALM2-AKAP2	0.622065479
B cells	AC007384.1	0.60578921
B cells	RHBDD1	0.604874683
B cells	LRBA	0.603074241
B cells	MBNL2	0.603062979
B cells	CRELD2	0.601982515
B cells	KLF13	0.591789883
B cells	SKAP1	0.585888364
B cells	IGLV3-1	0.585187649
B cells	FCHSD2	0.585093582
B cells	SEC24A	0.584467826
B cells	TUBA4A	0.583214259
B cells	RASSF6	0.577984152
B cells	SMYD3	0.573063689
B cells	TMEM243	0.569002109
B cells	ZBP1	0.567608537
B cells	TOX	0.565258167
B cells	RAB11A	0.564861881

B cells	HIVEP1	0.564028935
B cells	LPIN1	0.558088709
B cells	NEDD9	0.55807375
B cells	MCTP2	0.55558914
B cells	DANCR	0.554307278
B cells	GMDS-DT	0.548826322
B cells	TAF4B	0.545912559
B cells	ZHX2	0.544869131
B cells	BLNK	0.544355555
B cells	SLAMF7	0.544314627
B cells	ACOXL	0.538400814
B cells	TRAM2	0.534804002
B cells	TNFRSF13B	0.531939187
B cells	AL591518.1	0.528662736
B cells	LINC01934	0.526552252
B cells	CD70	0.525606527
B cells	ATP8A1	0.52422888
B cells	TSHZ2	0.524138864
B cells	ANGPTL1	0.523126582
B cells	TMC3-AS1	0.521153051
B cells	CHODL	0.518282325
B cells	CAMKMT	0.516524716
B cells	P2RY10	0.510108144
B cells	ANKRD44	0.509705299
B cells	KCNQ5	0.509672477
B cells	KCNN3	0.503919643
B cells	KRT10	0.501708485
B cells	GPHN	0.501048706
B cells	LAX1	0.5008046
B cells	PARP15	0.500723132
B cells	IQCB1	0.499527007
B cells	RORA	0.497963645
B cells	TUT4	0.497822054
B cells	CARD11	0.497816023
B cells	EPB41	0.490786324
B cells	FAM3C	0.488905093
B cells	AP002075.1	0.484952708
B cells	COL19A1	0.48346739
B cells	MANEA	0.481557583
B cells	SIDT1	0.478858186
B cells	SVIP	0.478125898

B cells	TNRC6B	0.477514303
B cells	IGHD	0.470628754
B cells	HMCES	0.470122467
B cells	AC009522.1	0.469911992
B cells	STK4	0.469610004
B cells	AC079793.1	0.464910917
B cells	TVP23C	0.46459306
B cells	CPNE5	0.458928672
B cells	MICAL3	0.456275802
B cells	VPREB3	0.456140842
B cells	ETS1	0.4556552
B cells	ESR2	0.455414083
B cells	ITGA6	0.454398646
B cells	PNOC	0.453699526
B cells	PDLIM1	0.451762842
B cells	FCMR	0.448238415
B cells	HIST1H2BD	0.447815019
B cells	ODC1	0.446659162
B cells	BMP6	0.444418189
B cells	CDKAL1	0.443400854
B cells	COL4A4	0.441673301
B cells	FCRL2	0.441525287
B cells	IFT57	0.439286359
B cells	GBF1	0.436226197
B cells	MIATNB	0.43440699
B cells	CD24	0.426274511
B cells	TLK1	0.425102221
B cells	SYNGR1	0.420710091
B cells	JADE3	0.420127876
B cells	CDC42SE2	0.41988387
B cells	AC012236.1	0.41977732
B cells	RIPOR2	0.418284681
B cells	PLP2	0.417556894
B cells	SIPA1L3	0.417041306
B cells	KLF12	0.416379481
B cells	PPM1K	0.412966923
B cells	P2RX5	0.412191398
B cells	NUGGC	0.411122181
B cells	AC016074.2	0.410781345
B cells	AC022182.1	0.408433774
B cells	ATP2A3	0.405040094

B cells	TMEM238	0.403842478
B cells	P2RY8	0.403739641
B cells	LINC02397	0.402047996
B cells	ORAI2	0.401630707
B cells	SRPRB	0.400405586
B cells	KHDRBS2	0.397200213
B cells	TMEM263	0.39707678
B cells	LINC01004	0.396301136
B cells	XKR6	0.395020508
B cells	TMEM154	0.394017987
B cells	ASXL1	0.393123976
B cells	SCMH1	0.393091065
B cells	TSHR	0.392368881
B cells	ANXA6	0.386659364
B cells	C16orf74	0.385585548
B cells	EPB41L4A	0.384515453
B cells	CYFIP2	0.383919734
B cells	SINHCAF	0.38317008
B cells	ANK3	0.382199388
B cells	GRK5	0.381844915
B cells	OCIAD2	0.38080901
B cells	NIBAN3	0.376709936
B cells	EIF1AY	0.374417918
B cells	CCDC32	0.374238581
B cells	PKIG	0.371735617
B cells	MACROD2	0.370543467
B cells	TEX9	0.367711941
B cells	E2F5	0.367400677
B cells	PBX4	0.361946138
B cells	TSBP1-AS1	0.359879261
B cells	LINC02576	0.358095558
B cells	ABCA5	0.357911642
B cells	PMM2	0.354203727
B cells	CAMK4	0.353761769
B cells	P2RX1	0.353507855
B cells	SCNN1B	0.351421637
B cells	LINC01473	0.350437842
B cells	PARM1	0.348518833
B cells	ST6GALNAC4	0.348513432
B cells	AC021678.2	0.347488861
B cells	OPTN	0.345218172

B cells	TSTD1	0.344188682
B cells	ARHGAP15	0.343742037
B cells	CAV1	0.341494856
B cells	TMEM117	0.34072029
B cells	HIST1H1E	0.339754859
B cells	AL355076.2	0.339349523
B cells	CHPF	0.33831405
B cells	ZNF107	0.33763595
B cells	LINC02541	0.334717823
B cells	HLA-DOB	0.334160058
B cells	DPEP1	0.333637931
B cells	ANKRD36B	0.332399552
B cells	TARSL2	0.332367302
B cells	SLC25A4	0.33223125
B cells	NXPE3	0.331676084
B cells	RASGRP1	0.331426314
B cells	RIC3	0.330337743
B cells	KIAA0040	0.329693125
B cells	SPAG1	0.329556291
B cells	FAM117A	0.328684439
B cells	ZNF827	0.328132776
B cells	ITGB7	0.32694634
B cells	SYTL1	0.326771623
B cells	BFSP2	0.326234394
B cells	LINC00571	0.325501262
B cells	CCDC69	0.324396713
B cells	VCPKMT	0.322910146
B cells	RORA-AS1	0.322236362
B cells	ACAP1	0.318247535
B cells	AC079781.5	0.31522726
B cells	RAPGEF5	0.313398857
B cells	MAP3K9	0.312497802
B cells	TRAF3	0.312299967
B cells	SLAMF6	0.310231929
B cells	ZFAT	0.308704179
B cells	C11orf24	0.305875658
B cells	8-Mar	0.302889612
B cells	C12orf74	0.302130827
B cells	PAWR	0.301378174
B cells	AFF2	0.299739919
B cells	IL21R	0.298444252

B cells	LINC01484	0.298429119
B cells	MCEE	0.297678054
B cells	LBH	0.296088016
B cells	ZNF215	0.295429557
B cells	DNAH8	0.294023684
B cells	DENND2C	0.289853208
B cells	MPP6	0.288380089
B cells	BCAS4	0.288354796
B cells	PPP1R9A	0.280881549
B cells	PATJ	0.2765179
B cells	ITM2A	0.276248532
B cells	PKHD1L1	0.275877285
B cells	COL4A3	0.272789848
B cells	YES1	0.269875317
B cells	C12orf65	0.268364033
B cells	AQP3	0.267989971
B cells	SYVN1	0.267628624
B cells	FAM102A	0.266158624
B cells	KNTC1	0.265242895
B cells	AIM2	0.265174664
B cells	CLNK	0.264971065
B cells	GNB5	0.263690603
B cells	KIZ	0.263600926
B cells	ALDH18A1	0.260778996
B cells	AC243960.1	0.258577194
B cells	FCRLA	0.257912072
B cells	SLAMF1	0.251769228
B cells	LINC01781	0.251713677
B cells	CFAP54	0.250946806
B cells	GRAMD1C	0.250840334
B cells	PTPN4	0.273702604
B cells	PCED1B	0.310286874
B cells	USP48	0.535177292
B cells	HSPA13	0.320611012
B cells	TMEM131	0.374400964
B cells	PTPN1	0.260064369
B cells	TXNDC15	0.478587923
B cells	EHMT1	0.680361503
B cells	TXNDC11	0.621183636
B cells	EAF2	0.505337472
B cells	AL162253.2	0.345993067

B cells	IGHV3-66	1.646626967
B cells	MIR4435-2HG	0.605822204
B cells	AHI1	0.279126907
B cells	STEAP1B	0.377844451
B cells	ZBTB38	0.642553297
B cells	U62317.4	0.33286814
B cells	XRRA1	0.26031321
B cells	TMEM131L	0.261028051
B cells	AC239799.2	0.391500984
B cells	SGO1-AS1	0.253937144
B cells	PGM3	0.258626501
B cells	STAG1	0.374404167
B cells	PCED1B-AS1	0.282580435
B cells	LIN52	0.264424938
B cells	FBH1	0.330168884
B cells	UMAD1	0.345367512
B cells	AC092546.1	0.27772988
B cells	CD38	0.631640487
B cells	NSD3	0.381188454
B cells	AL592429.2	0.32585317
B cells	ERC1	0.428206094
B cells	LRRK1	0.445259586
B cells	SEC24D	0.548945958
B cells	ELL2	0.345713289
B cells	HIST1H2AC	0.557568337
B cells	CLPTM1L	0.418627539
B cells	BET1	0.252503218
B cells	SNRPN	0.292871002
B cells	SREBF2	0.299731345
B cells	ATF7IP	0.474538457
B cells	DAPP1	0.337263743
B cells	HIST1H1C	0.599361052
B cells	SCAPER	0.377980792
B cells	CYTOR	1.095413166
B cells	SEL1L	0.758977979
B cells	ZNF791	0.276967402
B cells	LARP1B	0.334805896
B cells	GORASP2	0.302535624
B cells	IL2RG	0.269753014
B cells	TIFA	0.26349383
B cells	CHD7	0.28021416

B cells	ESR1	0.5001838
B cells	ATP11B	0.288456152
B cells	RFX3	0.313149221
B cells	HIST1H4C	0.302375723
B cells	RPS6KA5	0.32156828
B cells	RPL3	0.523271676
B cells	SELENOK	0.624164758
B cells	XRN1	0.441925169
B cells	UBE2G1	0.304133612
B cells	RNF19A	0.364238748
B cells	VPS37B	0.392665553
B cells	SMAP2	0.373062084
B cells	HIST1H2BJ	0.273397603
B cells	NFX1	0.284270145
B cells	AUTS2	0.434451529
B cells	PRDX2	0.381234126
B cells	LINC00910	0.468807541
B cells	DUSP5	0.377144312
B cells	RPS5	0.401133383
B cells	OGT	0.378654632
B cells	UAP1	0.251034342
B cells	VWA8	0.268681359
B cells	SPCS1	1.079745346
B cells	MRPS31	0.321760497
B cells	EZR	0.274632611
B cells	SRPRA	0.331336063
B cells	IMMP2L	0.33392401
B cells	AC012447.1	0.382495437
B cells	ALG5	0.375495902
B cells	UBA6-AS1	0.267621338
B cells	SCFD1	0.39115707
B cells	BCL11A	0.253262452
B cells	SFMBT1	0.267733202
B cells	RNGTT	0.264815209
B cells	Z93241.1	0.275890451
B cells	SDF2L1	0.734842973
B cells	MAN1A2	0.351507386
B cells	MTMR12	0.263444361
B cells	C12orf57	0.275346793
B cells	ANKRD12	0.321100848
B cells	GABPB1	0.306584047

B cells	ASCC3	0.289159348
B cells	RASA2	0.298822562
B cells	MANF	0.707982299
B cells	BRAF	0.254908714
B cells	RIC1	0.280010601
B cells	SLC44A1	0.478629376
B cells	VOPP1	0.452140278
B cells	RBM6	0.339752188
B cells	BCAR3	0.273466978
B cells	CCNC	0.250815921
B cells	HIST1H2BG	0.293489885
B cells	TTC28	0.310012999
B cells	CD37	0.545181626
B cells	AC016831.7	0.371825947
B cells	SEC62	0.541828531
B cells	SRP54	0.311364093
B cells	STIM2	0.299686412
B cells	MAP4K4	0.256883258
B cells	PRKD3	0.255809117
B cells	ICAM2	0.256568073
B cells	ERN1	0.539194417
B cells	SMDT1	0.332375627
B cells	LINC00513	0.296130788
B cells	EEF1B2	0.396695468
B cells	PDCD4	0.287031427
B cells	CCPG1	0.394580364
B cells	CADM1	0.561402543
B cells	ARID2	0.310672938
B cells	6-Mar	0.259550164
B cells	CASK	0.256751215
B cells	EXOC4	0.26787937
B cells	CCDC50	0.294648635
B cells	ERGIC2	0.287630973
B cells	OSBPL9	0.330615108
B cells	ANAPC16	0.25544124
B cells	CLEC2D	0.288723842
B cells	SELENOS	0.679162471
B cells	TCEA1	0.279005772
B cells	ADK	0.280341648
B cells	SUB1	0.74161544
B cells	RABAC1	0.648416575

B cells	SND1	0.391757939
B cells	RPL22L1	0.274359154
B cells	DERL1	0.297981735
B cells	MON2	0.258781365
B cells	RUNX2	0.400353108
B cells	EIF2AK4	0.399391519
B cells	SP100	0.254428742
B cells	CCND3	0.275391076
B cells	R3HDM1	0.29038092
B cells	RPS4X	0.322210081
B cells	BTG2	0.707784591
B cells	SRM	0.257590924
B cells	SSR4	2.564688964
B cells	CLIC4	0.318468964
B cells	TSC22D3	0.59434998
B cells	BCL2L11	0.387572635
B cells	PEL1	0.616937665
B cells	GALNT2	0.340710138
B cells	TEX14	1.108163698
B cells	DENND1B	0.33446084
B cells	MEF2C	0.262485891
B cells	CASP3	0.271522464
B cells	TMEM140	0.263700312
B cells	ATXN1	0.490116508
B cells	NSMCE2	0.444950899
B cells	SPCS3	0.685545432
B cells	IGHV3-53	2.648495087
B cells	ARF4	0.297404136
B cells	ANKRD37	0.318687035
B cells	HSP90B1	1.293182021
B cells	SEC61B	0.768729097
B cells	HERPUD1	0.688951947
B cells	YPEL5	0.259356891
B cells	ARHGAP24	0.362607674
B cells	CUTA	0.323190493
B cells	MRPS24	0.303587404
B cells	SSR2	0.364395483
B cells	RPLP0	0.251199004
B cells	FNDC3B	0.948392126
B cells	HDLBP	0.422308802
B cells	KDELR1	0.43600709

B cells	TMEM107	0.268106924
B cells	PRDM1	0.3287783
B cells	SERP1	0.365162211
B cells	RPL36AL	0.33582272
B cells	CCSER1	0.252744915
B cells	IGHA2	3.302809124
B cells	CEMIP2	0.368056069
B cells	H1FX	0.93680862
B cells	IGLC3	4.325137273
B cells	TMEM59	0.317812084
B cells	SSR3	0.570497307
B cells	PPIB	0.375597437
B cells	RRBP1	0.408682184
B cells	MYDGF	0.349770271
B cells	MDM2	0.42105483
CD19+ TAMs	RNASE1	3.290767755
CD19+ TAMs	SELENOP	3.014380344
CD19+ TAMs	APOE	2.752114467
CD19+ TAMs	SLC40A1	2.746750281
CD19+ TAMs	APOA2	2.538999278
CD19+ TAMs	LGMN	2.534461043
CD19+ TAMs	FOLR2	2.293578007
CD19+ TAMs	APOC1	2.133389332
CD19+ TAMs	CTSD	2.09878348
CD19+ TAMs	MAF	1.938261725
CD19+ TAMs	DAB2	1.916545241
CD19+ TAMs	C1QB	1.905356348
CD19+ TAMs	A2M	1.890830463
CD19+ TAMs	C1QA	1.877578695
CD19+ TAMs	GPNMB	1.875451582
CD19+ TAMs	SPP1	1.824372018
CD19+ TAMs	C1QC	1.788469074
CD19+ TAMs	PLD3	1.752274902
CD19+ TAMs	FCGRT	1.660393642
CD19+ TAMs	LIPA	1.649375503
CD19+ TAMs	CTSB	1.64625461
CD19+ TAMs	MS4A7	1.643340472
CD19+ TAMs	MS4A4A	1.617640642
CD19+ TAMs	MRC1	1.431393169
CD19+ TAMs	GYPC	1.429518996
CD19+ TAMs	STAB1	1.414347414

CD19+ TAMs	VCAM1	1.412999712
CD19+ TAMs	NRP1	1.371969915
CD19+ TAMs	NUPR1	1.362024623
CD19+ TAMs	LILRB5	1.345166122
CD19+ TAMs	CTSL	1.326783229
CD19+ TAMs	MSR1	1.310124562
CD19+ TAMs	CCL4L2	1.306589432
CD19+ TAMs	CD163	1.302638802
CD19+ TAMs	APOC2	1.28733032
CD19+ TAMs	ARL4C	1.285350792
CD19+ TAMs	CD14	1.275070485
CD19+ TAMs	IGF1	1.271125713
CD19+ TAMs	CD63	1.267297754
CD19+ TAMs	GPR34	1.264436758
CD19+ TAMs	SLCO2B1	1.257764854
CD19+ TAMs	CD68	1.256820771
CD19+ TAMs	FTL	1.249004126
CD19+ TAMs	TREM2	1.223720602
CD19+ TAMs	ALB	1.189504873
CD19+ TAMs	CREG1	1.167159838
CD19+ TAMs	GRN	1.153102121
CD19+ TAMs	KCNMA1	1.152699997
CD19+ TAMs	WWP1	1.148290348
CD19+ TAMs	BLVRB	1.14794117
CD19+ TAMs	CD59	1.124151861
CD19+ TAMs	CTSZ	1.095230377
CD19+ TAMs	CD209	1.088308627
CD19+ TAMs	FABP5	1.070719295
CD19+ TAMs	PLTP	1.061173978
CD19+ TAMs	HLA-DRB5	1.058467687
CD19+ TAMs	ITM2B	1.057971675
CD19+ TAMs	CXCL12	1.052072944
CD19+ TAMs	TIMP2	1.048022427
CD19+ TAMs	ADAP2	1.045768663
CD19+ TAMs	ITSN1	1.024221283
CD19+ TAMs	CFD	1.018891411
CD19+ TAMs	APOC3	1.016629748
CD19+ TAMs	MT1G	1.014037822
CD19+ TAMs	CD81	1.013603252
CD19+ TAMs	C2	1.011732212
CD19+ TAMs	ASAH1	1.002145925

CD19+ TAMs	CD163L1	0.999159851
CD19+ TAMs	FCHO2	0.99185275
CD19+ TAMs	FCGR2A	0.990384377
CD19+ TAMs	PSAP	0.981315709
CD19+ TAMs	FUCA1	0.980722253
CD19+ TAMs	FRMD4A	0.977086425
CD19+ TAMs	TYROBP	0.976660709
CD19+ TAMs	SLC1A3	0.97637299
CD19+ TAMs	MARCKS	0.976051117
CD19+ TAMs	CD74	0.975351682
CD19+ TAMs	MS4A6A	0.974098367
CD19+ TAMs	CTSC	0.969983964
CD19+ TAMs	C3AR1	0.966034752
CD19+ TAMs	FCGR3A	0.962631441
CD19+ TAMs	TSPAN4	0.960906511
CD19+ TAMs	SDCBP	0.959644238
CD19+ TAMs	TMEM176B	0.952373202
CD19+ TAMs	RAP2B	0.948169295
CD19+ TAMs	MCOLN1	0.93687894
CD19+ TAMs	HLA-DPA1	0.936304497
CD19+ TAMs	MAFB	0.931052559
CD19+ TAMs	FMN1	0.929970554
CD19+ TAMs	LGALS3	0.92952993
CD19+ TAMs	HLA-DRB1	0.927925977
CD19+ TAMs	CXCL16	0.924595278
CD19+ TAMs	CCL4	0.921221594
CD19+ TAMs	NRP2	0.905230308
CD19+ TAMs	MPEG1	0.903183663
CD19+ TAMs	FRMD4B	0.900965645
CD19+ TAMs	SDC3	0.891648592
CD19+ TAMs	HLA-DQA1	0.890821314
CD19+ TAMs	MERTK	0.882626922
CD19+ TAMs	NPL	0.867173587
CD19+ TAMs	CD9	0.866771193
CD19+ TAMs	NPC2	0.864936097
CD19+ TAMs	ATP1B1	0.860131069
CD19+ TAMs	HLA-DQB1	0.857854345
CD19+ TAMs	SGK1	0.857258929
CD19+ TAMs	HLA-DMA	0.857151456
CD19+ TAMs	F13A1	0.848268886
CD19+ TAMs	MT-CYB	0.848081003

CD19+ TAMs	FMNL2	0.844102119
CD19+ TAMs	HLA-DPB1	0.842823479
CD19+ TAMs	GADD45B	0.842394894
CD19+ TAMs	HLA-DRA	0.841268734
CD19+ TAMs	ACP5	0.840054679
CD19+ TAMs	GATM	0.836059142
CD19+ TAMs	VSIG4	0.835933348
CD19+ TAMs	CD84	0.831983086
CD19+ TAMs	GLUL	0.829044432
CD19+ TAMs	ABCA1	0.823144146
CD19+ TAMs	TSC22D1	0.822188731
CD19+ TAMs	MT-CO3	0.81889247
CD19+ TAMs	MFSD1	0.81654977
CD19+ TAMs	LAMP1	0.810510483
CD19+ TAMs	STARD13	0.807509497
CD19+ TAMs	FCER1G	0.805547037
CD19+ TAMs	CSF1R	0.805467582
CD19+ TAMs	PDK4	0.798812645
CD19+ TAMs	FAM20A	0.798313113
CD19+ TAMs	ME1	0.795497294
CD19+ TAMs	PLA2G7	0.793633975
CD19+ TAMs	CSTB	0.790283581
CD19+ TAMs	IGSF6	0.789698503
CD19+ TAMs	LRP1	0.78757899
CD19+ TAMs	CCL3	0.7865266
CD19+ TAMs	AP2A2	0.781350427
CD19+ TAMs	VMO1	0.776072212
CD19+ TAMs	SERPING1	0.775380531
CD19+ TAMs	CPM	0.772600116
CD19+ TAMs	AXL	0.769075293
CD19+ TAMs	PTMS	0.765771449
CD19+ TAMs	MAN2B1	0.762932031
CD19+ TAMs	HLA-E	0.757744812
CD19+ TAMs	PDGFC	0.756371773
CD19+ TAMs	IQGAP2	0.752871766
CD19+ TAMs	DOCK4	0.749978301
CD19+ TAMs	DST	0.748537955
CD19+ TAMs	TTY14	0.745930139
CD19+ TAMs	CXCL3	0.741054831
CD19+ TAMs	CEBPD	0.733215868
CD19+ TAMs	BNC2	0.73316218

CD19+ TAMs	ZFHX3	0.732910918
CD19+ TAMs	LTC4S	0.731958507
CD19+ TAMs	FARP1	0.731254586
CD19+ TAMs	HLA-A	0.729263977
CD19+ TAMs	TUBA1B	0.726243984
CD19+ TAMs	HMOX1	0.725768476
CD19+ TAMs	TPP1	0.723871572
CD19+ TAMs	GAA	0.722979168
CD19+ TAMs	ZFP36L1	0.722684756
CD19+ TAMs	ID2	0.719794237
CD19+ TAMs	SLC16A10	0.71970179
CD19+ TAMs	AKR1B1	0.715350842
CD19+ TAMs	RNASET2	0.715172697
CD19+ TAMs	TLR4	0.706653748
CD19+ TAMs	TMEM37	0.700802942
CD19+ TAMs	CCL3L1	0.698715882
CD19+ TAMs	HEXA	0.691562367
CD19+ TAMs	HLA-DQA2	0.69000523
CD19+ TAMs	ABCC5	0.684361206
CD19+ TAMs	FPR3	0.683972278
CD19+ TAMs	BST2	0.682058401
CD19+ TAMs	SNX6	0.676141904
CD19+ TAMs	MT1X	0.674262691
CD19+ TAMs	HLA-DMB	0.674079143
CD19+ TAMs	MT-ATP6	0.674048199
CD19+ TAMs	CD4	0.672760849
CD19+ TAMs	LGALS3BP	0.670317989
CD19+ TAMs	MT-ND1	0.6697393
CD19+ TAMs	LYVE1	0.666189889
CD19+ TAMs	EPB41L2	0.660774145
CD19+ TAMs	ANKH	0.658527589
CD19+ TAMs	BCAT1	0.657748791
CD19+ TAMs	CTSA	0.65727844
CD19+ TAMs	CALM3	0.653081743
CD19+ TAMs	EGR1	0.646880354
CD19+ TAMs	PLXND1	0.645838506
CD19+ TAMs	MGST3	0.645410782
CD19+ TAMs	LAIR1	0.645153024
CD19+ TAMs	CCL8	0.643237399
CD19+ TAMs	SPATS2L	0.641534832
CD19+ TAMs	ITGB5	0.641264696

CD19+ TAMs	STMN1	0.64120384
CD19+ TAMs	LAMP2	0.639532706
CD19+ TAMs	SASH1	0.63879473
CD19+ TAMs	SIGLEC1	0.638498419
CD19+ TAMs	GADD45G	0.637280392
CD19+ TAMs	KCTD12	0.635035053
CD19+ TAMs	IGSF21	0.634186973
CD19+ TAMs	SCN1B	0.630100748
CD19+ TAMs	SLC7A8	0.628934217
CD19+ TAMs	EBI3	0.627933482
CD19+ TAMs	SESN1	0.625801382
CD19+ TAMs	DPP7	0.621323143
CD19+ TAMs	TTYH3	0.61834114
CD19+ TAMs	NFIA	0.611838054
CD19+ TAMs	GAS2L3	0.608172468
CD19+ TAMs	PRDX1	0.607435989
CD19+ TAMs	EPHX1	0.607261682
CD19+ TAMs	PRNP	0.606388213
CD19+ TAMs	KIF1B	0.603915258
CD19+ TAMs	APLP2	0.601799827
CD19+ TAMs	OTUD1	0.601725072
CD19+ TAMs	RHOB	0.598659898
CD19+ TAMs	CLTC	0.597304486
CD19+ TAMs	TNFAIP2	0.592875223
CD19+ TAMs	IFI27	0.591852282
CD19+ TAMs	TIMP3	0.591371961
CD19+ TAMs	NCOA4	0.590847285
CD19+ TAMs	GM2A	0.58793349
CD19+ TAMs	HRH1	0.585495142
CD19+ TAMs	MT-ND4	0.583783574
CD19+ TAMs	RAB20	0.581458573
CD19+ TAMs	FTH1	0.581424034
CD19+ TAMs	BRI3	0.579809278
CD19+ TAMs	GPX4	0.579010271
CD19+ TAMs	GPR155	0.578192942
CD19+ TAMs	GOLIM4	0.577349988
CD19+ TAMs	VEGFB	0.576975238
CD19+ TAMs	ATP6V0B	0.575762265
CD19+ TAMs	COLEC12	0.574539178
CD19+ TAMs	TMIGD3	0.572376407
CD19+ TAMs	UNC93B1	0.57192875

CD19+ TAMs	C5AR1	0.570939032
CD19+ TAMs	RNASE6	0.568185688
CD19+ TAMs	LPAR6	0.566094118
CD19+ TAMs	OTOA	0.564843083
CD19+ TAMs	AMBP	0.564636322
CD19+ TAMs	ADAM9	0.562997844
CD19+ TAMs	MT-ND3	0.562584439
CD19+ TAMs	FCGBP	0.562338885
CD19+ TAMs	C6orf62	0.560791918
CD19+ TAMs	SERPINB6	0.560506549
CD19+ TAMs	HNMT	0.56004068
CD19+ TAMs	SMS	0.559905365
CD19+ TAMs	ALDH1A1	0.559504127
CD19+ TAMs	MPP1	0.557834118
CD19+ TAMs	MYO1E	0.557647796
CD19+ TAMs	FGL2	0.556237028
CD19+ TAMs	GPX3	0.554916053
CD19+ TAMs	B2M	0.554885482
CD19+ TAMs	DBI	0.553457797
CD19+ TAMs	C1orf54	0.553262889
CD19+ TAMs	PSD3	0.5531246
CD19+ TAMs	TMBIM6	0.552796296
CD19+ TAMs	ATP6AP1	0.552674228
CD19+ TAMs	MITF	0.549643922
CD19+ TAMs	GNPDA1	0.548163513
CD19+ TAMs	PIK3IP1	0.547813397
CD19+ TAMs	VAT1	0.54527336
CD19+ TAMs	MT-ND2	0.542729555
CD19+ TAMs	CPVL	0.542497415
CD19+ TAMs	CLTA	0.542262055
CD19+ TAMs	DHRS3	0.541287277
CD19+ TAMs	SRGAP1	0.541239022
CD19+ TAMs	RGS10	0.540398197
CD19+ TAMs	ARHGAP18	0.540328033
CD19+ TAMs	SLC22A23	0.535746207
CD19+ TAMs	FEZ2	0.533535289
CD19+ TAMs	SLC15A3	0.53245417
CD19+ TAMs	P4HA1	0.531413923
CD19+ TAMs	LAPTM4A	0.530832243
CD19+ TAMs	IFRD1	0.530760646
CD19+ TAMs	PAX8-AS1	0.530078399

CD19+ TAMs	OSBPL1A	0.529925493
CD19+ TAMs	BCAP31	0.529583219
CD19+ TAMs	ATP6V0C	0.52950461
CD19+ TAMs	AP1B1	0.527787768
CD19+ TAMs	CYFIP1	0.526216006
CD19+ TAMs	EGFL7	0.524849822
CD19+ TAMs	CMKLR1	0.524115824
CD19+ TAMs	CD28	0.523839681
CD19+ TAMs	NAIP	0.523198451
CD19+ TAMs	GCLC	0.522639302
CD19+ TAMs	TTR	0.519699967
CD19+ TAMs	CALM2	0.519091474
CD19+ TAMs	HLA-DOA	0.518327517
CD19+ TAMs	PEBP1	0.516823318
CD19+ TAMs	PRXL2A	0.516539171
CD19+ TAMs	CD93	0.514620673
CD19+ TAMs	GPR137B	0.513986789
CD19+ TAMs	AC100849.1	0.513568397
CD19+ TAMs	IDH1	0.513447214
CD19+ TAMs	PLEKHA1	0.511682263
CD19+ TAMs	UGCG	0.508669765
CD19+ TAMs	CST3	0.506567085
CD19+ TAMs	PHLDA1	0.505423329
CD19+ TAMs	CCL13	0.505060038
CD19+ TAMs	SPRED1	0.504780986
CD19+ TAMs	LILRB4	0.504530479
CD19+ TAMs	RND3	0.503896429
CD19+ TAMs	DDAH2	0.502962457
CD19+ TAMs	IER3	0.500999686
CD19+ TAMs	GAS6	0.500146301
CD19+ TAMs	NINJ1	0.49965259
CD19+ TAMs	ARL6IP1	0.49784466
CD19+ TAMs	SLC18B1	0.496300795
CD19+ TAMs	MT-CO1	0.496063256
CD19+ TAMs	GDF15	0.494949931
CD19+ TAMs	TMEM176A	0.494723424
CD19+ TAMs	ITGAV	0.494164606
CD19+ TAMs	RGS1	0.493705495
CD19+ TAMs	WLS	0.492041472
CD19+ TAMs	RGL1	0.491116441
CD19+ TAMs	MKNK1	0.490661248

CD19+ TAMs	PLAU	0.486009063
CD19+ TAMs	SDS	0.485482735
CD19+ TAMs	LY96	0.485350962
CD19+ TAMs	CAPZB	0.484947691
CD19+ TAMs	SERINC1	0.484926096
CD19+ TAMs	ATP6V0E1	0.484152772
CD19+ TAMs	EVA1B	0.481480407
CD19+ TAMs	EMP2	0.481142881
CD19+ TAMs	PDGFB	0.4795825
CD19+ TAMs	CD164	0.479377379
CD19+ TAMs	SCARB2	0.477831503
CD19+ TAMs	ATP6AP2	0.477687131
CD19+ TAMs	CCL2	0.476086576
CD19+ TAMs	LAPTM5	0.474925903
CD19+ TAMs	CYTH4	0.474894364
CD19+ TAMs	SCD	0.473944505
CD19+ TAMs	ATP6V1F	0.47254628
CD19+ TAMs	GFRA2	0.471349643
CD19+ TAMs	RGS2	0.466640528
CD19+ TAMs	TNFRSF1A	0.463931665
CD19+ TAMs	MGAT1	0.461345987
CD19+ TAMs	GIMAP5	0.459220646
CD19+ TAMs	CITED2	0.458858496
CD19+ TAMs	DNASE1L3	0.458655455
CD19+ TAMs	GSN	0.457484552
CD19+ TAMs	HOMER3	0.457141641
CD19+ TAMs	ETV5	0.455647167
CD19+ TAMs	CYBA	0.453997134
CD19+ TAMs	PMP22	0.452783883
CD19+ TAMs	IL2RA	0.451631544
CD19+ TAMs	MGLL	0.451017187
CD19+ TAMs	KCNJ5	0.448885818
CD19+ TAMs	DSC2	0.448557228
CD19+ TAMs	DIRC3	0.447660184
CD19+ TAMs	SCAMP2	0.445559625
CD19+ TAMs	FSCN1	0.444531684
CD19+ TAMs	DNPH1	0.441807705
CD19+ TAMs	QKI	0.441511586
CD19+ TAMs	PLA2G15	0.44042319
CD19+ TAMs	TNFSF13	0.440195401
CD19+ TAMs	SLC38A6	0.438309672

CD19+ TAMs	TENT5A	0.438184552
CD19+ TAMs	NFIC	0.4379106
CD19+ TAMs	DENND4C	0.435293593
CD19+ TAMs	CD302	0.434995615
CD19+ TAMs	GNB4	0.434857961
CD19+ TAMs	CRYL1	0.434349667
CD19+ TAMs	MGAT4A	0.432886006
CD19+ TAMs	MXD4	0.431818007
CD19+ TAMs	SLAMF8	0.431244517
CD19+ TAMs	COMT	0.430931787
CD19+ TAMs	RAC1	0.429941899
CD19+ TAMs	ADGRG6	0.429154703
CD19+ TAMs	CCDC152	0.428803805
CD19+ TAMs	MFHAS1	0.428050322
CD19+ TAMs	EDA	0.427309389
CD19+ TAMs	M6PR	0.426287867
CD19+ TAMs	BLVRA	0.425514617
CD19+ TAMs	RNF130	0.425498732
CD19+ TAMs	COLGALT1	0.425445017
CD19+ TAMs	CCL18	0.424699696
CD19+ TAMs	TCEAL9	0.422816713
CD19+ TAMs	ARHGAP5	0.422497069
CD19+ TAMs	SPATA7	0.421596546
CD19+ TAMs	RAPH1	0.420631761
CD19+ TAMs	TGOLN2	0.419794843
CD19+ TAMs	BEX4	0.419482686
CD19+ TAMs	SPIRE1	0.419364704
CD19+ TAMs	SGPL1	0.416661046
CD19+ TAMs	AAK1	0.413709237
CD19+ TAMs	EPB41L3	0.413667167
CD19+ TAMs	MYL6	0.413388415
CD19+ TAMs	BNIP3L	0.412203964
CD19+ TAMs	NCF4	0.411937265
CD19+ TAMs	PPT1	0.410302513
CD19+ TAMs	BMP2K	0.410097088
CD19+ TAMs	IER5L	0.410005461
CD19+ TAMs	GNS	0.41000349
CD19+ TAMs	VAMP8	0.409574741
CD19+ TAMs	NENF	0.407614251
CD19+ TAMs	RHOBTB3	0.407605319
CD19+ TAMs	CD99	0.407555351

CD19+ TAMs	TMSB4X	0.406315346
CD19+ TAMs	CCND1	0.405969838
CD19+ TAMs	RAB5C	0.404741363
CD19+ TAMs	NEU1	0.40403695
CD19+ TAMs	RASSF4	0.403423168
CD19+ TAMs	HES1	0.403262725
CD19+ TAMs	FNIP2	0.401537083
CD19+ TAMs	UACA	0.401402462
CD19+ TAMs	SIRPA	0.40036941
CD19+ TAMs	SCPEP1	0.399864918
CD19+ TAMs	TGFBR1	0.399694513
CD19+ TAMs	ARHGAP10	0.39885887
CD19+ TAMs	TRIM14	0.398614782
CD19+ TAMs	HGF	0.396819234
CD19+ TAMs	IL18	0.396453867
CD19+ TAMs	RTN4	0.396083065
CD19+ TAMs	CREBL2	0.395991628
CD19+ TAMs	EPS8	0.395658955
CD19+ TAMs	RNASEK	0.395147674
CD19+ TAMs	NTAN1	0.393716056
CD19+ TAMs	PEPD	0.393471807
CD19+ TAMs	IL4I1	0.393210125
CD19+ TAMs	TANC2	0.39257715
CD19+ TAMs	HPGDS	0.392533825
CD19+ TAMs	FABP3	0.392277687
CD19+ TAMs	SMPDL3A	0.392233552
CD19+ TAMs	SULT1A1	0.39207856
CD19+ TAMs	GLMP	0.391829619
CD19+ TAMs	PIK3R1	0.3893586
CD19+ TAMs	SESN3	0.388783091
CD19+ TAMs	MYO5A	0.386937194
CD19+ TAMs	SAT1	0.38579691
CD19+ TAMs	CLIC2	0.384914044
CD19+ TAMs	TGFBI	0.384237329
CD19+ TAMs	RBM47	0.384009795
CD19+ TAMs	APH1A	0.383791864
CD19+ TAMs	ITGA9	0.383650598
CD19+ TAMs	STOM	0.383278642
CD19+ TAMs	CD151	0.382197102
CD19+ TAMs	ZFYVE16	0.382052575
CD19+ TAMs	MFSD12	0.381919917

CD19+ TAMs	CLEC2B	0.380921705
CD19+ TAMs	GLDN	0.38042056
CD19+ TAMs	RNF13	0.380172525
CD19+ TAMs	HSD17B14	0.379661166
CD19+ TAMs	AKR1A1	0.378763374
CD19+ TAMs	ZDHHC14	0.377913923
CD19+ TAMs	H2AFJ	0.377514285
CD19+ TAMs	TMEM219	0.377031323
CD19+ TAMs	MMD	0.376752027
CD19+ TAMs	PLEKHO2	0.376451235
CD19+ TAMs	SEPTIN11	0.374638242
CD19+ TAMs	DRAM2	0.3741726
CD19+ TAMs	SNX5	0.373724273
CD19+ TAMs	CALR	0.372564171
CD19+ TAMs	NRIP1	0.372326589
CD19+ TAMs	TNFSF12	0.371095221
CD19+ TAMs	PRKACB	0.37067084
CD19+ TAMs	CANX	0.369474642
CD19+ TAMs	LHFPL2	0.368673724
CD19+ TAMs	ARRB2	0.368297826
CD19+ TAMs	CORO1B	0.367847137
CD19+ TAMs	HLA-B	0.366532142
CD19+ TAMs	ARHGAP21	0.366095962
CD19+ TAMs	OLMALINC	0.364727431
CD19+ TAMs	DIP2A	0.3642343
CD19+ TAMs	APOH	0.364129644
CD19+ TAMs	ADM	0.363937671
CD19+ TAMs	PEAK1	0.363176913
CD19+ TAMs	PXDC1	0.362900233
CD19+ TAMs	CMTM3	0.362650768
CD19+ TAMs	IGFLR1	0.362045685
CD19+ TAMs	CCR1	0.361013523
CD19+ TAMs	SLC35F6	0.36093349
CD19+ TAMs	MT-CO2	0.360843515
CD19+ TAMs	PER3	0.359332175
CD19+ TAMs	TMEM14C	0.359250626
CD19+ TAMs	TNFRSF21	0.359195506
CD19+ TAMs	CEBPA	0.358722238
CD19+ TAMs	RAB13	0.358457988
CD19+ TAMs	GUSB	0.358136438
CD19+ TAMs	SCP2	0.355256203

CD19+ TAMs	SCN9A	0.35444073
CD19+ TAMs	ANXA4	0.354024535
CD19+ TAMs	STX4	0.352165623
CD19+ TAMs	ACP2	0.351952949
CD19+ TAMs	NCKAP1L	0.351814482
CD19+ TAMs	TMEM35B	0.351282411
CD19+ TAMs	GABARAP	0.350714223
CD19+ TAMs	HEXB	0.349307015
CD19+ TAMs	FERMT3	0.348736788
CD19+ TAMs	ARRDC2	0.347606753
CD19+ TAMs	C1orf56	0.347439612
CD19+ TAMs	NAGK	0.347264548
CD19+ TAMs	AMDHD2	0.347130656
CD19+ TAMs	HS3ST2	0.346660833
CD19+ TAMs	NCKAP5	0.346482106
CD19+ TAMs	GNAS	0.346325528
CD19+ TAMs	LMNA	0.346113998
CD19+ TAMs	MT-ND5	0.345984196
CD19+ TAMs	INSIG1	0.344245104
CD19+ TAMs	RNH1	0.341748705
CD19+ TAMs	BIN1	0.341644625
CD19+ TAMs	PLAAT3	0.341597428
CD19+ TAMs	GASK1B	0.340819831
CD19+ TAMs	TUBB	0.340312123
CD19+ TAMs	SNX18	0.340154912
CD19+ TAMs	ORM1	0.339890039
CD19+ TAMs	PCBD1	0.339385347
CD19+ TAMs	ABHD12	0.339375323
CD19+ TAMs	FUOM	0.339208928
CD19+ TAMs	HAVCR2	0.338792011
CD19+ TAMs	SH3PXD2A	0.338422989
CD19+ TAMs	PIK3R3	0.338256924
CD19+ TAMs	FAM20C	0.338251131
CD19+ TAMs	RBMS1	0.337978578
CD19+ TAMs	SHMT1	0.337020693
CD19+ TAMs	LGALS9	0.336697641
CD19+ TAMs	POMP	0.335872312
CD19+ TAMs	IRF2BP2	0.335538934
CD19+ TAMs	AIG1	0.334657784
CD19+ TAMs	PLXNB2	0.334180715
CD19+ TAMs	TLN1	0.333966578

CD19+ TAMs	CTTNBP2NL	0.333334536
CD19+ TAMs	LPL	0.333284622
CD19+ TAMs	ITGB2	0.332417702
CD19+ TAMs	MGST2	0.332301047
CD19+ TAMs	ARL6IP5	0.331672798
CD19+ TAMs	SORBS3	0.331187633
CD19+ TAMs	CRHBP	0.331150378
CD19+ TAMs	ARPIN	0.32979864
CD19+ TAMs	CHID1	0.329311408
CD19+ TAMs	AP2S1	0.328956825
CD19+ TAMs	SLC46A3	0.328545464
CD19+ TAMs	CNRIP1	0.328535544
CD19+ TAMs	RHOC	0.327066713
CD19+ TAMs	S100A13	0.325916604
CD19+ TAMs	OSTF1	0.325302513
CD19+ TAMs	SPPL2A	0.322506604
CD19+ TAMs	TPT1	0.321897569
CD19+ TAMs	RAB3IL1	0.321674683
CD19+ TAMs	UCP2	0.321455074
CD19+ TAMs	MDH1	0.321209863
CD19+ TAMs	TWF2	0.320738005
CD19+ TAMs	QPRT	0.32069077
CD19+ TAMs	RENBP	0.320318975
CD19+ TAMs	FEM1B	0.320198121
CD19+ TAMs	ARHGAP4	0.319762742
CD19+ TAMs	MAT2A	0.319478184
CD19+ TAMs	SLC11A2	0.31939895
CD19+ TAMs	LITAF	0.318302914
CD19+ TAMs	SYNGR2	0.31824409
CD19+ TAMs	CYBRD1	0.317889515
CD19+ TAMs	CCDC107	0.317686552
CD19+ TAMs	SPINK1	0.316898362
CD19+ TAMs	MAMDC2	0.316336846
CD19+ TAMs	C20orf194	0.313737089
CD19+ TAMs	TNFRSF14	0.313634117
CD19+ TAMs	ATOX1	0.313606192
CD19+ TAMs	USF2	0.313035643
CD19+ TAMs	TMEM70	0.311943742
CD19+ TAMs	DTNA	0.311766738
CD19+ TAMs	BLOC1S1	0.311307758
CD19+ TAMs	APPL2	0.311292653

CD19+ TAMs	SNHG12	0.31107359
CD19+ TAMs	SUCNR1	0.309916662
CD19+ TAMs	MSRB2	0.309883626
CD19+ TAMs	ACTG1	0.309304178
CD19+ TAMs	GNG10	0.308918436
CD19+ TAMs	CTSF	0.308859646
CD19+ TAMs	PI4K2A	0.308668507
CD19+ TAMs	MTSS1	0.30852664
CD19+ TAMs	ENG	0.307238925
CD19+ TAMs	OTULINL	0.306954308
CD19+ TAMs	LAMTOR1	0.306502571
CD19+ TAMs	IGFBP4	0.306203851
CD19+ TAMs	CYB5A	0.30599866
CD19+ TAMs	NAGLU	0.305229554
CD19+ TAMs	ARPC5	0.304400256
CD19+ TAMs	ITPRIPL2	0.303210979
CD19+ TAMs	HNRNPH1	0.303164175
CD19+ TAMs	TCN2	0.303127105
CD19+ TAMs	ARHGEF12	0.302791895
CD19+ TAMs	PITHD1	0.302293779
CD19+ TAMs	DEGS1	0.302125148
CD19+ TAMs	SH2B3	0.301096126
CD19+ TAMs	DHRS7	0.300920889
CD19+ TAMs	CYB5R1	0.299463674
CD19+ TAMs	SDC2	0.299383175
CD19+ TAMs	PRKN	0.298867966
CD19+ TAMs	OAZ2	0.298507868
CD19+ TAMs	SERPINF1	0.297697296
CD19+ TAMs	ETS2	0.296595577
CD19+ TAMs	OGFRL1	0.2962876
CD19+ TAMs	SPIN1	0.296243908
CD19+ TAMs	H1FO	0.296010607
CD19+ TAMs	BAIAP2	0.295947913
CD19+ TAMs	GRINA	0.295365551
CD19+ TAMs	ADORA3	0.293358172
CD19+ TAMs	FAM91A1	0.293222889
CD19+ TAMs	CEP170	0.293006973
CD19+ TAMs	OLFML2B	0.292822243
CD19+ TAMs	LACC1	0.292324877
CD19+ TAMs	SMIM30	0.291208054
CD19+ TAMs	LY86	0.29113305

CD19+ TAMs	HCST	0.29049392
CD19+ TAMs	CCDC47	0.290368314
CD19+ TAMs	TM2D2	0.289741432
CD19+ TAMs	SUMF2	0.289524752
CD19+ TAMs	EVL	0.28752045
CD19+ TAMs	HEBP1	0.287489239
CD19+ TAMs	HECTD2	0.286917784
CD19+ TAMs	STON2	0.286868972
CD19+ TAMs	RAB32	0.286525645
CD19+ TAMs	FGFR1	0.286104794
CD19+ TAMs	APMAP	0.285700079
CD19+ TAMs	HSPB1	0.284471212
CD19+ TAMs	IFNGR1	0.284211167
CD19+ TAMs	RRAGD	0.28284892
CD19+ TAMs	P4HB	0.282620765
CD19+ TAMs	EPAS1	0.282598723
CD19+ TAMs	SLC39A1	0.281545348
CD19+ TAMs	GAL3ST4	0.281520096
CD19+ TAMs	DDR3K1	0.280298089
CD19+ TAMs	MMP14	0.28016654
CD19+ TAMs	VKORC1	0.279566424
CD19+ TAMs	NUCB1	0.279461037
CD19+ TAMs	TCEAL4	0.279171378
CD19+ TAMs	IL18BP	0.278449584
CD19+ TAMs	GBA	0.278288458
CD19+ TAMs	DBNDD2	0.278112793
CD19+ TAMs	TM6SF1	0.277956693
CD19+ TAMs	ANXA5	0.276704513
CD19+ TAMs	BCL2L1	0.276534898
CD19+ TAMs	SAMD4A	0.275115027
CD19+ TAMs	CLN8	0.274305752
CD19+ TAMs	EYA2	0.274274837
CD19+ TAMs	SGPP1	0.274272691
CD19+ TAMs	TMBIM1	0.274128399
CD19+ TAMs	LEPROT	0.270714885
CD19+ TAMs	TFPT	0.268896661
CD19+ TAMs	TRIM47	0.267541119
CD19+ TAMs	ARPC1B	0.267210855
CD19+ TAMs	PFKL	0.267074347
CD19+ TAMs	CXCL9	0.267069716
CD19+ TAMs	CCDC88A	0.26684799

CD19+ TAMs	RASAL2	0.264803726
CD19+ TAMs	ADIPOR1	0.264672032
CD19+ TAMs	TMEM86A	0.264364849
CD19+ TAMs	CD33	0.263944475
CD19+ TAMs	SLC43A3	0.263815625
CD19+ TAMs	NMRK1	0.261425121
CD19+ TAMs	MRC2	0.261262455
CD19+ TAMs	MPPED2	0.260691865
CD19+ TAMs	CNTLN	0.259860893
CD19+ TAMs	LINC00472	0.259013258
CD19+ TAMs	ZNF358	0.258965105
CD19+ TAMs	ALDH9A1	0.258328056
CD19+ TAMs	TMEM106A	0.25736182
CD19+ TAMs	PTTG1IP	0.256774603
CD19+ TAMs	BEX3	0.256641248
CD19+ TAMs	RPP25	0.256339568
CD19+ TAMs	CHCHD6	0.255934224
CD19+ TAMs	SNX24	0.255672286
CD19+ TAMs	PPIA	0.255242782
CD19+ TAMs	CLN6	0.254815399
CD19+ TAMs	PYCARD	0.254068411
CD19+ TAMs	SLC22A18	0.253709924
CD19+ TAMs	TNFRSF11A	0.253632553
CD19+ TAMs	NAGA	0.253509241
CD19+ TAMs	SLC12A5	0.252864231
CD19+ TAMs	MATK	0.252213507
CD19+ TAMs	IQGAP1	0.326989065
CD19+ TAMs	MCRIP1	0.254963685
CD19+ TAMs	DNASE2	0.286698441
CD19+ TAMs	HLA-C	0.319711046
CD19+ TAMs	GNB2	0.260372932
CD19+ TAMs	AP2M1	0.265414953
CD19+ TAMs	TLE5	0.280884795
CD19+ TAMs	CHMP1B	0.368499412
CD19+ TAMs	NCEH1	0.256038457
CD19+ TAMs	ARHGDI1A	0.267508278
CD19+ TAMs	RDX	0.406554251
CD19+ TAMs	CXCL2	0.594433695
CD19+ TAMs	SNX9	0.840236172
CD19+ TAMs	ZNF331	0.665368328
CD19+ TAMs	PAPSS2	0.353866162

CD19+ TAMs	APH1B	0.292380591
CD19+ TAMs	DAPK1	0.371818982
CD19+ TAMs	NDFIP1	0.267708232
CD19+ TAMs	DYNLL1	0.293370535
CD19+ TAMs	WASHC4	0.293826674
CD19+ TAMs	NECAP2	0.265141668
CD19+ TAMs	TRAPPC5	0.288154976
CD19+ TAMs	TMEM50A	0.297983814
CD19+ TAMs	CLIC1	0.298461669
CD19+ TAMs	ATP6V0A1	0.296190671
CD19+ TAMs	ATP6V1C1	0.271285278
CD19+ TAMs	FAM13A	0.297043123
CD19+ TAMs	PLCL1	0.348295871
CD19+ TAMs	TMBIM4	0.279379538
CD19+ TAMs	CREM	0.493443103
CD19+ TAMs	VPS28	0.283356068
CD19+ TAMs	BSG	0.267449509
CD19+ TAMs	PPP1CB	0.423424556
CD19+ TAMs	SELENOW	0.290196203
CD19+ TAMs	AHNAK	0.306597679
CD19+ TAMs	CBR1	0.251980541
CD19+ TAMs	ANXA11	0.277392082
CD19+ TAMs	TCF12	0.379447448
CD19+ TAMs	RANBP2	0.590398943
CD19+ TAMs	C9orf16	0.397797095
CD19+ TAMs	DHRS9	0.25415643
CD19+ TAMs	IL10RA	0.25385869
CD19+ TAMs	OS9	0.251077242
CD19+ TAMs	GSTO1	0.283397017
CD19+ TAMs	PTBP3	0.319087438
CD19+ TAMs	FXYD5	0.312805492
CD19+ TAMs	GATAD1	0.26193292
CD19+ TAMs	NHSL1	0.516097467
CD19+ TAMs	CEPT1	0.252082189
CD19+ TAMs	GNA13	0.460537329
CD19+ TAMs	NORAD	0.27642695
CD19+ TAMs	MT2A	0.718106849
CD19+ TAMs	EIF4A3	0.36016246
CD19+ TAMs	CAPG	0.468787029
CD19+ TAMs	WDR61	0.252641227
CD19+ TAMs	S100A11	0.301787644

CD19+ TAMs	DYNC1H1	0.257189207
CD19+ TAMs	EIF3D	0.2572143
CD19+ TAMs	SMURF2	0.262328079
CD19+ TAMs	SNX2	0.253595376
CD19+ TAMs	MMP9	0.383324355
CD19+ TAMs	RPS27L	0.260339926
CD19+ TAMs	MPC2	0.256777412
CD19+ TAMs	NAMPT	0.588383771
CD19+ TAMs	LNCAROD	0.306515595
CD19+ TAMs	CD72	0.277438875
CD19+ TAMs	PDK3	0.25595727
CD19+ TAMs	SLC3A2	0.277468102
CD19+ TAMs	DYNLRB1	0.251092286
CD19+ TAMs	TNS3	0.266800944
CD19+ TAMs	WASF2	0.304755717
CD19+ TAMs	RBPJ	0.250123342
CD19+ TAMs	ATP2A2	0.520450232
CD19+ TAMs	PLA2G4C	0.275493308
CD19+ TAMs	TCF4	0.317094185
CD19+ TAMs	P2RY13	0.293798333
CD19+ TAMs	CD40	0.258794107
CD19+ TAMs	REX1BD	0.259631775
CD19+ TAMs	SRP14	0.256094577
CD19+ TAMs	FOS	0.317078391
CD19+ TAMs	ZFAND5	0.631400544
CD19+ TAMs	AC084871.1	0.36671899
CD19+ TAMs	B4GALT1	0.371239844
CD19+ TAMs	FUS	0.278089373
CD19+ TAMs	FILIP1L	0.454646837
CD19+ TAMs	CEBPB	0.309371434
CD19+ TAMs	CHCHD10	0.26075932
CD19+ TAMs	BAX	0.258785692
CD19+ TAMs	ARRDC3	0.301206968
CD19+ TAMs	NFE2L2	0.255995942
CD19+ TAMs	TALDO1	0.283405892
CD19+ TAMs	KLF6	0.483810975
CD19+ TAMs	CREBRF	0.280580233
CD19+ TAMs	ID3	0.263107752
CD19+ TAMs	C4orf48	0.254673661
CD19+ TAMs	UQCR11	0.265126354
CD19+ TAMs	SLC31A2	0.300059555

CD19+ TAMs	EIF4A2	0.2699903
CD19+ TAMs	FHIT	0.326673349
CD19+ TAMs	DDX3X	0.298504381
CD19+ TAMs	CSGALNACT1	0.339469978
CD19+ TAMs	RNF144B	0.389020973
CD19+ TAMs	FOXO3	0.304155882
CD19+ TAMs	SAMSN1	0.401026514
CD19+ TAMs	LDLRAD4	0.356235071
CD19+ TAMs	GLA	0.256065957
CD19+ TAMs	CD83	0.379473933
CD19+ TAMs	MMP19	0.4025614
CD19+ TAMs	CHKA	0.384909705
CD19+ TAMs	ABCG1	0.265622469
CD19+ TAMs	SERINC5	0.269337157
CD19+ TAMs	PDE8A	0.543291961
CD19+ TAMs	WDR45B	0.383786764
CD19+ TAMs	PRMT9	0.273199651
CD19+ TAMs	AVPI1	0.255958851
CD19+ TAMs	ALPK3	0.313509921
CD19+ TAMs	SLC19A2	0.25673093
CD19+ TAMs	ADAMDEC1	0.279564906
CD19+ TAMs	ACSL1	0.615487287
CD19+ TAMs	JUNB	0.409139662
CD19+ TAMs	AC007319.1	0.29308236
CD19+ TAMs	RAB31	0.301375106
CD19+ TAMs	SH3BP5	0.328097456
CD19+ TAMs	PFKFB3	0.270662321
CD19+ TAMs	ICAM1	0.262391819
CD19+ TAMs	MT1E	0.420698365
CD19+ TAMs	FOXK2	0.317446339
CD19+ TAMs	HIF1A	0.259362529
CD19+ TAMs	RAB7A	0.371992401
CD19+ TAMs	MAP1LC3B	0.282452846
CD19+ TAMs	UBE2D3	0.31220936
CD19+ TAMs	MANBA	0.32837071
CD19+ TAMs	ATP1B3	0.632237887
CD19+ TAMs	NR4A2	0.38153332
CD19+ TAMs	IFIT2	0.258227696
CD19+ TAMs	ZFP36	0.493950691
CD19+ TAMs	SRGN	0.323366016
CD19+ TAMs	DDX3Y	0.294700194

CD19+ TAMs	LGALS1	0.295823092
CD19+ TAMs	TFRC	0.384779558
CD19+ TAMs	UST	0.580468203
CD19+ TAMs	MAFF	0.28910063
CD19+ TAMs	TTN	0.329275431
CD19+ TAMs	SIAH2	0.293876934
CD19+ TAMs	NFKB1	0.589416132
CD19+ TAMs	KLF2	0.304061094
CD19+ TAMs	ELL2	0.271398093
CD19+ TAMs	CCNH	0.391547718
CD19+ TAMs	ATF6	0.456523194

Supplementary Table 7. Classical M1 and M2 macrophage marker genes expression in CD19+ TAMs and CD19- TAMs, related to Fig. 3.

Gene	avg.exp	pct.exp	Cluster	avg.exp.scaled
MARCO	0.31911087	15.50013554	CD19- TAMs	0.707106781
IRF1	2.369314177	66.16427216	CD19- TAMs	0.707106781
CD80	0.215234481	14.37245866	CD19- TAMs	-0.707106781
CD86	2.061100569	73.04960694	CD19- TAMs	0.707106781
CD40	0.380807807	25.56248306	CD19- TAMs	-0.707106781
IL1B	7.452805638	53.60260233	CD19- TAMs	0.707106781
TNF	0.87975061	24.96069396	CD19- TAMs	0.707106781
IL1A	0.10750881	4.597451884	CD19- TAMs	0.707106781
NOS2	0.000271076	0.027107617	CD19- TAMs	-0.707106781
IL6	0.022933044	1.192735159	CD19- TAMs	-0.707106781
CXCL9	1.298021144	12.42071022	CD19- TAMs	0.707106781
CXCL10	1.753537544	15.20737327	CD19- TAMs	0.707106781
CXCL11	0.163513147	4.066142586	CD19- TAMs	0.707106781
CCR7	0.079587964	4.212523719	CD19- TAMs	0.707106781
IDO1	0.170344267	5.578747628	CD19- TAMs	0.707106781
VEGFA	1.279425319	36.06397398	CD19- TAMs	0.707106781
VEGFB	0.507834101	32.67552182	CD19- TAMs	-0.707106781
VEGFC	0.000325291	0.032529141	CD19- TAMs	0.707106781
VEGFD	0.001680672	0.135538086	CD19- TAMs	-0.707106781
IRF4	0.141772838	8.262401735	CD19- TAMs	0.707106781
FN1	1.894985091	17.57657902	CD19- TAMs	0.707106781
CLEC7A	1.875142315	72.97370561	CD19- TAMs	0.707106781
TGFB1	1.330008132	62.87340743	CD19- TAMs	0.707106781
TGFB2	0.078991597	4.440227704	CD19- TAMs	-0.707106781
IL1RN	1.061100569	25.87693142	CD19- TAMs	0.707106781
IL1R2	0.594524261	16.41095148	CD19- TAMs	0.707106781
IL4R	0.393819463	28.77202494	CD19- TAMs	0.707106781
IL10	0.76416373	17.34345351	CD19- TAMs	0.707106781
ARG2	0.264028192	12.27975061	CD19- TAMs	0.707106781
CCL2	0.138465709	3.822174031	CD19- TAMs	-0.707106781
CCL4	8.174247764	47.33532123	CD19- TAMs	-0.707106781
CCL5	0.27975061	10.74545947	CD19- TAMs	-0.707106781
CCL18	0.095310382	1.718622933	CD19- TAMs	-0.707106781
CCL22	0.01854161	1.051775549	CD19- TAMs	0.707106781
CCL24	0.023963134	1.832474925	CD19- TAMs	-0.707106781
CD274	0.091190024	6.408240716	CD19- TAMs	-0.707106781
PDCD1	0.005529954	0.525887774	CD19- TAMs	-0.707106781

CD276	0.148495527	11.67796151	CD19- TAMs	-0.707106781
CD200R1	0.107454595	8.181078883	CD19- TAMs	-0.707106781
TNFSF12	0.350121984	26.99376525	CD19- TAMs	-0.707106781
MMP9	0.505773922	14.74112226	CD19- TAMs	-0.707106781
MMP14	0.137544405	11.37435619	CD19- TAMs	-0.707106781
MMP19	0.282895094	11.13038764	CD19- TAMs	-0.707106781
CSF1R	2.514990512	83.38303063	CD19- TAMs	-0.707106781
CD163	2.48669016	66.98834372	CD19- TAMs	-0.707106781
MSR1	2.515803741	68.22445107	CD19- TAMs	-0.707106781
MARCO1	0.130183934	4.428226244	CD19+ TAMs	-0.707106781
IRF11	1.227279452	49.41565166	CD19+ TAMs	-0.707106781
CD801	0.248039844	17.40716998	CD19+ TAMs	0.707106781
CD861	1.803984417	71.22639183	CD19+ TAMs	-0.707106781
CD401	0.618768184	38.59164653	CD19+ TAMs	0.707106781
IL1B1	2.487400759	35.8597564	CD19+ TAMs	-0.707106781
TNF1	0.556930815	26.47566448	CD19+ TAMs	-0.707106781
IL1A1	0.051925637	2.830514325	CD19+ TAMs	-0.707106781
NOS21	0.000394497	0.039449677	CD19+ TAMs	0.707106781
IL61	0.024360176	1.439913211	CD19+ TAMs	0.707106781
CXCL91	1.166872134	24.22703289	CD19+ TAMs	-0.707106781
CXCL101	1.448296267	27.24986439	CD19+ TAMs	-0.707106781
CXCL111	0.114058879	5.493367523	CD19+ TAMs	-0.707106781
CCR71	0.054835051	2.934069727	CD19+ TAMs	-0.707106781
IDO11	0.071403915	2.791064648	CD19+ TAMs	-0.707106781
VEGFA1	0.628482667	27.90571527	CD19+ TAMs	-0.707106781
VEGFB1	1.107451058	60.2988313	CD19+ TAMs	0.707106781
VEGFC1	0.000147936	0.00493121	CD19+ TAMs	-0.707106781
VEGFD1	0.00493121	0.438877657	CD19+ TAMs	0.707106781
IRF41	0.074116081	5.365156073	CD19+ TAMs	-0.707106781
FN11	0.899206075	24.99630159	CD19+ TAMs	-0.707106781
CLEC7A1	1.189999507	54.28275556	CD19+ TAMs	-0.707106781
TGFB11	1.088268652	57.22668771	CD19+ TAMs	-0.707106781
TGFB21	0.141081907	9.172049904	CD19+ TAMs	0.707106781
IL1RN1	0.391784605	14.73938557	CD19+ TAMs	-0.707106781
IL1R21	0.314265989	11.33191972	CD19+ TAMs	-0.707106781
IL4R1	0.307362296	24.55249273	CD19+ TAMs	-0.707106781
IL101	0.631934514	19.49307165	CD19+ TAMs	-0.707106781
ARG21	0.186005227	11.74121012	CD19+ TAMs	-0.707106781
CCL21	0.530598156	18.46738005	CD19+ TAMs	0.707106781
CCL41	9.277232605	64.32269836	CD19+ TAMs	0.707106781
CCL51	0.350609004	16.76611273	CD19+ TAMs	0.707106781

CCL181	0.376399231	15.73055871	CD19+ TAMs	0.707106781
CCL221	0.012328024	0.542433059	CD19+ TAMs	-0.707106781
CCL241	0.033236353	2.722027713	CD19+ TAMs	0.707106781
CD2741	0.113910942	9.172049904	CD19+ TAMs	0.707106781
PDCD11	0.006903693	0.631194832	CD19+ TAMs	0.707106781
CD2761	0.279994083	22.31372356	CD19+ TAMs	0.707106781
CD200R11	0.281720006	21.30282558	CD19+ TAMs	0.707106781
TNFSF121	0.584693525	40.7811036	CD19+ TAMs	0.707106781
MMP91	0.679964495	19.90729326	CD19+ TAMs	0.707106781
MMP141	0.325509147	25.48449135	CD19+ TAMs	0.707106781
MMP191	0.482124365	14.78376646	CD19+ TAMs	0.707106781
CSF1R1	3.984811874	93.46121604	CD19+ TAMs	0.707106781
CD1631	5.85369101	90.90684945	CD19+ TAMs	0.707106781
MSR11	5.663395631	95.09837763	CD19+ TAMs	0.707106781

Supplementary Table 8. Key Resources Table

REAGENT or RESOURCE	SOURCE	IDENTIFIER
Antibodies		
<i>In vivo</i> mAb anti-mouse CD73	bioxcell	Cat#BE0209
<i>In vivo</i> Plus anti-mouse PD-L1 (B7-H1)	bioxcell	Cat#BP0101
<i>In vivo</i> mAb anti-human CD19	bioxcell	Cat#BE0281
FC: anti-Human CD45	Biolegend	Cat#368516
FC: anti-Human CD14	Biolegend	Cat#325603
FC: anti-Human CD11b	Biolegend	Cat#301322
FC: anti-Human CD19 (For CD19 ⁺ TAMs sorting and ImageStream)	Biolegend	Cat#302234
FC: anti-Human CD68	Biolegend	Cat#333808
FC: anti-Human CD73	Biolegend	Cat#344013
FC: anti-Human CD19 (For flow cytometry analysis)	Biolegend	Cat#302206
FC: anti-Human CD274	Biolegend	Cat#329740
FC: anti-Human CD64	Biolegend	Cat#305027
FC: anti-Human PD-1	Biolegend	Cat#367405
FC: anti-Human CD80	Biolegend	Cat#305217
FC: anti-Human CCR2	Biolegend	Cat#357203
FC: anti-Human ARG-1	Biolegend	Cat#369705
FC: anti-Human CD163	Biolegend	Cat#333610
FC: anti-Human CD206	Biolegend	Cat#321103
FC: anti-Human CD19 (For flow cytometry in Fig 5f)	BD Bioscience	Cat#557921
FC: anti-Human PAX5	BD Bioscience	Cat#562814
FC: anti-Human Ki-67	BD Bioscience	Cat#563757d
FC: anti-Human CD86	BD Bioscience	Cat#562432
FC: anti-Human HLA_DR	BD Bioscience	Cat#564231
FC: anti-Human CD326	BD Bioscience	Cat#745841
FC: anti-Human Fc Block	BD Bioscience	Cat#564219
FC: anti-Mouse F4/80 (For CD19 ⁺ macrophages sorting)	Biolegend	Cat#123110
FC: anti-Mouse F4/80 (For flow cytometry analysis)	Biolegend	Cat#123114
FC: anti-Mouse Ly6C	Biolegend	Cat#128036
FC: anti-Mouse CD274	Biolegend	Cat#124312
FC: anti-Mouse CD279	Biolegend	Cat#135218
FC: anti-Mouse CD45.1	Biolegend	Cat#110723
FC: anti-Mouse CD45.2	Biolegend	Cat#109813
FC: anti-Mouse Ki-67	Biolegend	Cat#652410
FC: anti-Mouse Ly6G	Biolegend	Cat#127605
FC: anti-Mouse CD3	Biolegend	Cat#100203
FC: anti-Mouse CD8a	Biolegend	Cat#100722
FC: anti-Mouse PD-1	Biolegend	Cat#135218

FC: anti-Mouse CD19 (For CD19 ⁺ macrophages sorting)	Biolegend	Cat#152410
FC: anti-Mouse CD169	Biolegend	Cat#142406
FC: anti-Mouse CD209b	Thermo Fisher Scientific	Cat# 17-2093-82
FC: anti-Mouse CLEC4F	Biolegend	Cat#156804
FC: anti-Mouse CD11c	Biolegend	Cat#117306
FC: anti-Mouse CD170	Biolegend	Cat#155508
FC: anti-Mouse CD115	Biolegend	Cat#135510
FC: anti-Mouse Ly-6G/Ly6c (Gr-1)	Biolegend	Cat#108438
FC: anti-Mouse CD45	BD Bioscience	Cat#563053
FC: anti-Mouse CD11b	BD Bioscience	Cat#562287
FC: anti-Mouse MHCII (I-A/I-E)	BD Bioscience	Cat#562564
FC: anti-Mouse CD19 (For flow cytometry analysis)	BD Bioscience	Cat#557921
FC: anti-Mouse CD11c	BD Bioscience	Cat#560584
FC: anti-Mouse CD4	BD Bioscience	Cat#552051
FC: anti-Mouse CD45R/B220	BD Bioscience	Cat#563893
FC: anti-Mouse Fc Block	BD Bioscience	Cat#553142
FC: 7-AAD	BD Bioscience	Cat#559925
FC: Fixable Viability Stain 780	BD Bioscience	Cat#565388
FC: Fixable viability stain 700	BD Bioscience	Cat#564997
Chip, Wb: Rabbit IgG, monoclonal-Isotype Control	abcam	Cat#ab172730
Chip, Wb: Anti-PAX5 antibody	abcam	Cat#ab227635
Wb: Anti-PGC1 alpha antibody	abcam	Cat#ab106814
Wb: Anti-LAMP1 antibody	abcam	Cat#ab24170
Wb: Anti-CD63 antibody	abcam	Cat#ab134045
Wb: LC3B (E7X4S) XP [®] Rabbit mAb	Cell Signaling Technology	Cat#43566S
Wb: SQSTM1/p62 (D5L7G) Mouse mAb	Cell Signaling Technology	Cat#88588S
Wb: NT5E antibody	Affinity	Cat#DF6763
Wb: Cathepsin B (D1C7Y) XP [®] Rabbit mAb	Cell Signaling Technology	Cat#31718T
Wb: Cathepsin H Antibody - Internal	Affinity	Cat#DF8514
Wb: Phospho-TFEB (Ser142) antibody	Affinity	Cat#AF3845
Wb: β -Actin Mouse Monoclonal Antibody	Beyotime	Cat#AF5009
Wb: GAPDH Mouse Monoclonal Antibody	Beyotime	Cat#AF5001
Wb: Histone H3 Mouse Monoclonal Antibody	Beyotime	Cat#AF0009
Wb: HRP-labeled Goat Anti-Mouse IgG(H+L)	Beyotime	Cat#A0216
Wb: HRP-labeled Goat Anti-Rabbit IgG(H+L)	Beyotime	Cat#A0208
Wb: LAMP-5 antibody	santa cruz	Cat#sc-398190
Wb: LAMP2 Monoclonal antibody	proteintech	Cat#66301-1-Ig
Wb, IF: TFEB Polyclonal antibody	proteintech	Cat#13372-1-AP
Wb, IF: PD-L1/CD274 monoclonal antibody	proteintech	Cat#2B11D11

Wb, IF: CD19 antibody	Affinity	Cat#DF7030
IF: CD68	abcam	Cat#ab213363
IF: PD-L1	abcam	Cat#ab213524
IF: F4/80	abcam	Cat#ab6640
IF: Alexa Fluor® 488 Anti-F4/80	Abcam	Cat#ab204266
IF: Alexa Fluor® 647 Anti-PD-L1 antibody	Abcam	Cat#ab224030
IF: CD19	Cell Signaling Technology	Cat#3574S
IF: Anti-rabbit IgG (H+L), F(ab') ₂ Fragment (Alexa Fluor® 555 Conjugate)	Cell Signaling Technology	Cat#4413S
IF: Anti-mouse IgG (H+L), F(ab') ₂ Fragment (Alexa Fluor® 488 Conjugate)	Cell Signaling Technology	Cat#4408S
IF: Anti-mouse IgG (H+L), F(ab') ₂ Fragment (Alexa Fluor® 647 Conjugate)	Cell Signaling Technology	Cat#4410S
IHC: Anti-CD45 antibody	abcam	Cat#ab40763
IHC: Ki-67 (D2H10) Rabbit mAb (IHC Specific)	Cell Signaling Technology	Cat#9027S
IHC: CD8α (D4W2Z) XP® Rabbit mAb (Mouse Specific)	Cell Signaling Technology	Cat#98941S
IHC: CD4 (D7D2Z) Rabbit mAb	Cell Signaling Technology	Cat#25229S
IHC: NCAM1 (CD56) (E7X9M) XP® Rabbit mAb	Cell Signaling Technology	Cat#99746S
IHC: Ki-67 (8D5) Mouse mAb	Cell Signaling Technology	Cat#94497
IHC: PD-1 (D7D5W) XP® Rabbit mAb (Mouse Specific)	Cell Signaling Technology	Cat#84651s
IHC: CD45 (D3F8Q) Rabbit mAb	Cell Signaling Technology	Cat#70257S
IHC: FoxP3 (D6O8R) Rabbit mAb	Cell Signaling Technology	Cat#12653S
IHC: FoxP3 (D2W8E™) Rabbit mAb (IHC Specific)	Cell Signaling Technology	Cat#98377S
IHC: CD8α (D8A8Y) Rabbit mAb	Cell Signaling Technology	Cat#85336S
IHC: CD31 (PECAM-1) (89C2) Mouse mAb	Cell Signaling Technology	Cat#3528S
IHC: CD4 (D7D2Z) Rabbit mAb (BSA and Azide Free)	Cell Signaling Technology	Cat#27520SF
IHC: PD-1 (D4W2J) XP® Rabbit mAb	Cell Signaling Technology	Cat#86163S
mIHC: CD14	Abcam	Cat#ab245235
mIHC: CD68	Abcam	Cat#ab192847
mIHC: CD20	Cell Signaling Technology	Cat#48750S
mIHC: CD19	Abcam	Cat#ab134114
Bacterial and virus strains		
pMSCV-IRES-GFP II	Addgene	Cat#52107
Lentivirus	Jikai	N/A
Biological samples		

Tumor samples	The First Affiliated Hospital of Zhejiang University	NA
Adjacent normal tissues	The First Affiliated Hospital of Zhejiang University	NA
PBMC from HCC patients	The First Affiliated Hospital of Zhejiang University	NA
Critical commercial assays		
5'-Nucleotidase (CD73) Activity Assay kit	Abcam	Cat#ab235945
cytofix/Cytoperm Fixation/ Permeabilization Kit	BD Bioscience	Cat#554714
Nuclear and Cytoplasmic Protein Extraction Kit	Beyotime	Cat#P0028
Adenosine Assay	Cell Biolabs	Cat#MET-5090
Chromium Next GEM Single Cell 3' GEM, Library & Gel Bead Kit v3.1	10X Genomics	Cat#1000121
Chromium Next GEM Chip G Single Cell Kit,	10X Genomics	Cat#1000120
Opal 6-plex manual detection kit	Akoya Biosciences	Cat#NEL861001KT
Experimental models: Cell lines		
THP-1	ATCC	N/A
Hepa1-6	ATCC	N/A
Plat-E	ATCC	N/A
iBMDM	Zhejiang University	N/A
Experimental models: Organisms/strains		
C57BL/6 (males, 6-12 weeks old)	Nanjing University	N/A
<i>Pax5^{fllox/fllox}</i>	Cyagen Biosciences	N/A
<i>CD19^{fllox/fllox}</i>	Cyagen Biosciences	N/A
<i>muMT</i>	Zhejiang University	N/A
<i>Lyz-Cre</i>	Jackson Laboratory	Cat#018956
Oligonucleotides		
Primers, see Table S5	This manuscript	N/A
Software and algorithms		
Venny (2.1)	https://bioinfogp.cnb.csic.es/tools/venny/index.html	https://bioinfogp.cnb.csic.es/tools/venny/
WebGestalt	http://www.webgestalt.org/	https://doi.org/10.1093/nar/gkz401
MAST	https://doi.org/10.1186/s13059-015-0844-5	https://www.bioconductor.org/packages/release/bioc/html/MAST.html

STAR	doi:10.1093/bioinformatics/bts635	http://code.google.com/p/rna-star/
GSVA (v1.36.0)	https://doi.org/10.1186/1471-2105-14-7	http://www.bioconductor.org/packages/release/bioc/html/GSVA.html
Monocle2 (v2.10.1)	https://doi.org/10.1038/nmeth.4402	https://github.com/cole-trapnelllab/monocle-release
Seurat	doi:10.1038/nbt.4096.	https://github.com/satijalab/seurat
Cell Ranger (v3.0.1)	10x Genomics, https://doi.org/10.1038/ncomms14049	https://10xgenomics.com
GSEA (v4.1.0)	https://doi.org/10.1073/pnas.0506580102	https://www.gsea-msigdb.org/gsea/index.jsp
WebGestalt (v2019)		https://www.webgestalt.org/
Wave desktop (v2.6.1)	Agilent	https://www.agilent.com.cn/zh-cn/product/cell-analysis/real-time-cell-metabolic-analysis/xf-software/seahorse-wave-desktop-software-740897#relatedproducts
ACCENSE	doi:10.1073/pnas.1321405111.	http://cellaccense.com/
Bowtie 2 (v2.3.4.3)	doi:10.1038/nmeth.1923	http://bowtie-bio.sourceforge.net/bowtie2/index.shtml
Deeptools (3.02)	doi:10.1093/nar/gku365	https://deeptools.readthedocs.io/en/develop/
ChIPseeker (1.12.1)	https://doi.org/10.1093/bioinformatics/btv145	https://bioconductor.org/packages/release/bioc/html/ChIPseeker.html
MEME (5.1)	doi:10.1093/nar/gkp335.	https://meme-suite.org/meme/
Prism (v8.0)	Graph Pad	https://www.graphpad.com/
Flow Jo (v10.5.3)	Treestar	https://www.flowjo.com/
Image J	Freeware/NIH	https://imagej.nih.gov/ij/
MicroVigene	Vigene Tech	http://www.vigenetech.com/MicroVigene.htm

DAVID	doi: 10.1038/nprot.200 8.211	https://david.ncicrf.gov/summary.jsp
R 4.0.5	R Project	https://www.r-project.org
Deposited data		
Sc-RNA-seq	This paper	N/A
Sc-RNA-seq (published)	Bioproject	PRJCA010606
Sc-RNA-seq (published)	Bioproject	PRJCA007744
Cut&Tag	This paper	ftp://ftp.ncbi.nlm.nih.gov/genomes/all/GCF/000/00
RNA-seq	This paper	N/A
Other		
Protein Block	Abcam	Cat#ab64226
Seahorse XF 1.0 M glucose solution	Agilent	Cat#103577-100
Seahorse XF 100 mM pyruvate solution	Agilent	Cat#103579-100
Seahorse XF 200 mM glutamine solution	Agilent	Cat#103578-100
Seahorse XF RPMI Medium	Agilent	Cat#103576-100
Seahorse XFe24 FluxPak	Agilent	102340-100
Leukocyte Activation Cocktail, with BD GolgiPlug™	BD Bioscience	Cat#550583
Lyso-Tracker Red	Beyotime	Cat#C1046
Cell lysis buffer for Western and IP	Beyotime	Cat#p0013
EdU	Beyotime	Cat#ST067
FCCP	Cayman	Cat#15218
Antimycin A1	Cayman	Cat#18433
oligomycin A	Cayman	Cat#11342
Clodronate Liposomes & Control Liposomes	Clodronate Liposomes	Cat#CP-005-005
Corning® Cell-Tak™ Cell and Tissue Adhesive	Corning	Cat#354240
Dipyridamole	Glpbio	Cat#GC17673
EHNA hydrochloride	Glpbio	Cat#GC10935
NBMPR	Glpbio	Cat#GC10835
MitoTracker™ Deep Red FM	Invitrogen	Cat#M22426
pHrodo™ Red, SE	Invitrogen	Cat#P36600
MitoSOX™ Red	Invitrogen	Cat#M36008
LysoSensor™ Yellow/Blue DND-160	Invitrogen	Cat#L7545
CellLight™ Mitochondria-GFP	Invitrogen	Cat#C1050
staurosporine	Merck	Cat#569397-100ug
NEOFECT™ DNA transfection reagent	Neofect	Cat#TF201201
Animal-free recombinant murine M-CSF	Peprtech	Cat#AF-315-02
<i>TFEB</i> siRNA (h)	santa cruz	Cat#sc-38509
IACS-010759	Selleck	Cat#1570496-34-2
Adenosine 5'-monophosphate monohydrate	Sigma-Aldrich	Cat#A2252

Adensine 5'-pyrophosphoric acid (5'-ADP)	Sigma-Aldrich	Cat#3768-14-7
CD73 inhibitor-AMP-CP	Sigma-Aldrich	Cat#3768-14-7
Hyaluronidase	Worthington	Cat#LS005477
ProLong™ Gold and Diamond Antifade Mountants	Invitrogen	Cat#S36939
Rhod-2 dextran conjugate	ABD Bioquest	Cat#20451
Calbryte™ 630 AM	ABD Bioquest	Cat#20720
Goat serum	Zsbio	Cat#ZLI-9056
Anti-CD3ε	Biolegend	Cat#100302
Anti-CD28	Biolegend	Cat#102116
MojoSort™ Streptavidin Nanobeads	Biolegend	Cat#480016
MojoSort™ Magnet	Biolegend	Cat#480019
FBS	NEWZERUM	Cat#FBS-E500
IL-2	Novoprotein	Cat#C013
2-mercaptoethanol	Gibco	Cat#21985023
40 ,6-diamidino-2-phenylindole (DAPI)	Sigma-Aldrich	Cat#D9542